Novel strategies and targets for the detection and cure of Diabetes Mellitus

Dissertation

zur Erlangung des Grades eines Doktors der Naturwissenschaften

im Fachbereich Biologie/Chemie
der Universität Bremen

vorgelegt von
Katharina Stolz

Bremen, 01.10.2015

1. Gutachter: Prof. Dr. Kathrin Mädler

2. Gutachter: Prof. Dr. Annette Schürmann

Erklärung gemäß §6 Abs. 5 der Promotionsordnung

Hiermit versichere ich, dass ich die vorliegende Dissertation mit dem Titel „Novel strategies and targets for the detection and cure of Diabetes Mellitus“ selbständig verfasst und keine anderen als die angegebenen Quellen und Hilfsmittel benutzt habe.

Bremen, den 01.10.2015

……..
Katharina Stolz

Table of contents

I. Table of figures

II. Abbreviations

APC	Antigen presenting cell
ATP	Adenosin triphosphate
AUC	Area under curve
CAT	Catalase
CD	Cluster of Differentiation
CTLA-4	Cytotoxic T-lymphocyte antigen
DAMP	Damage associated molecular pattern
DAP12	DNAX activation protein of 12 kDa
DC	Dendritic cell
DNA	Deoxyribonucleic acid
DTBZ	Dihydrotetrabenazine
ER	Endoplasmatic reticulum
GABA	Gamma-aminobutric acid
GAD65	Glutamic acid decarboxylase
GLP	Glucagon-like peptide
GLUT	Glucose transporter
GPX	Glutathione peroxidase
GRPP	Glicentin-related polypeptide
GSIS	Glucose stimulated insulin secretion
HFD	High fat diet
HLA	Human leukocyte antigen
HMGB	High mobility group protein
HOMA	Homeostasis model assessment
IAA	Insulin auto antibody
IA-2	Tyrosine phosphatase-like protein
IAPP	Islet amyloid polypeptide
IFN	Interferon
IL	Interleukin
IL2RA	Interleukin-2 receptor alpha chain
ipGTT	Intraperitoneal glucose tolerance test
ITIM	Immunoreceptor tyrosine-based inhibition motif
ITAM	Immunoreceptor tyrosine-based activation motif

LPS	Lipopolysaccharide
MAG	Myelin-associated glycoprotein
MHC	Major Histocompatibility Complex
mRNA	Messenger ribonucleic acid
Nampt	Nicotinamide phosphoribosyltransferase
NAD	Nicotinamide adenine dinucleotide
Neu3	Neuraminidase 3
ND	Normal diet
NF-κB	Nuclear factor κB
NMN	Nicotinamide mononucleotide
NNT	Nicotinamide nucleotide transhydrogenase
NOD mouse	Non-Obese Diabetic Mouse
OVA	Ovalbumin
PBMC	Peripheral blood monocytes
pDC	Plasmacytoid dendritic cell
PET	Positron emission tomography
PC	Prohormone convertase
PP	Pancreatic polypeptide
PRPP	Phosphoribosylpyrophosphate
PTPN22	Protein tyrosine phosphatase non-receptor type 22
ROS	Reactive oxygen species
Siglec	Sialic acid binding immunoglobulin-like lectin
SOD	Superoxide dismutase
SPECT	Single-photon emission computed tomography
SPIO	Superparamagnetic iron oxide
ST8Sia I	α- 2,8-sialyltransferase
STZ	Streptozotocin
TNF	Tumor necrosis factor
T1D	Type 1 diabetes mellitus
T2D	Type 2 diabetes mellitus
VMAT	Vesicularmonoamine transporter
ZnT8	Zinc-transporter 8

1.1 Summary

Diabetes mellitus is one of the most challenging health problems of the 21st century, affecting 382 million people worldwide. It occurs when the pancreatic β-cells do not produce sufficient amounts of insulin, in Type 2 Diabetes accompanied by loss of glucose clearance by peripheral tissues due to insulin resistance, all together resulting in hyperglycemia. Insulin resistance is closely associated to obesity switch, in which adipocyte inflammation leads to altered secretion of so called adipocytokines, which in turn have influence on other tissues and the islet cells. A newly identified adipocytokine named Nampt was investigated during the first part of this work, together with its enzymatic product NMN, both essential players of intracellular NAD synthesis. Neither Nampt nor NMN showed any influence on cell survival and apoptosis in isolated human islets and did not alter insulin secretion during chronic exposure, but both potentiated insulin secretion if added acutely to high glucose concentrations. Therefore targeting the NAD synthesis could provide therapeutic strategies in the control of β-cell function.

Diabetes diagnostic, therapy and research would benefit from non-invasive accurate imaging of the functional β-cells *in vivo*. During my thesis we developed a strategy to monitor the functional β-cell mass by measuring Mn^{2+} uptake into β-cells by MRI. We were able to show Mn^{2+} signals correlating with functional *in vivo* tests in STZ and HFD induced diabetes mouse models, pointing to Mn^{2+} MRI as a useful tool to monitor functional β-cell mass *in vivo*.

Inflammation plays an important part in diabetes development, in insulin resistance as well as in β-cell destruction. One protein family that function as a modulator of the immune system, the Siglecs, was found to be expressed on human islet cells and Siglec-7 showed protective effects on diabetic milieu induced failure and apoptosis of human isolated islets. To see if mouse Siglecs display similar effects in the development of diabetes, we investigated their role in a Siglec-F knockout mouse model with HFD- or STZ-induced diabetes. FACS analyses revealed that mice, in contrast to humans, are not expressing Siglecs in endocrine cells, but in a very small cell population instead. Depletion of macrophages from isolated mouse islets decreased Siglec expression, indicating macrophages as the origin of Siglec signals. Due to the lacking expression, Siglec-F knockout did not influence blood glucose levels and *in vivo* and *in vitro* insulin secretion of diabetic mice compared to wildtype controls in STZ-experiments.

1.2 Zusammenfassung

Diabetes mellitus betrifft weltweit 382 Millionen Menschen und ist damit eine der größten Herausforderungen des 21. Jahrhunderts. Diabetes entsteht durch eine nicht ausreichende Insulinsekretion der β-Zellen des Pankreas, im Typ 2 Diabetes begleitet von der Insulinresistenz des peripheren Gewebes, was im Endeffekt zu Hyperglykämie führt. Insulinresistenz ist eng mit Fettleibigkeit assoziiert, während der Adipozyten entzündungsbedingt ihre Sekretion von sogenannten Adipozytokinen verändern und damit auch andere Gewebe wie die β-Zelle beeinflussen. Während meiner Arbeit habe ich ein neu identifiziertes Adipozytokin namens Nampt und dessen Produkt NMN untersucht, die beide essentielle Bestandteile der intrazellulären NAD Synthese sind. Bei chronischer Behandlung zeigten beide keinen Einfluss auf Zellviabilität, Apoptose und Insulinsekretion. Allerdings potenzierten sowohl Nampt als auch NMN die Insulinsekretion, wenn die Inkubation nur kurze Zeit zusammen mit erhöhter Glukosekonzentration durchgeführt wurde. Dieses Ergebnis zeigt, dass die NAD Synthese ein potenzieller Therapie Ansatzpunkt für die Steigerung der β-Zellaktivität sein kann.

Die Diagnostik, Therapie und Erforschung von Diabetes würde sehr von einer genauen Bildgebung der funktionalen β-Zellmasse *in vivo* profitieren. Während dieser Arbeit haben wir eine MRT Messung zur Darstellung der funktionalen β-Zellmasse durch Mn^{2+} Aufnahme entwickelt. Wir konnten zeigen, dass die gemessenen Mn^{2+} Signale mit funktionalen *in vivo* Tests übereinstimmten und so die besondere Eignung von Mn^{2+} basierten MRT Messungen zur Bestimmung der funktionalen β-Zellmasse herausstellen.

Entzündungsprozesse spielen sowohl in Insulinresistenz, als auch bei der Zerstörung von β-Zellen eine wichtige Rolle. Die Siglecs, eine Proteinfamilie die Antworten des Immunsystems reguliert, werden zellspezifisch in Inselzellen exprimiert. Unter diabetischen Bedingungen schützt Siglec-7 die β-Zelle und ihre Funktion in isolierten humanen Inseln. Die Untersuchung von, durch STZ- und HFD- induzierten diabetischen Mäusen sollte zeigen, ob Maus Siglecs ähnliche Effekte in der Diabetesentwicklung aufweisen. FACS Analysen zeigten, dass Mäuse, im Gegensatz zum Menschen, Siglecs nur in einer sehr geringen Zellpopulation exprimieren, nicht in endokrinen Zellen. Die Entfernung von Makrophagen aus isolierten Maus Inseln verminderte gleichzeitig auch die vorhandene Siglec Expression und weißt damit auf die Makrophagen als Siglec Quelle hin. Durch die fehlende Expression hatte der

knockout von Siglec-F *in vivo* und *in vitro* keinen Einfluss auf die Blutzuckerwerte in diabetischen Mäusen im STZ-Tiermodell.

2. Introduction

2.1 The pancreatic islet of Langerhans and glucose homeostasis

The pancreas is a glandular organ, located in the abdominal cavity behind the stomach. It is around 12,5 to 15 cm long and its weight varies from 60 to 100 mg. The pancreas secrets digestive enzymes into the small intestine, the so called pancreatic juice[1]. Besides its exocrine secretion it shows also an endocrine function. The endocrine part, the islets of Langerhans, represents only 1% of the total pancreas mass[2] and can be subdivided into five cell types depending on their secretory products insulin (β-cells), glucagon (α-cells), somatostatin (δ-cells), ghrelin (ε-cells) and pancreatic polypeptide (PP-cells)[3-5].

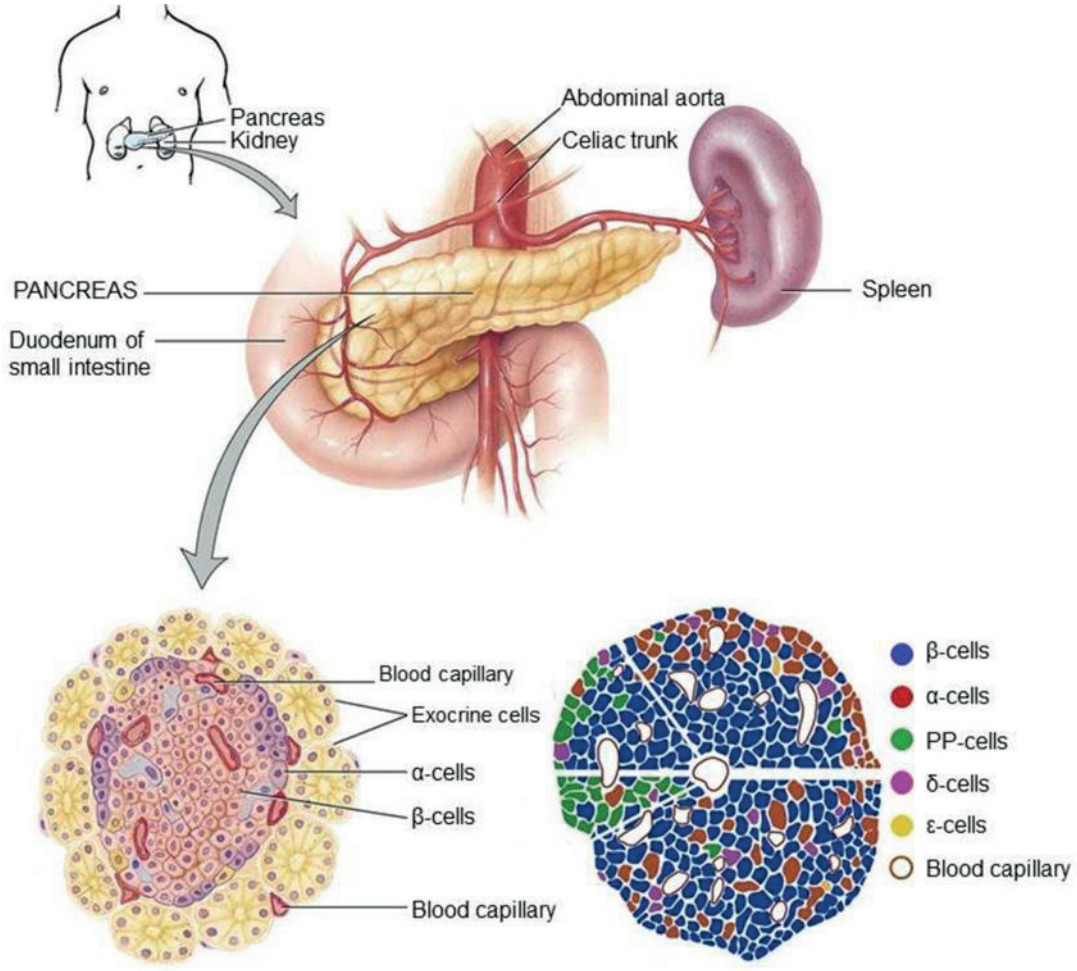

Figure 1: Anatomy and physiology of the pancreas and the islets of Langerhans
The pancreas sits across the back of the abdomen, behind the stomach. The head of the pancreas is on the right side of the abdomen and is connected to the duodenum. The islets of Langerhans are cell clusters within the pancreas, surrounded by exocrine cells. Islets consists of α-cells secreting glucagon, β-cells secreting insulin, δ-cells secreting somatostatin, ε-cells secreting ghrelin and PP-cells secreting pancreatic polypeptide. (modified from [6,7])

β-cells represent the majority of islet cells with around 50-80%. They release insulin upon stimuli like elevated blood glucose levels. Insulin leads to glucose uptake in peripheral tissues and inhibits glycogenolysis, all together leading to dropping blood sugar levels. Glucagon, secreted by α-cells, is the counterpart of insulin. It is secreted in the case of low blood glucose levels and induces glycogenolysis and gluconeogenesis in hepatic cells to restore normal blood glucose levels[8]. Somatostatin is secreted by around 5% of the islet cells, the δ-cells, and upon secretion it suppresses the release of several neuronal, gastrointestinal and pancreatic hormones, especially insulin and glucagon[9]. Ghrelin is secreted by ε-cells and plays a role in hunger stimulation. Pancreatic polypeptide acts mainly towards suppression of food intake, gastric emptying and increases energy expenditure[10].

2.1.1 Insulin

Insulin is synthesized as a single-chain 86-amino-acid precursor polypeptide named preproinsulin. Cleavage by proteolytic enzymes leads to proinsulin, consisting of A-, B- and C-chain. Conversion of proinsulin to insulin continues in maturing granules through the action of prohormone convertase 2 and 3 and carboxy peptidase H by cleavage of an internal 31-amino-acid residue fragment. This generates the C-peptide and the A- (21 amino acids) and B- (30 amino acids) chains of insulin, which are connected by disulfide bonds. C-peptide and insulin are stored in secretory granules and released together[11]. The key regulator for insulin release is glucose, although amino acids, ketones, various nutrients, gastrointestinal peptides, and neurotransmitters also influence insulin secretion[11,12]. Glucose is taken up through the glucose-transporter (GLUT), is getting phosphorylated by glucokinase and further metabolism generates adenosine triphosphate (ATP). The rise in ATP concentration results in closure of K_{ATP} channels leading to membrane depolarization, opening of voltage-gated Ca^{2+} channels followed by Ca^{2+} influx and exocytosis of insulin granules[12,13].

On its target cells insulin binds to its receptor and stimulates intrinsic tyrosine kinase activity, leading to receptor autophosphorylation and recruitment of intracellular signaling molecules. This initiates a complex cascade of intracellular reactions resulting in metabolic and mitogenic effects, for example translocation of GLUT4 to the cell surface, glycogen synthesis, protein synthesis, lipogenesis or regulation of various genes[12].

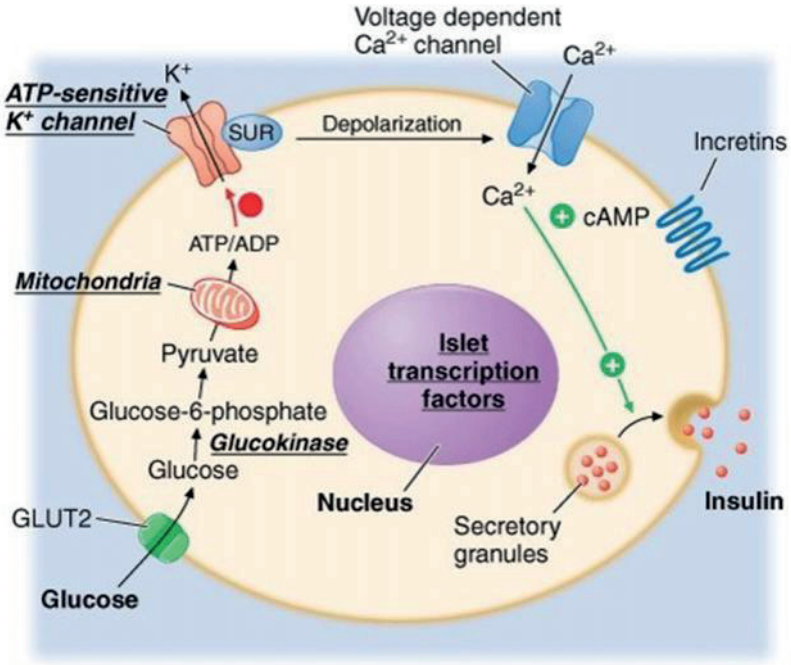

Figure 2: Mechanism of insulin secretion in β-cells
Glucose enters the cell via GLUT2 and gets further metabolized. This leads to elevated intracellular ATP levels, which in turn leads to closure of K^+ channels. This is accompanied by membrane depolarization and Ca^{2+} influx, resulting in exocytotic release of insulin from storage granules. (adapted from [12])

2.1.2 Glucagon

Mammalians express proglucagon as an 18 kDa protein containing three homologous hormonal sequences: glucagon, glucagon-like peptide 1 (GLP1), and glucagon-like peptide 2 (GLP2), separated by two intervening peptides, IP-1 and IP-2, and preceded by an N-terminal extension called glicentin-related polypeptide (GRPP)[14]. This peptide is expressed in the α-cells in the islets of Langerhans and in the endocrine L-cells of the intestinal mucosa and different processing results in formation of different peptides. α-cells express high levels of prohormone convertase (PC) 2, which processes proglucagon to glucagon, whereas the intestinal L-cells express PC3 that processes GLP1, an insulinotropic hormone[14,15]. α-cells secrete glucagon upon dropping blood glucose levels, whether inhibition during high glucose levels is directly by glucose or by paracrine mechanisms is under debate[8]. Gamma-aminobutyric acid (GABA)[16], Zn^{2+}, somatostatin[17] and insulin[18] are paracrine stimulators that contribute to the regulation of glucagon release[19,20]. Glucagon acts mainly on the liver, where it binds to its receptor and stimulates glycogenolysis and gluconeogenesis and inhibits glycolysis, leading to increased hepatic glucose output[8]. Its action is mediated by the activation of adenylyl cyclase and the PKA pathway mainly by the upregulation of glucose-6-phosphatase and phosphoenolpyruvate carboxykinase[8].

2.2 Diabetes

Diabetes mellitus is a multifactorial disease and one of the most challenging health problems in the 21st century. 382 million people worldwide suffer from diabetes[21] and till 2030 it is considered to be the 7th leading cause of death[22]. Diabetes is a metabolic syndrome that occurs, if the body is not producing enough insulin or cannot use it effectively, which leads to hyperglycemia. The elevated circulating glucose levels damage tissues with time, this can lead to cardiovascular disease, blindness, kidney failure, and lower-limb amputation[21]. Diabetes can be divided into different forms. Type 1 Diabetes mellitus (T1D) is an autoimmune reaction, in which the immune system destroys the insulin producing β-cells in the pancreas, causing absolute insulin deficiency. These patients need artificial insulin every day for the rest of their life to control their blood glucose levels and live a normal life. T1D is usually diagnosed in children or young adults, but can affect every age group[21].

With around 85% to 95% of all diabetes cases Type 2 Diabetes mellitus (T2D) is the most common one. T2D is a combination of insufficient amounts of produced insulin and peripheral tissue insulin-resistance. It is normally diagnosed in adults and many people live with undiagnosed T2D till the consequences of the illness take place. The majority of the T2D-patiens can live without extra insulin administration and control their disease by a change of lifestyle and additional medications[21].

2.2.1 Type 1 Diabetes mellitus

Genetic predisposition and different environmental factors can lead to autoimmune destruction of pancreatic β-cells and cause Type 1 Diabetes mellitus[23]. Several gene loci have been identified, that are increasing the risk to develop T1D, like human leukocyte antigen (HLA), the insulin gene, protein tyrosine phosphatase non-receptor type 22 (PTPN22), interleukin-2 receptor alpha chain (IL2RA) and cytotoxic T-lymphocyte antigen 4 (CTLA-4)[24]. Circulating antibodies against β-cell antigens are detectable already months or years before the onset of diabetes and can be used as markers for diabetic risk. The most common auto-antibodies are directed against glutamic acid decarboxylase (GAD65), tyrosine phosphatase-like protein (IA-2) and insulin (IAA) and zinc-transporter 8 (ZnT8)[23]. Not all antibody positive individuals develop diabetes and concordance in monozygotic twins, who share the genetic predisposition, is only 50%, indicating the importance of a number of environmental

factors[23,25]. Putative factors are viral infection, dietary factors (e.g. cow milk), vaccination and toxins, but definitive proof is lacking for any of them[23,26].

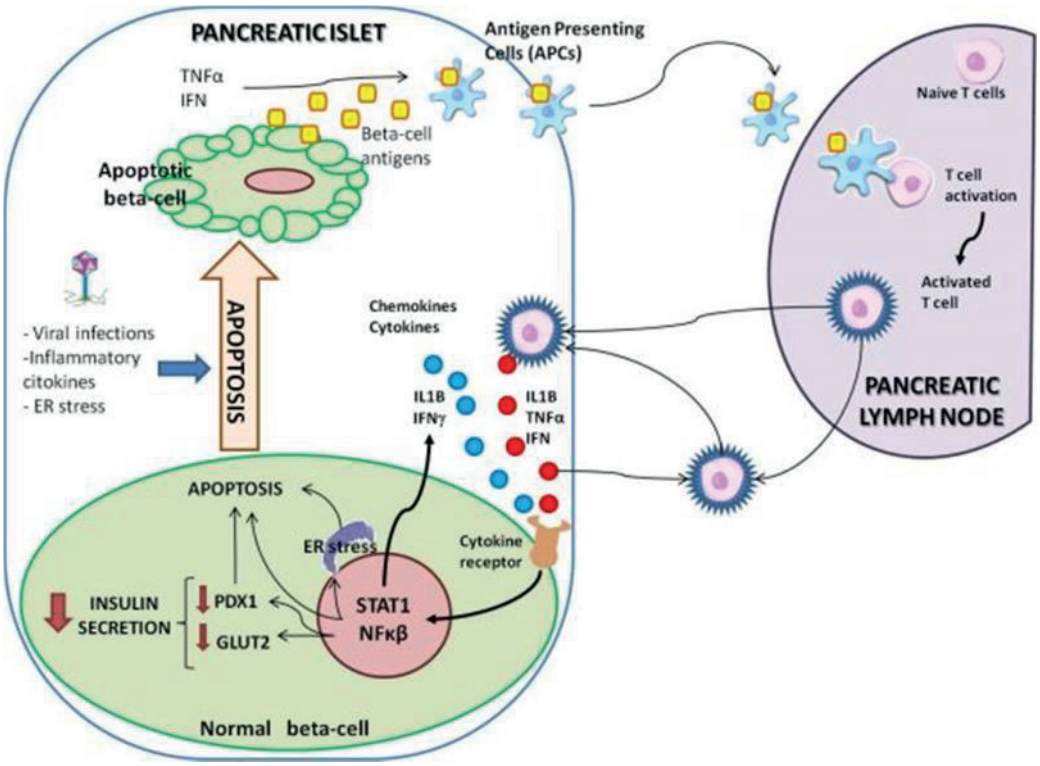

Figure 3: Cellular mechanisms of β-cell death Necrotic β-cells may release β-cell antigens, which lead to activation of antigen presenting cells. These in turn activate naive T-cells which migrate in the pancreas and release inflammatory factors back in the islets. Inflammatory cytokines lead to insufficient insulin production and secretion. Activation of transcription factors NFκB and STAT-1 trigger ER stress, apoptotic processes and β-cell release of cytokines, even amplifying the autoimmune attack. (adapted from [27])

Most data concerning T1D progression were derived from rodent models like the NOD mouse, but there is indication that it is closely related to the human disease[24]. Clinical symptoms develop late, after the loss of around 70% of the β-cell population. Loss of β-cells in human and mouse is due to apoptosis, mediated by infiltrating immune cells[23]. Cytotoxic T-cells get activated in response to cells presenting β-cell antigens and migrate into the islets of Langerhans. The activated T-cells can directly kill the β-cell through perforin or Fas/Fas ligand (FasL) interactions, secrete soluble mediators that induce β-cell death or activate macrophages[28].

Till now, the only treatment available for T1D patients consists of lifelong exogenous administration of human recombinant insulin. Alternatively therapeutic strategies are

whole pancreas- or only islet transplantation, but both require lifelong immunosuppression, and due to the limited availability of islets only few patients benefits from this techniques. To overcome the limitation some research is concentrating on Xenotransplantation, using porcine islets for transplantation, or stem cell derived β-cells[29].

Another idea for the treatment of early onset T1D is the inhibition of the immunsystem activation by antibodies. CD3 is required for T-cell activation and first clinical trials show improvement in stimulated C-peptide responses and reduced need for exogenous insulin[30]. T-cell activation requires also co-stimulatory stimulus, delivered through CD28 signaling after binding to CD80 and CD86 on antigen presenting cells. Blocking of this signaling by soluble T-cell receptors that bind to CD80 and CD86, is preventing their interaction with CD28 and led to higher C-peptide response[31]. Also antibodies against CD20, a B-cell specific antigen, reduced the decline in β-cell function[32]. Immunization of NOD mice with typical autoantigens like GAD65, insulin or plasmid DNA encoding mouse proinsulin II alone protected them from the development of diabetes, but clinical trials were not able to show the same effect in humans[32,33].

2.2.2 Type 2 Diabetes mellitus

Type 2 is the most common form of diabetes and the number of people with T2D is growing rapidly worldwide[22]. Patients β-cells are still producing insulin, but not enough to overcome insulin resistance in peripheral tissues (predominantly muscle, fat and liver) resulting from obesity, physical inactivity and genetic predisposition[34]. However, only 20% of those people with severe insulin resistance become diabetic, the other 80% are able to compensate by higher insulin secretion[35] and higher β-cell mass[36] to maintain near-normal blood glucose levels[37]. During the first phase of T2D progression insulin secretion increases to overcome insulin resistance in peripheral tissues[38]. The second phase can last for years and is characterized by loss of the compensatory effect of the β-cells due to a decline of β-cell mass and therefore increasing blood glucose levels. At some critical point β-cell mass becomes inadequate due to increased apoptosis[39] and glucose level rises in a short period of time (period three) to stage four, the definite diabetes. Normally, patients in this phase still produce enough insulin to not progress to ketoacidosis and hold this status for their entire lifespan. Patients with severe β-cell loss, ketoacidosis and true

dependence on insulin for survival are mainly found in T1D[38]. T2D is normally diagnosed when continuous high blood sugar levels have already damaged the body and the complications of diabetes occur. β-cell mass is reduced up to 50% in T2 diabetic patients[40], but mostly the disease can still be reversed with exercise and weight reduction[41].

Because most insulin resistant individuals are not developing diabetes, maintenance of functional β-cells is the crucial part. The main reason for decrease in β-cell mass is apoptosis induced by different stimuli like elevated glucose levels, free fatty acids, islet amyloid polypeptide (IAPP) and cytokines[42]. Under normal conditions glucose is an important compound for β-cells and induces ATP production, insulin secretion and proliferation. Chronically elevated glucose levels act toxic to the β-cell, the so called glucotoxicity[43], leading to overstimulation of the β-cells till the cells insulin biosynthesis is insufficient to meet the high insulin demand to maintain normoglycemia[44]. The highly adapted demand in protein production leads to endoplasmatic reticulum (ER) stress, which results in production of reactive oxygen species (ROS)[42,45]. β-cells exhibit only poor DNA repair capacity and low expression of the antioxidant enzymes superoxide dismutase 1 and 2 (SOD1-2), glutathione peroxidase 1 (GPX1) and catalase (CAT) and are therefore prone to oxidative stress[44,45]. ER stress is even worse in combination with elevated saturated fatty acid levels like palmitate[45]. Proinflammatory cytokines and chemokines released by adipose tissue and immune cells under hyperglycemic conditions contribute to the inflammatory process in pancreatic islets, too, leading to macrophage islet infiltration and increased IL1β production[44].

2.2.3 Insulin resistance

Chronic insulin resistance is characteristic for T2D and one of the defining clinical features for the metabolic syndrome, but diabetes develops only in combination with failure of insulin production in β-cells. Insulin resistance in muscle results in decreased glucose disposal whereas it leads to elevated glucose production in the liver. In adipose tissue it leads to increase in free fatty acid release from adipocytes and circulating free fatty acids are worsening insulin resistance in skeletal muscle, by inhibition of pyruvate dehydrogenase, or directly activate proinflammatory response [46,47]. Obesity and the concomitant development of inflammation are major components of insulin resistance. Inflammation in adipocytes due to hypertrophy,

hyperplasia and hypoxia leads to the release of cytokines, chemokines, adipocytokines and other proinflammatory signals[48]. This attracts pro-inflammatory macrophages into the adipose tissue, further activating the inflammatory response. Hepatic inflammation in obesity is triggered by fatty liver disease and increased stress pathway response and leads to inhibition of glycogenolysis and gluconeogenesis[46,47].

2.3 Adipokines

Adipose tissue secrets more than 600 peptides and hormones, collectively called adipokines or adipocytokines[49], among them leptin, adiponectin, resistin and several cytokines like tumor necrosis factor α (TNFα), interleukin 1β (IL1β) and interleukin 6 (IL6)[50]. In adipose tissue they contribute to immune cell migration, metabolism and function. They modulate processes in the whole body including brain, liver, vasculature, heart and pancreatic β-cells[49]. In obesity, adipose tissue depots are enlarged, leading to dysregulation of adipokine secretion.

The first adipokine that was associated with pancreatic effects is leptin, which is acting on satiety center of the hypothalamus to restrict food intake and enhance energy expenditure. Humans and rodents that lack a functional leptin protein manifests voracious feeding and obesity and leptin treatment is reversing this abnormalities[51]. Typical animal models used for obesity and type 2 diabetes are the *ob/ob* mice, that lack the leptin protein or the *db/db* mice that display deficient leptin receptor activity[52]. β-cells express the leptin receptor that allows the protein to act directly on the cells. Surprisingly, the majority of obese human individuals exhibit higher circulating concentration of leptin than normal weight individuals, but this elevated level fail to modulate weight due to leptin resistance[53]. Different factors are involved in leptin resistance development, like impaired leptin transport in the blood–brain barrier, endoplasmic reticulum stress, and impaired leptin signaling[54]. In β-cells, leptin has an inhibitory effect on insulin secretion and reduces preproinsulin gene expression[50,51]. In addition, leptin was found to affect proliferation, apoptosis and cell size depending on the studied model[54].

Another well-established adipokine is adiponectin, which in opposite to leptin shows negative correlation with the body mass index[50]. Mice lacking functional adiponectin or its receptors develop insulin resistance, while extra adiponectin administration shows insulin-sensitizing properties[51]. In liver and muscle, adiponectin is enhancing

energy consumption and fatty acid oxidation, even improving insulin sensitivity. Expression of adiponectin receptors was found on primary and clonal β-cellsand upon binding adiponectin exhibits beneficial effects on apoptosis and proliferation, whereas its effect on insulin secretion is still under debate[50].

2.3.1 Nampt and NMN

Nicotinamide phosphoribosyltransferase (Nampt or visfatin) is expressed in many cells and tissues and has been identified as an adipokine with enzymatic function in synthesizing nicotinamide mononucleotide (NMN) from nicotinamide and phosphoribosylpyrophosphate (PRPP)[49]. NMN is a key intermediate for the synthesis of nicotinamide adenine dinucleotide (NAD), which is in turn essential for the function of pancreatic β-cells. Nampt exists in an intracellular (iNampt) and extracellular (eNampt) form and eNampt exhibits higher NAD biosynthetic activity compared to iNampt[55]. It is the rate limiting component of NAD biosynthesis[56] and Nampt-deficient heterozygous mice show impaired glucose tolerance and reduced insulin secretion that was reversed by additional administration of NMN[55,57]. Additionally some studies showed Nampt acting like a cytokine and taking part in proinflammatory immune responses[58] as well as anti-apoptotic effects[59]. Circulating eNampt levels are elevated in T2D patients and significantly correlated with markers of insulin resistance like fasted plasma glucose and HOMA-index[60]. iNAMPT and NAD levels in tissues are reduced by HFD feeding and ageing, contributing to the pathogenesis of T2D[57]. A recent study suggests positive effects for Nampt in preserving β-cell mass by stimulating proliferation and inhibition of apoptosis[59]. Because iNampt expression is altered in T2D and its absence contributed to glucose tolerance and insulin secretion, we investigated, whether Nampt or its product NMN directly influence β-cell survival and function.

2.4 β-cell imaging

T1D and T2D are associated with a functional loss of β-cell mass and therefore preserving β-cell mass is the main focus to cure diabetes. Our current knowledge about β-cell mass in normal and diabetic patients relies mainly on autopsy data, therefore a noninvasive *in vivo* quantification of β-cell mass would be an important tool to monitor the natural course of β-cell mass and the efficiency of novel antidiabetic therapies. Till now T2D is diagnosed when β-cells already fail, but early

diagnosis of changes in β-cell mass and early treatment strategies could already rescue these patients from the development of diabetes.

Positron emission tomography (PET), single-photon emission computed tomography (SPECT) and magnetic resonance imaging (MRI) are methods allowing noninvasive *in vivo* imaging of β-cells. Imaging the pancreatic islets *in vivo* is challenging due to their small size (100–400 µm in diameter) and their high dispersion throughout the pancreas (only 2% of the total mass)[61]. PET and SPECT are highly sensitive, but depend on high specific radioactive agents and provide only low spatial resolution, at best in the millimeter range, which makes its use crucial for the detection of the small islets of Langerhans. Compared to PET and SPECT, MRI provides higher spatial resolution, enhanced soft tissue contrast, unlimited depth penetration and its lower sensitivity can be overcome by specific agents providing high contrast in MRI[62].

Despite the techniques for in vivo detection of islets, the choice of a specific labeling agent remains crucial. Radioactive ligands like radiolabeled dihydrotetrabenazine (DTBZ) were shown to visualize β-cells in PET and SPECT[63,64] and preclinical studies with ^{11}C-DTBZ in diabetic rodents showed lower pancreatic radiotracer activity in diabetic rodents compared to nondiabetic animals[65,66]. Contrary other studies showed, that the vesicularmonoamine transporter 2 (VMAT2), the target of DTBZ, is also expressed in PP-cells and that not all β-cells express this transporter[67,68]. This reduces the quantification potential of PET imaging of β-cell mass by targeting VMAT2, but there are a lot of other potential probes for β-cell labeling[69]. Radiolabeled antibodies against β-cell specific proteins or lipids are an additional idea for imaging probes for PET, but the large immunoglobulin size leads to slow clearance from the blood resulting in low radioactive ratios in the pancreas compared to vessels[62,70]. To overcome this limitations radiolabeled single-chain antibodies were developed, which showed a linear correlation between β-cell mass and probe accumulation[71]. D-mannoheptulose is transported into isolated islets and was thought to provide a new agent for β-cell imaging[72], but it inhibits insulin secretion and increases the blood glucose level, which makes it useless for the application in patients with diabetes[73]. Other promising targets are radiolabeled Exendin-3 and -4, which are binding to the GLP1 receptor. This receptor is enriched in β-cells and studies showed colocalization of Exendins and β-cells[74,75]. But earlier studies indicate that chronic hyperglycemia leads to decreasing receptor levels in rats and humans, which implies underestimation of β-cell mass in diabetes[76].

MRI is not dependent on radiolabeled ligands, but still needs contrast agents for higher contrast. Paramagnetic gadolinium based agents have been used to monitor transplanted islets[77], but prolonged presence of gadolinium in the body is detrimental to human health, which is limiting its clinical use in patients[78]. Superparamagnetic iron oxide (SPIO) nanoparticles with dextran-coated iron oxide cores were also used for labeling β-cells before transplantation and allowed detection after several days without inhibitory effects on function but the clinical use of this method is still immature[79-81]. These methods allow the measurement of β-cell mass, but not of β-cell function. Mn^{2+} is a very promising T_1 contrast agent. There is Ca^{2+} influx upon glucose stimulation of β-cells and during this progress Mn^{2+} enters the cell, resulting in higher MRI signals[82] after glucose stimulation. Time-dependent changes in pancreas signal intensity after intravenous administration of glucose or saline to normal and diabetic mice were already reported[83], indicating Mn^{2+}-enhanced MRI imaging as a promising tool in functional β-cell mass measurement.

Imaging *in vivo* β-cell mass is a promising tool to monitor diabetes onset and progression. One of the leading causes for diabetes is inflammation, influencing adipocytokine production as well as β-cell function and survival. The inflammatory signaling and activation of immune cells are caused by secreted stimulators or via cell-cell interactions. A protein family called Siglecs (sialic acid-binding immunoglobulin (Ig)-like lectins) exhibit an extracellular binding domain, as well as intracellular signaling motifs and mediate such interactions in the immune system. Therefore we hypothesized an involvement of this modulating protein family in inflammatory responses during the progression of diabetes.

2.5 Sialic acid binding immunoglobulin-like lectins (Siglecs)

Most animal cells are coated with a variety of glycan chains with different roles in cell–cell communication, adhesion, membrane structure and cellular signaling[84]. Sialic acids are acidic sugars with a nine-carbon backbone and represent the most common sugar residue in the periphery of many glycans. This exposed location makes them well-suited for recognition by molecules, leading to the development of alone 50 different sialic acids in deuterostomes[84]. In vertebrate, Siglecs are the largest known family of lectins that recognize sialic acid-containing glycans. They are type I transmembrane surface proteins with an amino-terminal V-set immunoglobulin

domain that binds to sialic acid containing glycans. Proximal to the V-set domain Siglecs consists of a number of C2-set immunoglobulin domains, varying from one to sixteen[85,86]. They can be divided into two subgroups, based on their sequence similarity and evolutionary conservation. Siglec-1 (also known as Sialoadhesin or CD 169), Siglec-2 (also known as CD22), Siglec-4 (also known as myelin-associated glycoprotein, MAG) and Siglec-15 are distantly related (25-30% identity) and have clear orthologues in all mammalian species. The other group are the Siglec-3 or CD33-related Siglecs. They share 50-99% identity and are still evolving by gene duplication, exon shuffling, exon loss and gene conversion, which leads to important differences in CD33-related Siglecs among mammalian species. CD33 related Siglecs in human are numbered (e.g. Siglecs -3, -5, -6, -7, -8, -9, -10, -11, -12 and -14), while the murine CD33-related are lettered (Siglecs –E, -F, -G and –H).

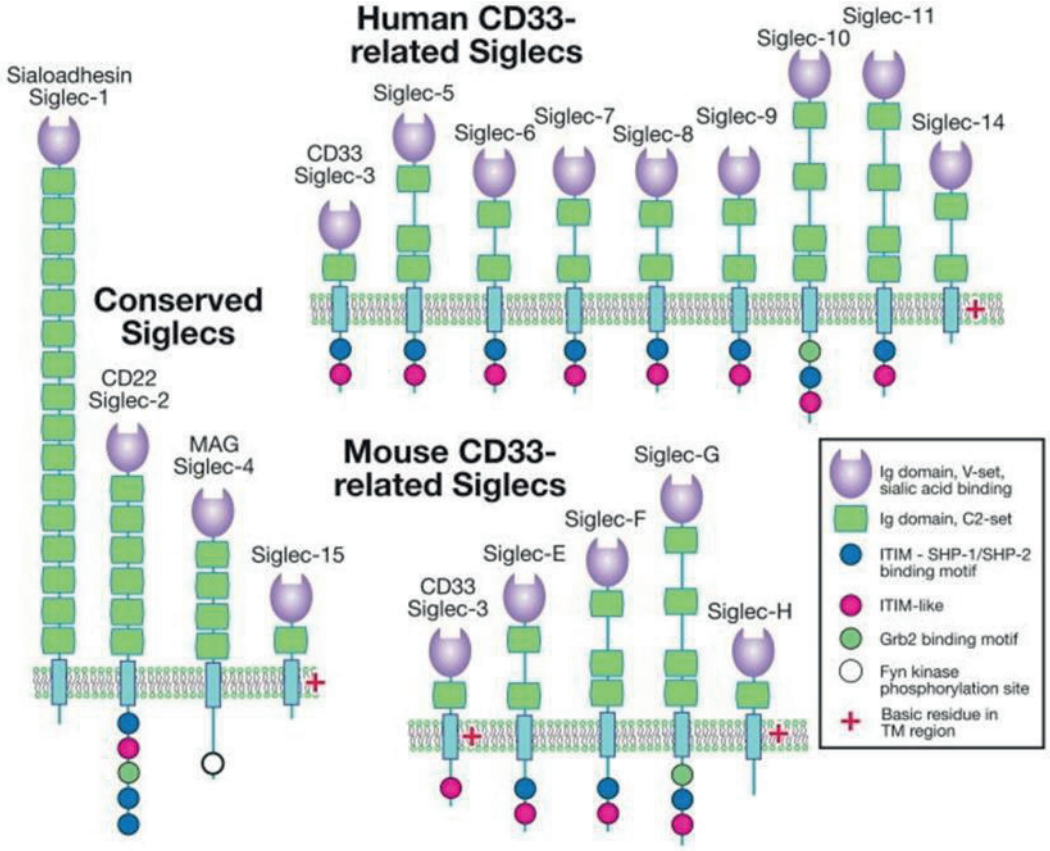

Figure 4: Domain structure of the known Siglecs in human and mice
There are two subgroups of Siglecs: One in mammals conserved group containing sialoadhesin (Siglec-1), CD22 (Siglec-2), MAG (Siglec-4) and Siglec-15. The other group contains CD33-related Siglecs, human Siglec-3, -5, -6, -7, -8, -9, -10, -11 and -14 and mouse Siglec-3, -E, -F, -G and -H. In humans, Siglec-12 has lost its arginine residue required for sialic acid binding and Siglec-13 is deleted. The plus sign indicates the presence of a charged residue in the transmembrane domain, which has been shown to interact with the adaptor protein DAP12. (adapted from[87])

Besides the discrimination of their evolutionary conservation, Siglecs can be divided into three groups based on their cytoplasmatic tails. Siglec-1 and -4 are lacking any inhibitors motifs in their cytoplasmatic tails providing most probably a pure adhesion function. Most Siglecs belong to group two, which display inhibitory function by their intracellular immunoreceptor tyrosine-based inhibition motifs (ITIMs) (mouse Siglecs-2, -E, -F and –G and human Siglecs -2, -3, -5, -6, -7, -8, -9, -10 and -11). The remaining Siglecs (mouse Siglec-3, -15 and –H and human Siglec-14 and -15) contain a positively charged region in their tail which can associate with a disulfide-linked homodimer of DAP12 (DNAX activation protein of 12 kDa), which in turn contains an immunoreceptor tyrosine-based activation motif (ITAM)[88].

Because CD33- related Siglecs are evolving quickly and developed different numbers in between species, it is hard to find real paralogues for mice and human. In humans it is clear that several Siglecs arise from gene duplication, like the Siglecs -7, -8 and -9, but in respect to sequence homology only mouse Siglec-E is similar[89,90]. Only Siglec-7 and -9 have a similar expression pattern and Siglec-E exhibits combined features of Siglecs-7 and -9[90,91]. Also human Siglecs-10 and -11 arose from gene duplication, but display different ligand binding profiles[92] and only Siglec-10 has a clear orthologue in mice, Siglec-G[93]. While Siglec-10 is broadly expressed in B-cells, eosinophils, monocytes and a subpopulation of natural killer cells[94], Siglec-G expression is restricted to B-cells[95]. Siglec-H lacks ITIM-like motifs and depends on the presence of the ITAM-containing adaptor protein DAP12. It is expressed predominantly on plasmacytoid dendritic cell (pDC) precursors[96] and has no orthologue in man.

Siglecs are expressed in a highly cell-type-restricted pattern, sialoadhesin for example is a macrophage specific adhesion molecule and CD22 is a well characterized B-cell inhibitory receptor[85,86,88]. In mice CD33 is mainly expressed in granulocytes, Siglec-E in neutrophils, monocytes and conventional dendritic cells, Siglec-F is primarily expressed in eosinophils, Siglec-G in B-cells and some dendritic cells and Siglec-H is primarily expressed in plasmacytoid dendritic cells[88]. Despite Siglec-4 (expressed in cells of the nervous system) and Siglec-6 (on placental trophoblasts), Siglecs are mainly expressed on cells of the innate immune system in a highly cell-type-restricted pattern and display a lot of different functions there[88,97]. Sialoadhesin is a macrophage specific adhesion molecule that has been shown to participate in the phagocytosis of pathogens. It binds to its ligand on other cells

(trans-interaction) and leads to internalization of *Neisseria meningitides*[98], *Trypanosoma cruzi*[99] and porcine respiratory and reproductive syndrome virus[100]. Siglec-5 is also able to promote *Neisseria meningitides* phagocytosis[98], but because Siglec-5 is mainly bound to ligands on the same cell (cis-interaction) is has been shown to participate in endocytosis and this was also shown for Siglecs-2, -7, -9 and -F[101].

Cell death or damage results in the release of damage associated molecular patterns (DAMPs) like HMGB1 (high mobility group protein B1). HMGB1 can associate with the sialoglycoprotein CD24 and this complex interferes with Siglec-10 and Siglec-G in mice, leading to reduced NF-κB activation and thereby controlling inflammation in the context of tissue damage[102]. Murine plasmacytoid dendritic cells (pDC) can be divided into two groups, one is expressing only low levels of Siglec-H and secretes large amounts of type I interferon, whereas the other group exhibits higher levels of Siglec-H and remarkably lower levels of type I interferons[103]. This is in contrast with the predicted activating effects of Siglec-H by DAP12, but was confirmed by anti-Siglec-H antibodies inhibiting IFN-α production[104]. In contrast Siglec-14 promotes activating effects upon overexpression, leading to enhanced TNF-α production[105]. Sialoadhesin expression is induced in human monocyte-derived dendritic cells that have been exposed to rhinoviruses and this DCs are stimulating T-cells[106]. On the other hand, Siglec-7 expression declines after LPS stimulation on immature DCs[107].

Siglecs seem to have also regulatory function on immune responses. Siglec-E expression can be induced on macrophages by ligands for TLR2, 4, 7 and 9 and is than attenuating NF-κB activation and TNF and IL1 secretion[108]. Upregulation of pro-inflammatory cytokines by LPS were also observed for the overexpression of Siglec-9 in a macrophage cell line. In parallel, the anti-inflammatory cytokine IL10 was strongly induced upon Siglec-9 overexpression[109].

2.5.1 Siglecs and diabetes

Assuming Siglecs as possible modulators of inflammatory responses, we wanted to investigate their expression on islet infiltrating macrophages in diabetes development and their possible protective role by downregulation of pro-inflammatory cytokines. Previous work in our lab showed unexpected expression of Siglecs not only on macrophages, but also and more importantly on the islet cells themselves. They are expressed in a cell type specific manner, Siglecs -1, -2, -7 and -10 in β-cells, Siglecs

-3, -5 and -8 in α-cells[110]. Expression levels changed with diabetes in opposite directions. While the β-cell Siglecs -7 and 10 were significantly down regulated in T2 diabetic pancreas samples obtained from autopsy, the α-cell Siglec-3 was upregulated compared to healthy control individuals. In opposite to Siglec-7 protein, its ligands showed clear upregulation in T2D in α- and β-cells, providing a possible mechanism of intercellular crosstalk. Overexpression of Siglec-7 in healthy and T2D islets improved GSIS, reduced apoptosis and diminished IL1β and IL6 secretion under diabetogenic conditions. T2D islets and islets treated with diabetogenic conditions induced peripheral blood monocytes (PBMCs) migration, which was diminished upon restoration of Siglec-7 in these islets. In contrary silencing of Siglec-7 in islets reduced insulin release. Protective effects of Siglec-7 were due to diminished IκBα and p65 phosphorylation, leading to reduced NFκB activation and subsequent cytokine production[110].

Besides its differential expression in diabetes in islets, Siglec-7 expression in PBMCs changed with their activation profile. Activation by Lipopolysaccharide (LPS) or a high glucose and palmitate mixture led to activation of PBMCs was accompanied by loss of Siglec-7 expression[110].

These findings suggest that Siglecs do not only modulate immune responses of the immune system, it appears that they can also influence β-cell survival. Previous studies were done *in vitro*, to investigate the Siglecs role in diabetes development *in vivo* we started our research in a Siglec knockout mouse model. Because Siglec-7, that was investigated in humans so far, lacks a functional paralogue in mice, we decided to go for a Siglec-F knockout model. Since Siglec-F is already known to participate in immune responses in airway inflammation and chronic inflammation is important in T1D and T2D, Siglec-Fs participation in STZ- and HFD- induced diabetes mellitus was investigated.

2.5.2 Siglec-F

Siglec-F appears to be the most closely related functional paralog of human Siglec-8, but it is expressed on many other cell types[86]. Siglec-F, like Siglec-8, has a cytoplasmic ITIM-like motif and is recognizing the ligand 6′-sulfated sialyl Lewis X or sialyl Lewis X in which the penultimate galactose is sulfated in the 6 position (NeuAcα2-3Galβ1-4(Fucα1-3)(6-O-sulfo)GlcNAc)[111]. It was initially identified in immature cells of the myelomonocytic lineage and in a subset of CD11b-positive

cells[112] and Siglec-F mRNA was also found in mouse eosinophils[113]. This was quiet unexpected, because Siglec-F sequence is relative similar to that of human Siglec-5, which is not expressed by eosinophils, but Siglec-F expression was confirmed later on[90,111]. Further studies showed Siglec-F expression on alveolar macrophages, some T-cells and weakly on neutrophils[114,115], but not on mouse mast cells, like human Siglec-8 is[116]. Ovalbumin (OVA) induced lung inflammation leads to upregulation of Siglec-F on blood and bone marrow eosinophils together with the upregulation of Siglec-F ligands in lung tissue[117]. Crosslinking of Siglec-F by antibodies leads to increased apoptosis in eosinophils *in vivo* and *in vitro*[118,119], hinting to a Siglec-F dependent feedback loop controlling allergic responses. Administration of a specific Siglec-F antibody also reduced numbers of eosinophils in OVA induced eosinophilic gastrointestinal diseases and eosinophilic esophagitis, but these studies did not observe changes in apoptosis[120,121]. Modulating effect of Siglec-F in eosinophilic inflammation was proven by Siglec-F knockout mice. Mice lacking Siglec-F display same basal levels of eosinophils, but increased eosinophilia upon OVA challenge and therefore increased inflammation due to lacking feedback loop of Siglec-F activation[117].

3. Results

This thesis consists of three publications. Each publication represents an individual part of the research that I have done and my participation in the progress of publication is mentioned in the beginning of every part. The publications are:

- The Adipocytokine Nampt and Its Product NMN Have No Effect on Beta-Cell Survival but Potentiate Glucose-Stimulated Insulin Secretion (published in Plos one, January 16, 2013)

- Manganese mediated magnetic resonance imaging signals correlate with functional β-cell mass during diabetes progression (Accepted for publication in Diabetes)

- Siglec-7 is down-regulated in inflamed islets and activated peripheral blood mononuclear cells; restores β-cell function and survival (under revision)

3.1 The Adipocytokine Nampt and Its Product NMN Have No Effect on Beta-Cell Survival but Potentiate Glucose-Stimulated Insulin Secretion

Robert Spinnler[1,2♦], Theresa Gorski[1♦], Katharina Stolz[3♦], Susanne Schuster[1], Antje Garten[1], Annette G. Beck-Sickinger[4], Marten A. Engelse[5], Eelco J. P. de Koning[5,6], Antje Körner[1], Wieland Kiess[1], Kathrin Maedler[3]

1 Center for Pediatric Research Leipzig (CPL), Department for Women and Child Health, University of Leipzig, Leipzig, Germany; **2** Leipzig University Medical Center, IFB Adiposity Diseases, Leipzig, Germany; **3** Center for Biomolecular Interactions, University of Bremen, Bremen, Germany; **4** Institute of Biochemistry, Faculty of Bioscience, Pharmacy and Psychology, University of Leipzig, Leipzig, Germany; **5** Department of Nephrology, Leiden University Medical Center, Leiden, The Netherlands; **6** Hubrecht Institute, Utrecht, The Netherlands

♦ These authors contributed equally to this work

My contribution:

Performance and analysis of TUNEL analysis in human islets (Figure 2)

Performance and analysis of GSIS in human islets (Figure 3)

Treatment and sample collection for NAD level analysis in human islets (Figure 4)

OPEN ACCESS Freely available online

PLOS ONE

The Adipocytokine Nampt and Its Product NMN Have No Effect on Beta-Cell Survival but Potentiate Glucose Stimulated Insulin Secretion

Robert Spinnler[1,2☯], Theresa Gorski[1☯], Katharina Stolz[3☯], Susanne Schuster[1*], Antje Garten[1], Annette G. Beck-Sickinger[4], Marten A. Engelse[5], Eelco J. P. de Koning[5,6], Antje Körner[1], Wieland Kiess[1], Kathrin Maedler[3]

1 Center for Pediatric Research Leipzig (CPL), Department for Women and Child Health, University of Leipzig, Leipzig, Germany, **2** Leipzig University Medical Center, IFB Adiposity Diseases, Leipzig, Germany, **3** Center for Biomolecular Interactions, University of Bremen, Bremen, Germany, **4** Institute of Biochemistry, Faculty of Bioscience, Pharmacy and Psychology, University of Leipzig, Leipzig, Germany, **5** Department of Nephrology, Leiden University Medical Center, Leiden, The Netherlands, **6** Hubrecht Institute, Utrecht, The Netherlands

Abstract

Aims/Hypothesis: Obesity is associated with a dysregulation of beta-cell and adipocyte function. The molecular interactions between adipose tissue and beta-cells are not yet fully elucidated. We investigated, whether or not the adipocytokine Nicotinamide phosphoribosyltransferase (Nampt) and its enzymatic product Nicotinamide mononucleotide (NMN), which has been associated with obesity and type 2 diabetes mellitus (T2DM) directly influence beta-cell survival and function.

Methods: The effect of Nampt and NMN on viability of INS-1E cells was assessed by WST-1 assay. Apoptosis was measured by Annexin V/PI and TUNEL assay. Activation of apoptosis signaling pathways was evaluated. Adenylate kinase release was determined to assess cytotoxicity. Chronic and acute effects of the adipocytokine Nampt and its enzymatic product NMN on insulin secretion were assessed by glucose stimulated insulin secretion in human islets.

Results: While stimulation of beta-cells with the cytokines IL-1β, TNFα and IFN-γ or palmitate significantly decreased viability, Nampt and NMN showed no direct effect on viability in INS-1E cells or in human islets, neither alone nor in the presence of pro-diabetic conditions (elevated glucose concentrations and palmitate or cytokines). At chronic conditions over 3 days of culture, Nampt and its product NMN had no effects on insulin secretion. In contrast, both Nampt and NMN potentiated glucose stimulated insulin secretion acutely during 1 h incubation of human islets.

Conclusion/Interpretation: Nampt and NMN neither influenced beta-cell viability nor apoptosis but acutely potentiated glucose stimulated insulin secretion.

Citation: Spinnler R, Gorski T, Stolz K, Schuster S, Garten A, et al. (2013) The Adipocytokine Nampt and Its Product NMN Have No Effect on Beta-Cell Survival but Potentiate Glucose Stimulated Insulin Secretion. PLoS ONE 8(1): e54106. doi:10.1371/journal.pone.0054106

Editor: Makoto Kanzaki, Tohoku University, Japan

Received June 28, 2012; **Accepted** December 10, 2012; **Published** January 16, 2013

Funding: The work was supported by Deutsche Forschungsgemeinschaft KFO 152 "Atherobesity" & Emmy Noether Programm, the LIFE program (Leipzig Interdisciplinary Research Cluster of Genetic Factors, Clinical Phenotypes and Environment), the IFB (Integrated Research and Treatment Center AdiposityDiseases), BMBF (Bundesministerium für Bildung und Forschung), the German Diabetes Society (DDG) and the Kompetenznetz Adipositas-Verbund LARGE (TP01) and Kompetenznetz Diabetes and the European Research Council (ERC 260336). Provision of human islets were supported by the National Center for Research Resources (NCRR), the National Institute of Diabetes and Digestive and Kidney Diseases (NIDDK) and the Juvenile Diabetes Research Foundation (JDRF) and through the European Consortium for Islet Transplantation (ECIT), Islets for Research Distribution Program. The funders had no role in study design, data collection and analysis, decision to publish, or preparation of the manuscript.

Competing Interests: The authors would also like to confirm that Kathrin Mädler is co-author of this manuscript and a PLOS ONE Editorial Board member. This does not alter the authors' adherence to all the PLOS ONE policies on sharing data and materials.

* E-mail: Susanne.Schuster@medizin.uni-leipzig.de

☯ These authors contributed equally to this work.

Introduction

Obesity and the development of type 2 diabetes mellitus (T2DM) are strongly related. It has been suggested, that molecular signals from adipose tissue convey the information that beta-cells reside in an obese environment. T2DM results from a pancreatic islet failure to produce sufficient amounts of insulin and from a decrease in the sensitivity of glucose-metabolizing tissues to insulin [1]. A failure of beta-cell function and a reduction in beta-cell mass mainly caused by apoptosis are two of the factors underlying the complex etiology of T2DM. They are often associated with an increase in circulating cytokines, free fatty acids (FFAs) and chronic hyperglycaemia [2]. Obesity leads to dysregulation of adipose tissue function, up regulation of proinflammatory cytokine release and enhanced secretion of FFAs which all might contribute to pancreatic beta-cell damage.

Cytokines, alone or in combination, take part in the pathogenesis of diabetes causing pancreatic beta-cell dysfunction and decline of viability [3–5].

Additionally, gluco-lipotoxicity causes beta-cell failure in T2DM [6], and also saturated FFAs alone cause beta-cell apoptosis [7–10], whereas the monounsaturated FFA oleate is less toxic [7,10] and even protects against palmitate-induced apoptosis in beta-cells [10].

A metabolic dysregulation also results in an altered production and secretion of adipocytokines, which *per se* influences beta-cell survival and function. Specifically, the adipocytokines leptin and adiponectin influence beta-cell survival and death [9,11,12]. Leptin, secreted from white adipocytes, is an essential factor in regulating body weight and glucose homeostasis [12]. Leptin receptors are expressed by beta-cells [13]. *In vitro*, leptin stimulates the release of IL-1β, decreases the expression of the IL-1 receptor antagonist (IL-1Ra) in human islets [14] and upon chronic exposure induces beta-cell apoptosis [11] and impairs islet function in rodent and human beta-cells [9,11,12]. In INS-1 cells leptin alone does not modify caspase-3 activation or DNA fragmentation, whereas a combination of leptin with cytokines or FFAs suppress cytokine and palmitate induced apoptosis and DNA fragmentation [9]. While leptin levels are elevated in obesity, adiponectin is decreased [15] and correlates with impaired beta-cell function and survival. It binds to two subtypes of adiponectin receptors, AdipoR1 and AdipoR2. AdipoR1 is expressed in muscle, while AdipoR2 is mainly expressed in the liver and in beta-cells at similar levels [16]. *In vivo*, adiponectin exists as a globular fragment or as full-length form [17]. The C-terminal globular domain of adiponectin, gAcrp30, counteracts cytokine- and palmitate-induced beta-cell apoptosis [9], increases insulin secretion in islets from high fat diet-treated mice at high glucose concentrations [18,19] and prevents cytokine- and FFA-induced suppression of insulin secretion in INS-1 cells [9]. In contrast, adiponectin administration to human islets fails to prevent beta-cell apoptosis induced by FFAs [20].

Nicotinamide phosphoribosyltransferase (Nampt, also known as PBEF or visfatin) has been identified as a novel adipokine, with both intra- and extracellular enzymatic function. Rather than exerting insulin-mimetic effects *in vitro* or *in vivo*, Nampt catalyses the rate-limiting step in mammalian NAD biosynthesis [21]. Nicotinamide mononucleotide (NMN), the enzyme product of Nampt, has been shown to correct impaired islet function in $Nampt^{(+/-)}$ mice [21] and to restore suppressed insulin secretion in mouse models of impaired beta-cell function [22]. Nampt also acts in a cytokine-like manner, either in an anti-apoptotic [23,24] or a pro-inflammatory fashion [25]. Nampt levels in the circulation are elevated in non-obese and obese T2DM patients and correlate with increased IL-6 serum levels [26].

Since previous studies yielded contradicting data, we aimed to evaluate whether or not the adipocytokines leptin, adiponectin, Nampt or its enzyme product NMN affect beta-cell viability, cytotoxicity, apoptosis and beta-cell function.

Materials and Methods

Ethics Statement

We have received the human islets from the European Consortium for Islet Transplantation (ECIT), where six European-based centers for human islet transplantation have established collaboration with the aim establishing an integrated project to develop and expand clinical islet transplantation. Whenever islet isolation fails to be suitable for transplantation, centers provide them for islet research. Thus, these research projects apply to NIH regulations PHS 398, exemption 4. Human pancreata are harvested from brain dead donors, according to the European and National regulations for organ procurement. Human islet isolations are performed through approved protocols of the centers. Donors or their family members have given written consent to donate organs for transplantation and research, all documented by the transplantation centers. For this study, all islet preparations were received from the University of Leiden. The University of Bremen institutional review board specifically approved this study.

Cell Culture

The rat insulinoma cell line INS-1E was a generous gift from Prof. Claes Wollheim, Geneva, Switzerland and represents a highly differentiated clone of INS-1 cells [27]. INS-1E cells (passages 70–95) were grown in RPMI 1640 (PAA Laboratories, Pasching, Austria) culture medium containing 25 mM HEPES and supplemented with 2 mM L-glutamine (PAA), 50 µM β-mercaptoethanol (Sigma, Munich, Germany), 1 mM sodium pyruvate (Sigma) and 5% FCS (PAA) in an atmosphere of 5% CO_2 at 37°C. Subconfluent cells were maintained in culture by passaging of cultures every 3–4 days after plating.

Human islets were isolated from pancreata of four non-diabetic organ donors at the Leiden University Medical Center and cultured as described previously [28]. For long-term *in vitro* studies, islets were cultured on extracellular matrix–coated plates derived from bovine corneal endothelial cells (Novamed Ltd., Jerusalem, Israel), allowing the cells to attach to the dishes and spread, preserving their functional integrity.

Cells were cultured with IL-1β [0.1–100 ng/ml], IFN-γ [0.1–100 ng/ml] and TNFα [0.1–100 ng/ml] (R&D Systems, McKinley Place, MN, USA) or the adipocytokines leptin [1–500 ng/ml], gAcrp30 [1.67–835 ng/ml] (both PeproTech GmbH, Hamburg, Germany) or Nampt [1–25 ng/ml] (kindly provided by AdipoGen Inc., Incheon, South Korea) or the enzymatic product NMN [10–1000 µM] (Sigma) or camptothecin [2 µM] (Sigma) and etoposide [85 µM] (Calbiochem, Merck KGaA, Darmstadt, Germany) or palmitate [0.125–1 mM] and oleate [0.125–1 mM] (Sigma), dissolved as described previously [28].

Cell Viability, Cytotoxicity and Apoptosis

To measure viability and cytotoxicity, cells were seeded into 96well plates at 25,000 cells/well for 72 hours. Cells were incubated for 24 h in RPMI 1640 medium without FCS, but supplemented with 0.2% BSA (Life Technologies GmbH, Darmstadt, Germany) and then incubated in serum free medium in the absence or presence of the treatment conditions for 48–72 h. Viability and cytotoxicity were measured by WST-1 assay (Roche, Mannheim, Germany) and by ToxiLight®BioAssay Sample Kit (Lonza Inc., Rockford, IL,USA) respectively, according to manufacturer's instructions. Apoptosis in INS-1E cells was assessed by FITC-AnnexinV (An) and propidium iodide (PI) staining (BD, Heidelberg, Germany) and flow cytometric analysis (BD FACSCalibur). For each sample, 10,000 cells were counted. An-positive and double-stained An/PI positive cells were considered to be apoptotic. For detection of beta-cell apoptosis in human islets, 100 human islets were cultured in suspension dishes, treated for 72 h, and fixed with Bouins solution. Islet sections were prepared as described previously [29] and insulin and TUNEL staining was performed according to the manufacturer (In Situ Cell Death Detection Kit, TMR-red; Roche) [29].

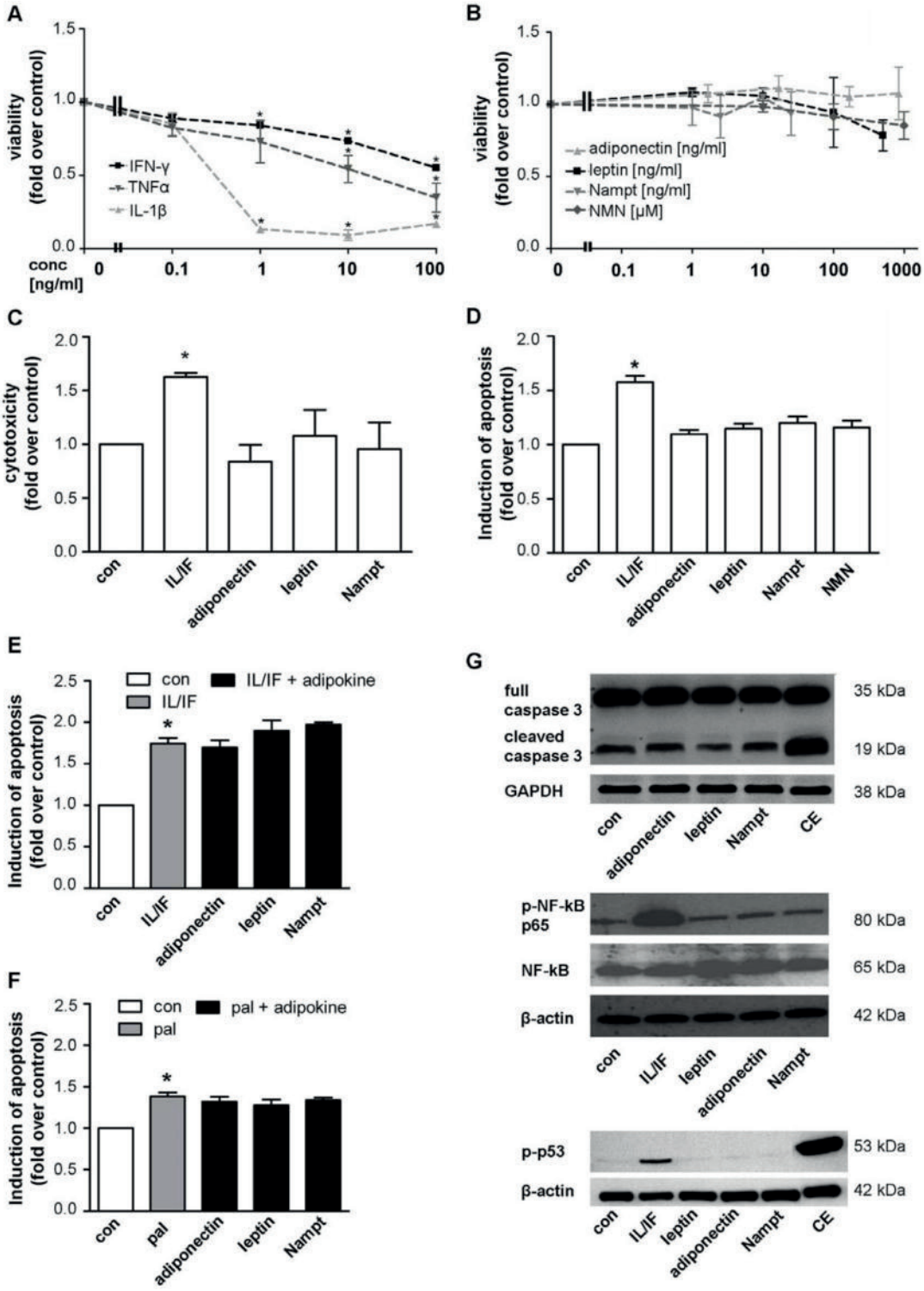

Figure 1. The adipocytokines leptin, adiponectin, Nampt and NMN have no direct effects on beta-cell survival in INS-1E cells. INS-1E cells were kept under serum-free conditions 24 h before and during the 48 h experiment. (**A,B**) INS-1E cells were exposed to cytokines (**A**: IL-1β, IFN-γ or TNFα) or adipocytokines (**B**: adiponectin, leptin, Nampt, NMN) at the indicated concentrations for 48 h and cell viability was measured by WST-1

assay. Data are shown as means ±SEM of 3 independent experiments performed in triplicates. Statistical analyses were performed by one-way ANOVA with Bonferroni's Multiple Comparison Test as posthoc test. **C,D**: INS-1E cells were exposed to adipocytokines (adiponectin 167 ng/ml, leptin 200 ng/ml, Nampt 2.5 ng/ml, NMN 100 μM) or a cytokine combination (10 ng/ml IL-1β+10 ng/ml IFN-γ) for 48 h. Cytotoxicity (**C**) was analyzed by measuring the release of adenylate kinase into the supernatant and (**D**) apoptosis was measured by FITC-annexinV (An) and propidium iodide (PI) staining and subsequent flow cytometric analysis of An-positive and double An/PI positive cells. Results were expressed relative to cells exposed to serum free medium (con) and as means ±SEM of three independent experiments performed in triplicates. **E,F**: INS-1E cells were exposed to a cytokine combination (IL/IF; 10 ng/ml IL-1β+10 ng/ml IFN-γ) (**E**) or 0.25 mM palmitate (pal) (**F**) for 48 h in the absence or presence of the adipocytokines (167 ng/ml adiponectin, 200 ng/ml leptin, 2.5 ng/ml Nampt) and induction of apoptosis was measured by An/PI staining and flow cytometric analysis. Data are shown as means ±SEM of triplicates of three independent experiments. Statistical analyses were performed by students t-test. G: INS-1E cells were exposed to the adipocytokines adiponectin (167 ng/ml), leptin (200 ng/ml) or Nampt (2.5 ng/ml) or a combination of camptothecin (2 μM) and etoposide (85 μM; CE, **upper and lower panel**) or a cytokine combination (10 ng/ml IL-1β+10 ng/ml IFN-γ, **middle and lower panel**). Western blot analyses were performed for full length and cleaved caspase-3 (**upper panel**), phospho-NF-κB p65 (Ser536) and NF-κB p65 (**middle panel**) and phospho-p53 (Ser15) (**lower panel**). GAPDH or beta-actin were used as loading control. All panels show one typical blot out of three independent experiments. *$p<0.05$ compared to untreated control.
doi:10.1371/journal.pone.0054106.g001

Measurement of Intracellular NAD Level

The concentrations of NAD in the whole cell extracts were analysed by a commercially available NAD/NADH assay kit (EnzyChrom™ NAD/NADH Assay Kit; Köln, Germany). Therefore, 500,000 cells/well were seeded in 6well plates and cultured as described above. After treatment for 2 or 48 h, cells were trypsinized and 2 wells per sample were pooled and lysed in 100 μl NAD extraction buffer. To homogenize the samples, cell extracts were undergo freeze/thaw cycles. NAD level were determined according to manufacturer's instructions. The cell pellet of each sample was resuspended in 100 μl 2% SDS, shaked for 10 min at 99°C and centrifuged for 5 min at 20,000×g and then used for protein determination (BCA Assay, Pierce Thermo Scientific). The NAD level of each sample was referred to the corresponding total protein amount of the sample.

Western Blotting

INS-1E cells were seeded into 6well plates at 500,000 cells/w ell and grown in culture medium. After 72 h, cells were incubated in serum free medium for 24 h. Thereafter, cells were incubated for 48 h for activated caspase-3, 6 h for p53 and 3 h for NF-κB detection under serum free conditions in the absence or presence of the treatment conditions. Equal amounts of protein from each treatment group were run on 10% or 15% SDS–polyacrylamide gels. After semi-dry transfer onto nitrocellulose, membranes (0.45 μm) were blocked and subsequently incubated with rabbit anti-phospho-p53 antibody (Ser15), rabbit anti-caspase-3 antibody, rabbit anti-phospho-NF-κB-p65 (Ser536) antibody, rabbit anti-NF-κB-p65 antibody (all Cell Signaling Technology Inc., Beverly, MA, USA), mouse anti-β-actin antibody (Sigma) or mouse anti-GAPDH antibody (Millipore, Billerica, USA) over night, followed by a 2 h incubation with anti-rabbit or anti-mouse IgG HRP-conjugated antibodies (Dako A/S, Glostrup, Denmark). Specific bands were visualized using ECL chemiluminescence substrate (Super Signal Pico, Pierce, USA) and CL-XPosure film (Thermo Scientific, Waltham, MA, USA).

Insulin Secretion Assays

Human islets used to perform glucose and IBMX/Forskolin stimulated insulin secretion (GSIS) experiments were kept in culture medium on matrix-coated plates derived from bovine corneal endothelial cells (Novamed Ltd.). For determining the chronic effects of the adipocytokines, islets were exposed for 72 h and then washed and pre-incubated (30 min) in Krebs Ringer bicarbonate buffer (KRB) containing 2.8 mM glucose and 0.5% BSA. For acute insulin release in response to glucose, islets were washed, KRB was then replaced by KRB 2.8 mM glucose for 1 h (basal), followed by an additional 1 h-incubation in KRB 16.7 mM glucose (stimulated).

To assess the acute effects of the adipocytokines, human islets were incubated after a 2 day- pre-incubation and recovery period for 1 h at 2.8 mM glucose, followed by a 1 h-incubation period at 2.8 mM glucose plus adipocytokines and an additional 1 h-incubation period at 16.7 mM glucose plus adipocytokines.

A second parallel experiment was designed to directly compare the adipocytokine effects after glucose stimulation. Human islets were acutely incubated with 2.8 mM for 1 h, followed by incubation at 16.7 mM glucose for 1 h and incubation at 16.7 mM glucose plus adipocytokines for 1 h.

A third parallel experiment was designed to investigate whether adipokines also influence secretory machinery in general. Human islets were acutely incubated with 2.8 mM for 1 h, followed by incubation at in the presence of IBMX (100 uM) and Forskolin (10 uM, Sigma) as described before [30].

Islets were extracted with 0.18 N HCl in 70% ethanol for determination of insulin content. Islet insulin was determined using human insulin ELISA (ALPCO, Salem, NH, USA) and expressed per content.

Statistical Analyses

Significant differences were determined using GraphPad Prism software 4 and the unpaired Student's t-test or by one-way ANOVA with Bonferroni's Multiple Comparison Test as posthoc test. The threshold of significance was set $p<0.05$.

Results

The Adipocytokines Leptin, Adiponectin, Nampt and NMN have no Direct Effects on Beta-cell Survival in INS-1E Cells

First, we confirmed the presence of the adiponectin receptors AdipoR1 and AdipoR2 as well as the leptin receptor (OB-R, LeptinR) in INS-1E cells (Fig. S1) [14,20], whereas the existence of a specific receptor for Nampt is currently unknown.

Cell viability in INS-1E cells was reduced by the cytokines IL-1β, IFN-γ and TNFα during 48 h exposure in a dose-dependent manner. IL-1β and IFN-γ reduced beta-cell viability starting at a concentration of 1 ng/ml and TNFα at a higher concentration of 10 ng/ml. At a cytokine concentration of 10 ng/ml the viability of INS-1E cells was reduced by 91.4±1.7% by IL-1β stimulation, 45.6±6.3% by TNFα and 26.3±2.0% by IFN-γ, respectively (Fig. 1A). For further experiments, a cytokine combination of IL-1β (10 ng/ml) and IFN-γ (10 ng/ml) was used as control. In contrast, the adipocytokines leptin, adiponectin, Nampt and NMN showed no effect on viability over a wide range of concentrations (Fig. 1B) at 48 h long-term exposure.

These results were confirmed by analyzing cytotoxicity and apoptosis during the treatment. Cytotoxicity was investigated by

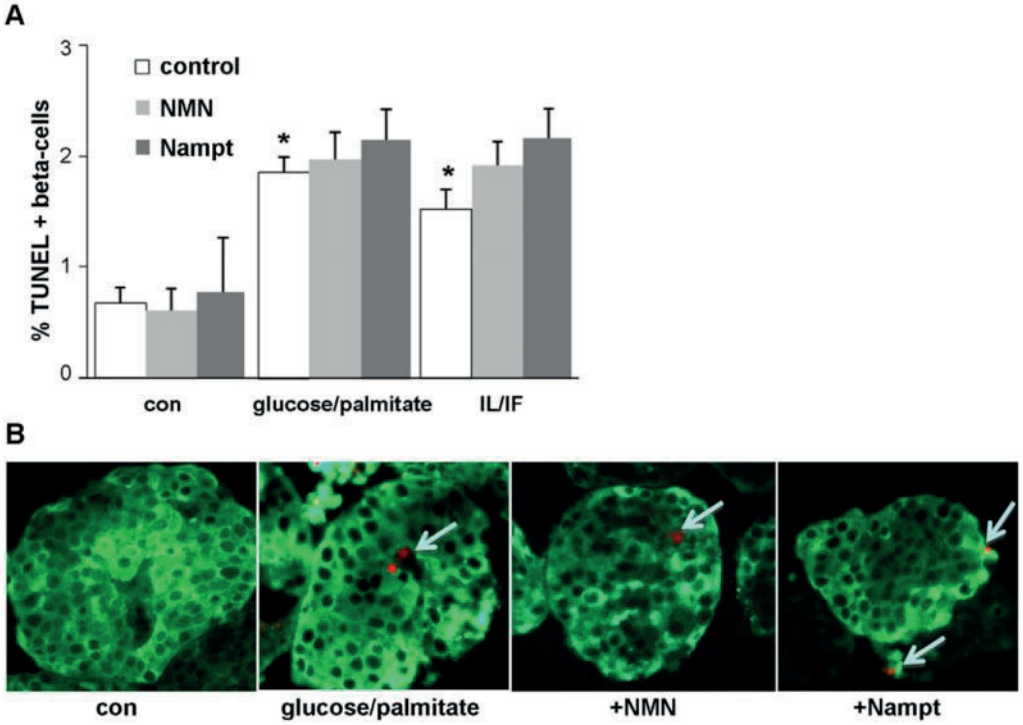

Figure 2. Nampt and NMN have no direct effects on beta-cell survival in human islets. (**A,B**) Human pancreatic islets were cultured in suspension with the mixture of 22.2 mM glucose/0.5 mM palmitate or 2 ng/ml IL-1β/1000 IU IFN-γ in the absence (con) or presence of NMN (100 μM) or Nampt (2.5 ng/ml) for 72 h. Apoptosis was analysed in paraffin embedded islet sections by the TUNEL assay (red nuclei, white arrows) and counter-stained in green for insulin (**B**). Results are means ±SEM of the %TUNEL-positive beta-cells (the average number of beta-cells counted were 1456±277 for each treatment group in each experiment) of three different experiments from three different organ donors. **B:** shows representative staining pictures. *$p<0.05$ compared to vehicle treated control.
doi:10.1371/journal.pone.0054106.g002

measuring the release of adenylate kinase from damaged cells and apoptosis by An/PI labeling and subsequent flow cytometric analysis. Analyses of cytotoxicity and apoptosis confirmed the toxic effects of the cytokines but not of adipocytokines on beta-cell survival (Fig. 1C,D, Fig. S3). Concentrations of the adipocytokines were chosen according to physiological levels (see Discussion). The cytokine combination IL-1β and IFN-γ (10 ng/ml each) induced cytotoxic (60.9±10.5%, Fig. 1C) as well as apoptotic (63.0±9.0%, Fig. 1D) effects after 48 h stimulation. To investigate whether adipocytokines may protect INS-1E cells from cytokine- or palmitate-induced apoptosis or may enhance apoptosis, INS-1E cells were stimulated with a combination of adipocytokines and cytokines or palmitate for 48 h. The apoptosis induced by cytokines (IL-1β/IFN-γ) and palmitate could not be ameliorated by the adipocytokines leptin, adiponectin or Nampt (Fig. 1E,F). Western blotting analysis revealed similar lacking effects of the adipocytokines adiponectin, leptin, or Nampt on different apoptotic pathways (Fig. 1G). The combination of cytokines IL-1β/IFN-γ or the pro-apoptotic cocktail of camptothecin and etoposide were used as positive controls for activation of different apoptotic pathways, such as cleavage of caspase-3 (Fig. 1G, upper panel), phosphorylation of NF-κB p65 subunit (Ser536) (Fig. 1G, middle panel) and of p53 (Ser15) (Fig. 1G, lower panel). To evaluate whether the INS-1E cell model used in our study is able to activate mechanisms to counteract apoptosis, we also investigated the protective effects of oleate on palmitate-induced cytotoxicity (Fig. S2A–C). A previously observed protection of beta-cells from palmitate-induced apoptosis by oleate [8,11,31] could have been confirmed in our study in INS-1E cells (Fig. S2D).

Nampt and NMN have no Direct Effects on Beta-cell Survival in Human Islets

Survival data from cell lines are difficult to extrapolate to primary cells. While Nampt and NMN did not induce beta-cell apoptosis in INS-1E cells, the direct effects of Nampt and NMN on the human beta-cell are unknown. Our next experiments investigated the effects of Nampt and NMN under control and diabetogenic conditions on beta-cell survival in human islets. The same physiological concentrations were used as in the cell line experiments. In addition to Nampt, we also exposed human islets to its enzymatic product NMN for 72 h. In confirmation with our results obtained in INS-1E cells, no effect of Nampt or NMN was observed on beta-cell apoptosis in human islets at control conditions (5.5 mM glucose) (Fig. 2A). Apoptosis was induced by 72 h exposure of human islets to the mixture of 22.2 mM glucose and 0.5 mM palmitate which induced a 2.7-fold induction in beta-cell apoptosis and by mixture of the cytokines IL-1β and IFN-γ, which induced a 2.3-fold increase in beta-cell apoptosis, compared to control conditions at 5.5 mM glucose ($p<0.05$, Fig. 2A,B). Addition of Nampt or NMN had no effect on beta-cell apoptosis in all conditions.

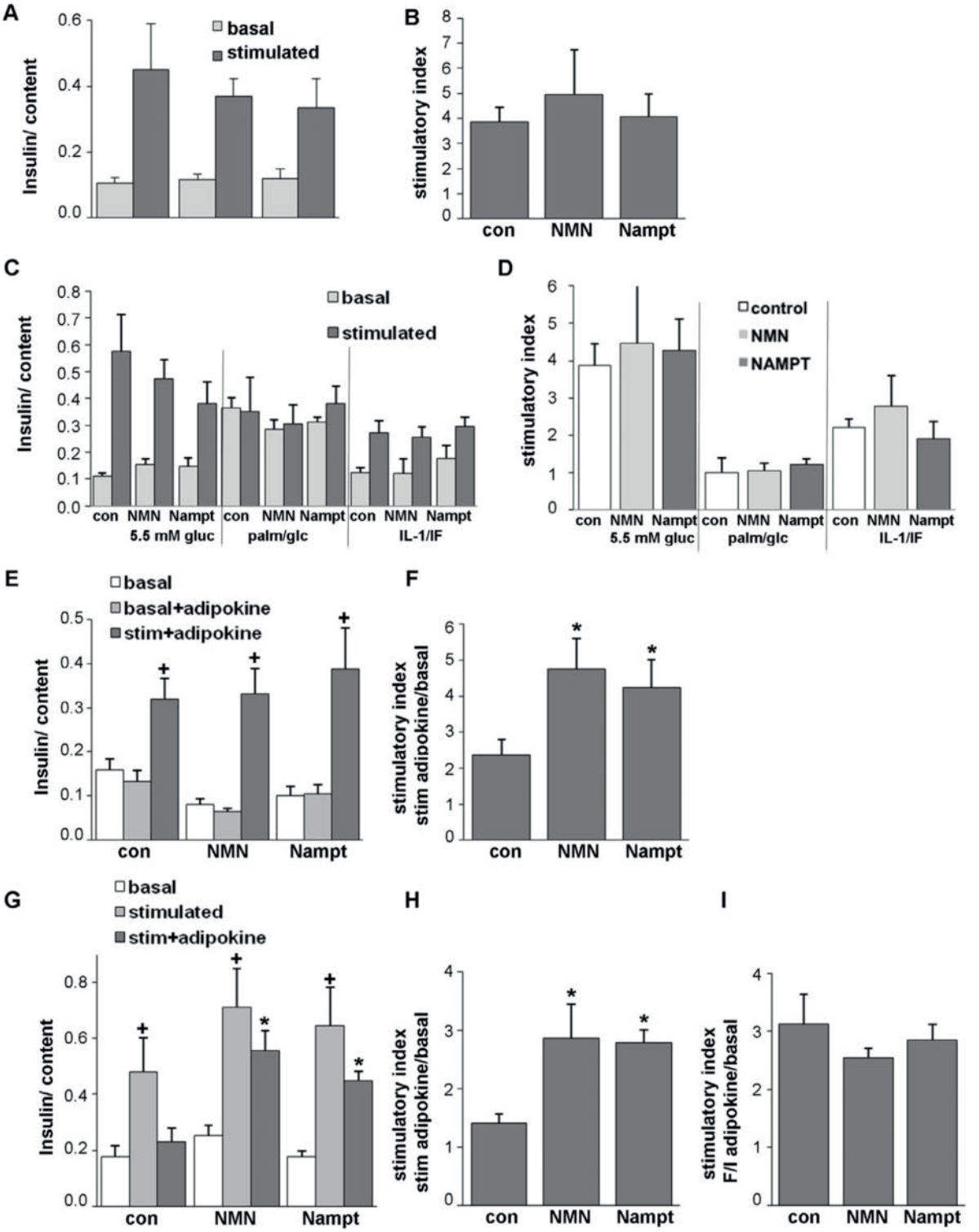

Figure 3. Nampt and NMN potentiate glucose stimulated insulin secretion (GSIS) in human islets. GSIS from human islets cultured on extracellular matrix coated dishes and chronically (**A–D**) or acutely (E–I) exposed to NMN (100 μM) and Nampt (2.5 ng/ml). (**A–D**) Islets were chronically exposed to the treatment conditions for 72 h (**A,B**: 5.5 mM glucose; **C,D**: 5.5 mM glucose, the mixture of 22.2 mM glucose/0.5 mM

palmitate or 2 ng/ml IL-1β/1000 IU IFN-γ), medium was changed and GSIS performed in the absence of the treatment conditions. Basal and stimulated insulin secretion indicate the amount secreted during 1 h incubations at 2.8 (basal) and 16.7 mM (stimulated) glucose following the 72 h culture period and normalized to insulin content. The stimulatory index was calculated (**B,D**). (**E,F**) Islets were pre-cultured for 48h and then exposed to 2.8 mM glucose for 1 h (basal), to 2.8 mM glucose including the adipocytokines for 1 h (basal+adipokine) and another subsequent hour to 16.7 mM glucose including the adipocytokines (stim+adipokine). The stimulatory index was calculated (**F**). (**G, H**) Islets were pre-cultured for 48 h and then exposed to 2.8 mM glucose for 1 h (basal), to 16.7 mM glucose for 1 h (stimulated) and another subsequent hour to 16.7 mM glucose including the adipocytokines (stim+adipokine). The stimulatory index was calculated (**H**). (**I**) Stimulatory index from human islets exposed to 2.8 mM glucose (basal) and subsequently to 1 h exposure to IBMX (100 mM)/Forskolin (10 mM) with or without Nampt or NMN was calculated. Results are means ±SEM from triplicates from three independent experiments from three donors. *$p<0.05$ to the respective untreated control, $^{+}p<0.05$ to 2.8 mM basal glucose.
doi:10.1371/journal.pone.0054106.g003

Nampt and NMN Potentiate Glucose Stimulated Insulin Secretion in Human Islets

Since Nampt and NMN failed to protect human islets from apoptosis induced by diabetogenic conditions, we tested whether it may influence insulin secretion under basal conditions in culture. Human islets were chronically exposed to Nampt or NMN at 5.5 mM glucose for 72 h and GSIS was analysed thereafter. Nampt and its enzymatic product NMN did not influence beta-cell insulin secretion upon chronic exposure (Fig. 3A,B). Next, we investigated whether Nampt and NMN have an effect on long-term glucolipotoxicity and cytokine toxicity, induced by 72 h exposure of human islets to the mixture of 22.2 mM glucose and 0.5 mM palmitate or by the mixture of the cytokines IL-1β and IFN-γ. Glucose stimulated insulin secretion was determined at the end of the 72 h culture. Glucose/palmitate as well as the cytokine mixture severely reduced the stimulatory index (Fig. 3C,D; 3.8- and 1.8-fold respectively, $p<0.05$). Neither Nampt nor NMN changed GSIS in any of the conditions (Fig. 3C,D). This is in line with the above described lack of influence of Nampt and NMN on beta-cell survival (Fig. 2).

To determine the acute effect of Nampt and NMN on insulin secretion, we cultured the islets in the presence of the adipocytokine at low and high glucose concentrations for 1 h, respectively. At low glucose, Nampt and NMN elicited no significant effect on insulin secretion when compared to low glucose alone (Fig. 3E, basal +adipokine vs. basal). At high glucose conditions the GSIS was improved by Nampt and NMN. While glucose alone induced a 2.4-fold induction of insulin secretion, this induction was 2.0- and 1.8-fold induced by NMN and Nampt, respectively ($p<0.05$, Fig. 3E,F, stim+adipokine vs. basal), when compared to 16.7 mM glucose alone. To exclude exhaustive effects on beta-cell insulin secretion, which could have occurred after stimulation with high glucose concentrations, we repeated the experiment by testing adipocytokine effects only at high glucose conditions. Again, human islets were pre-cultured for 2 days at 5.5 mM glucose, basal glucose of 2.8 mM (Fig. 3G, basal) was added for 1 h followed by 1 h exposure to high glucose (16.7 mM) (Fig. 3G, stimulated) and then to high glucose in the presence of Nampt or NMN (Fig. 3G, stim+adipokine). All islets showed similar GSIS before the addition of the adipocytokine (Fig. 3G, stimulated). In contrast, islets which were stimulated a 2nd subsequent hour with 16.7 mM glucose alone showed a decrease in GSIS (Fig. 3G, con, dark grey bar). Islets which were exposed to high glucose and Nampt or its enzymatic product NMN showed a restoration of insulin secretion, which was 2.0-fold increased by Nampt and NMN, respectively, when compared to 16.7 mM glucose alone ($p<0.01$, Fig. 3G,H, stim+adipokine vs. basal).

This effect of Nampt and NMN on the potentiation of glucose stimulated insulin secretion was dependent on the effect of glucose, since stimulation of insulin secretion with agents which raise intracellular levels of cAMP (forskolin and 3-isobutyl-Methylxanthine/IBMX) was not influenced by Nampt or NMN (Fig. 3I).

NAMPT and NMN Increase NAD Level and Ameliorate NAD Depletion

NAD level increased in human islets after short time incubation with NMN (2.2-fold) or Nampt (2.6-fold). Incubation for a longer time did not change NAD level in human islets (Fig. 4A). In INS-1E cells short time incubation with NMN or Nampt did not alter intracellular NAD level whereas the NAD level after 48 h

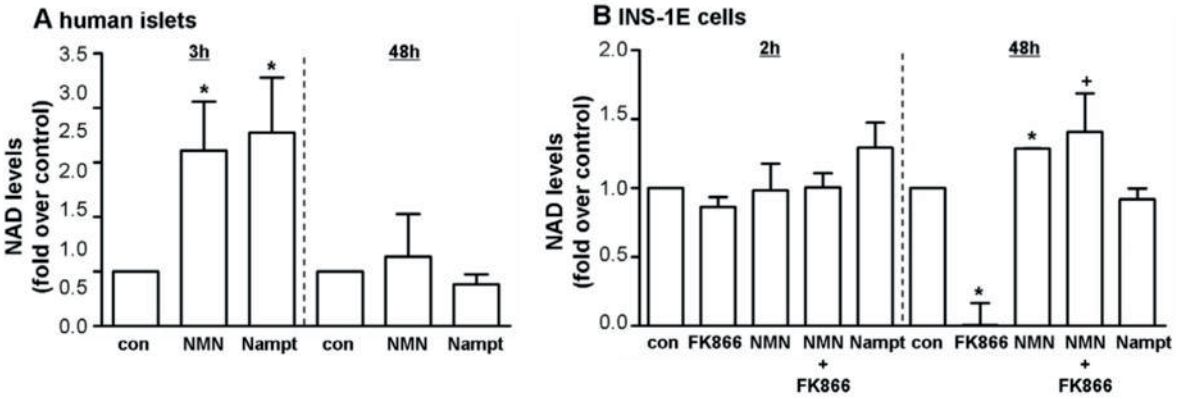

Figure 4. Nampt and NMN increase NAD level and ameliorate NAD depletion. Human islets (A) and INS-1E cells (B) were stimulated with NMN [100 μM] or Nampt [2.5 ng/ml] for a short time (2 or 3 h) or a long time exposure (48 h). NAD level were normalised to the total protein amount in each sample. FK866 [10 nM], a specific Nampt inhibitor, was used as a positive control in INS-1E cells. * $p<0.05$ compared to con (serum free medium);+$p<0.05$ compared to FK866 treated cells.
doi:10.1371/journal.pone.0054106.g004

incubation were slightly increased by NMN (0.3-fold). After 48 h, NMN restored intracellular NAD level after NAD depletion caused by FK866, a specific Nampt inhibitor (Fig. 4B).

Discussion

Because of the controversial data concerning the effects of adiponectin, leptin and Nampt on beta-cell survival [9;11;22–25], we aimed to evaluate whether or not these adipocytokines affect beta-cell viability, cytotoxicity and apoptosis. For the first time we also show presence of Nampt in beta-cells and human islets (Fig. S4A,B) and effects of Nampt and its enzyme product NMN on human beta-cell function and survival.

Previously, adiponectin (gAcrp30) and leptin were found to strongly inhibit palmitate-induced apoptosis, with a weaker effect on cytokine-induced apoptosis [9,11]. In contrast, another previous study showed that leptin and high glucose levels induce apoptosis in human and rat beta-cells [11]. However, we did not find any changes of INS-1E cell viability, cytotoxicity or apoptosis after stimulation with the adipocytokines. Neither NF-κB-, caspase-3- nor p53- mediated apoptotic pathways were influenced by adiponectin, leptin or Nampt under the experimental conditions we used. In cell line experiments, a number of experimental factors could explain such discrepancies; differences between cell lines (Min6 or INS-1E cells), cell passages or starvation conditions could result in different experimental outcomes. In our study, beta-cells were starved before the experiments started, whereas in a previous study, non-starving conditions were used [9]. The leptin and adiponectin concentrations in our study are in agreement with other *in vitro* studies [9,11,32]. Leptin at 200 ng/ml is within the upper range that is measured in obese people [33,34]. Adiponectin concentrations range from 1–5000 ng/ml in different studies [35,36] and strongly correlate with insulin sensitivity and beta-cell compensation [37]. In line with our results, also Staiger *et al.* did not detect any effects of adiponectin on beta-cell survival or insulin secretion despite functionally active receptors in human islets [20].

Results from clinical studies show that visfatin/Nampt levels are elevated in nonobese and obese patients with T2DM compared with control subjects [26]. Additionally, circulating serum levels of Nampt are elevated in obese compared to lean children [38], suggesting that Nampt is associated with beta-cell function in humans. To elucidate whether the demonstrated effects of Nampt depend upon its enzymatic activity, we tested NMN, the enzyme product of Nampt. In our study, physiological adipocytokine concentrations were used to test their effects. Nampt serum levels are 2.22 ng/ml in healthy adults and increase up to 2.75 ng/ml in patients with T2DM [39], thus 2.5 ng/ml was used in our cell culture studies. This amount corresponds to approximately 0.023 nM for the Nampt dimer, which is the molecular form of Nampt in human serum that is enzymatically active [40]. No physiological human serum concentrations for NMN have been published so far. Data from mice report a plasma concentration of 80–90 µM [21], thus, a dose of 100 µM NMN was used in our study. Nampt has also been shown to exert enzyme-independent cytokine-like anti-apoptotic effects [24,41]. There were no protective effects of Nampt and NMN on the beta-cell line INS-1E and human islets using multiple tested assays. Nampt and NMN also had no effect on the function of human islets upon chronic exposure. Further, pro-apoptotic signaling pathways, such as activation of p-53 and NF-κB were activated by cytokines in our study, which is in line with numerous previous publications [7,42,43], and were not modified by Nampt, although other adipocytokines can modify such pathways [9,11]. In Min6 beta-cells, palmitate-induced beta-cell apoptosis was inhibited by Nampt [23]. However, in that study, a Nampt concentration of 100 nM was tested, which is approximately 4300-fold higher than in physiological conditions.

In our study, Nampt as well as NMN did not change basal insulin release, but acutely potentiated GSIS under high glucose conditions, which is reminiscent of the effects of Glucagon-like peptide-1 (GLP-1), being only affective at high glucose concentrations, but additionally, GLP-1 shows protective effects on beta-cell survival [44]. Nampt-mediated systemic NAD biosynthesis is critical for beta-cell function and for the regulation of glucose homeostasis [21]. Nampt heterozygous ($Nampt^{+/-}$) female mice show impaired glucose tolerance due to a defect in GSIS. The administration of NMN has been demonstrated to restore GSIS in $Nampt^{(+/-)}$ mice *in vivo* and in islets *in vitro* [21] and also to protect against cytokine-mediated impairment of beta-cell function in mouse islets [22]. This strongly indicates that the observed defects are due to a lack of Nampt-mediated NAD biosynthesis. According to this, our data revealed that NMN restores intracellular NAD level after depletion caused by FK866, a specific Nampt inhibitor. As an NAD biosynthetic enzyme, Nampt regulates the activity of NAD-consuming enzymes such as sirtuins, which are involved in cellular homeostasis, glucose metabolism and stress responses [45]. We measured increased intracellular NAD level after short time incubation with NMN and Nampt in human islets which might explain the beneficial effects on GSIS. In a previous study of Bordone *et al.* sirtuin 1 (Sirt1) promoted insulin secretion in pancreatic beta-cells in response to glucose partly through repression of uncoupling protein 2 (Ucp2) and consequently increased levels of ATP [46]. We could not found any changes in ATP level (Fig. S4C) after stimulation with Nampt and NMN for 2, 48 and 72 h. Probably, the changes in NAD level are too small to detect alterations in ATP concentrations. Further, pancreatic beta-cell-specific Sirt1-overexpressing (BESTO) transgenic mice exhibited enhanced GSIS and improved glucose tolerance [47]. Additionally, it was found that old BESTO mice have significantly reduced plasma NMN levels and lost their ability to GSIS. NMN administration restored the improved glucose tolerance and enhanced GSIS in these aged female BESTO mice [48].

Our findings indicate that Nampt and NMN did not influence beta-cell survival. However, targeting NAD biosynthesis might represent novel therapeutic strategies in the control of beta-cell function.

Supporting Information

Figure S1 Expression of the adiponectin receptors (AdipoR1, AdipoR2) and the leptin receptor. Demonstration of mRNA expression of the adiponectin receptors (AdipoR1, AdipoR2) and the leptin receptor (LepR/Ob-R) in INS-1E cells and in visceral fat taken from rats.
(TIF)

Figure S2 Oleate protects from palmitate induced apoptosis in INS-1E cells. INS-1E cells were exposed to palmitate and oleate at increasing concentrations alone (**A**) or in combination for 72 h (**B**) or 24 h (**C**). Viability was measured by WST-1 analysis (**A,B**) and cytotoxicity was analyzed by measuring the release of adenylate kinase in the supernatant (**C**). Data show the mean ± SEM of quadruplicates of three independent experiments. *$p<0.05$ to untreated control, **$p<0.05$ to palmitate treated cells. (**D**) Western blot analysis was performed for control cells, 0.5 mM palmitate (pal) treated cells, 0.5 mM oleate (ol)

treated cells and for the combination (pal+ol) for full length and cleaved caspase-3. GAPDH was used as loading control. All panels show one typical blot out of three independent experiments.
(TIF)

Figure S3 Cytokines increased apoptosis in INS-1E cells. INS-1E cells were exposed to the cytokine combination (10+10 ng/ml IL/IF) and the adipocytokines (200 ng/ml leptin, 167 ng/ml adiponectin and 2.5 ng/ml Nampt) for 48 h. Apoptosis in INS-1E cells was assessed by FITC Annexin V (An) and propidium iodide (PI) staining and flow cytometric analysis. For each sample, 10,000 cells were counted. An-positive and double-stained An/PI positive cells were defined as apoptotic cells.
(TIF)

Figure S4 Nampt is expressed in human islets and the beta-cell line INS-1E. **(A)** Nampt mRNA was analysed in human islets and INS-1E cells by PCR. Human Nampt was amplified using the primers: forward ATGAATCCTGCGGCA-GAAGC and reverse CTAATGATGTGCTGCTTCCAGT [40]. To detect Nampt mRNA in rats forward primer CCACC-GACTCGTACAAGGTT and reverse primer ACTTCTTTGGCCTCCTGGAT were used. **(B)** Nampt protein was detected in lysates [10 µg protein] by using a monoclonal antibody (1:5000) in 5% non-fat dry milk (OMNI379, Axxora, Lörrach, Germany) in human islets and INS-1E cells. For normalisation GAPDH was used. **(C)** ATP level were measured according to manufacturer's instructions (CellTiter-Glo® Luminescent Cell Viability Assay, Promega, Madison, WI, USA) after 2, 48 and 72 h with NMN [100 µM], Nampt [2,5 ng/ml] or FK866 [10 nM], a specific Nampt inhibitor.
(TIF)

Acknowledgments

We thank Sandy Laue for excellent technical assistance. Nampt was kindly provided by Byung Soo Youn (AdipoGen Inc., Incheon, Sounth Korea). FK866 was kindly provided by TopoTarget A/S, Copenhagen, Denmark. Human islets were provided through the Leiden University Medical Center.

Author Contributions

Drafted the article or revised it critically and gave final approval of the version to be published: RS TG KS SS AG AGBS MAE EJPdK AK WK KM. Conceived and designed the experiments: RS TG KS SS AG AGBS AK WK KM. Performed the experiments: RS TG KS MAE EJPdK. Analyzed the data: RS TG KS KM WK. Contributed reagents/materials/analysis tools: AGBS AK MAE EJPdK. Wrote the paper: RS TG SS KM.

References

1. Wang C, Guan Y, Yang J (2010) Cytokines in the Progression of Pancreatic beta-Cell Dysfunction. Int J Endocrinol 2010: 515136.
2. Stumvoll M, Goldstein BJ, van Haeften TW (2005) Type 2 diabetes: principles of pathogenesis and therapy. Lancet 365: 1333–1346.
3. Pukel C, Baquerizo H, Rabinovitch A (1988) Destruction of rat islet cell monolayers by cytokines. Synergistic interactions of interferon-gamma, tumor necrosis factor, lymphotoxin, and interleukin 1. Diabetes 37: 133–136.
4. Maedler K, Dharmadhikari G, Schumann DM, Storling J (2009) Interleukin-1 beta targeted therapy for type 2 diabetes. Expert Opin Biol Ther 9: 1177–1188.
5. Eizirik DL, Mandrup-Poulsen T (2001) A choice of death–the signal-transduction of immune-mediated beta-cell apoptosis. Diabetologia 44: 2115–2133.
6. Poitout V, Robertson RP (2008) Glucolipotoxicity: fuel excess and beta-cell dysfunction. Endocr Rev 29: 351–366.
7. Kharroubi I, Ladriere L, Cardozo AK, Dogusan Z, Cnop M, et al. (2004) Free fatty acids and cytokines induce pancreatic beta-cell apoptosis by different mechanisms: role of nuclear factor-kappaB and endoplasmic reticulum stress. Endocrinology 145: 5087–5096.
8. Maedler K, Spinas GA, Dyntar D, Moritz W, Kaiser N, et al. (2001) Distinct effects of saturated and monounsaturated fatty acids on beta-cell turnover and function. Diabetes 50: 69–76.
9. Rakatzi I, Mueller H, Ritzeler O, Tennagels N, Eckel J (2004) Adiponectin counteracts cytokine- and fatty acid-induced apoptosis in the pancreatic beta-cell line INS-1. Diabetologia 47: 249–258.
10. Cunha DA, Hekerman P, Ladriere L, Bazarra-Castro A, Ortis F, et al. (2008) Initiation and execution of lipotoxic ER stress in pancreatic beta-cells. J Cell Sci 121: 2308–2318.
11. Maedler K, Schulthess FT, Bielman C, Berney T, Bonny C, et al. (2008) Glucose and leptin induce apoptosis in human beta-cells and impair glucose-stimulated insulin secretion through activation of c-Jun N-terminal kinases. FASEB J 22: 1905–1913.
12. Seufert J (2004) Leptin effects on pancreatic beta-cell gene expression and function. Diabetes 53 Suppl 1: S152–S158.
13. Kieffer TJ, Heller RS, Habener JF (1996) Leptin receptors expressed on pancreatic beta-cells. Biochem Biophys Res Commun 224: 522–527.
14. Maedler K, Sergeev P, Ehses JA, Mathe Z, Bosco D, et al. (2004) Leptin modulates beta cell expression of IL-1 receptor antagonist and release of IL-1beta in human islets. Proc Natl Acad Sci U S A 101: 8138–8143.
15. Koerner A, Kratzsch J, Kiess W (2005) Adipocytokines: leptin–the classical, resistin–the controversical, adiponectin–the promising, and more to come. Best Pract Res Clin Endocrinol Metab 19: 525–546.
16. Kharroubi I, Rasschaert J, Eizirik DL, Cnop M (2003) Expression of adiponectin receptors in pancreatic beta cells. Biochem Biophys Res Commun 312: 1118–1122.
17. Kadowaki T, Yamauchi T (2005) Adiponectin and adiponectin receptors. Endocr Rev 26: 439–451.
18. Gu W, Li X, Liu C, Yang J, Ye L, et al. (2006) Globular adiponectin augments insulin secretion from pancreatic islet beta cells at high glucose concentrations. Endocrine 30: 217–221.
19. Winzell MS, Nogueiras R, Dieguez C, Ahren B (2004) Dual action of adiponectin on insulin secretion in insulin-resistant mice. Biochem Biophys Res Commun 321: 154–160.
20. Staiger K, Stefan N, Staiger H, Brendel MD, Brandhorst D, et al. (2005) Adiponectin is functionally active in human islets but does not affect insulin secretory function or beta-cell lipoapoptosis. J Clin Endocrinol Metab 90: 6707–6713.
21. Revollo JR, Korner A, Mills KF, Satoh A, Wang T, et al. (2007) Nampt/PBEF/Visfatin regulates insulin secretion in beta cells as a systemic NAD biosynthetic enzyme. Cell Metab 6: 363–375.
22. Caton PW, Kieswich J, Yaqoob MM, Holness MJ, Sugden MC (2011) Nicotinamide mononucleotide protects against pro-inflammatory cytokine-mediated impairment of mouse islet function. Diabetologia.
23. Cheng Q, Dong WP, Qian L, Wu JC, Peng YD (2011) Visfatin inhibits apoptosis of pancreatic {beta}-cell line, MIN6, via the mitogen-activated protein kinase/phosphoinositide 3-kinase pathway. J Mol Endocrinol.
24. Li Y, Zhang Y, Dorweiler B, Cui D, Wang T, et al. (2008) Extracellular Nampt promotes macrophage survival via a nonenzymatic interleukin-6/STAT3 signaling mechanism. J Biol Chem 283: 34833–34843.
25. Romacho T, Azcutia V, Vazquez-Bella M, Matesanz N, Cercas E, et al. (2009) Extracellular PBEF/NAMPT/visfatin activates pro-inflammatory signalling in human vascular smooth muscle cells through nicotinamide phosphoribosyltransferase activity. Diabetologia 52: 2455–2463.
26. El Mesallamy HO, Kassem DH, El Demerdash E, Amin AI (2011) Vaspin and visfatin/Nampt are interesting interrelated adipokines playing a role in the pathogenesis of type 2 diabetes mellitus. Metabolism 60: 63–70.
27. Merglen A, Theander S, Rubi B, Chaffard G, Wollheim CB, et al. (2004) Glucose sensitivity and metabolism-secretion coupling studied during two-year continuous culture in INS-1E insulinoma cells. Endocrinology 145: 667–678.
28. Maedler K, Oberholzer J, Bucher P, Spinas GA, Donath MY (2003) Monounsaturated fatty acids prevent the deleterious effects of palmitate and high glucose on human pancreatic beta-cell turnover and function. Diabetes 52: 726–733.
29. Sauter NS, Schulthess FT, Galasso R, Castellani LW, Maedler K (2008) The antiinflammatory cytokine interleukin-1 receptor antagonist protects from high-fat diet-induced hyperglycemia. Endocrinology 149: 2208–2218.
30. Shu L, Matveyenko AV, Kerr-Conte J, Cho JH, McIntosh CH, et al. (2009) Decreased TCF7L2 protein levels in type 2 diabetes mellitus correlate with downregulation of GIP- and GLP-1 receptors and impaired beta-cell function. Hum Mol Genet 18: 2388–2399.
31. Eitel K, Staiger H, Brendel MD, Brandhorst D, Bretzel RG, et al. (2002) Different role of saturated and unsaturated fatty acids in beta-cell apoptosis. Biochem Biophys Res Commun 299: 853–856.
32. Kulkarni RN, Wang ZL, Wang RM, Hurley JD, Smith DM, et al. (1997) Leptin rapidly suppresses insulin release from insulinoma cells, rat and human islets and, in vivo, in mice. J Clin Invest 100: 2729–2736.
33. De Marinis L, Bianchi A, Mancini A, Gentilella R, Perrelli M, et al. (2004) Growth hormone secretion and leptin in morbid obesity before and after

biliopancreatic diversion: relationships with insulin and body composition. J Clin Endocrinol Metab 89: 174–180.
34. Chan JL, Heist K, DePaoli AM, Veldhuis JD, Mantzoros CS (2003) The role of falling leptin levels in the neuroendocrine and metabolic adaptation to short-term starvation in healthy men. J Clin Invest 111: 1409–1421.
35. Coppola A, Marfella R, Coppola L, Tagliamonte E, Fontana D, et al. (2009) Effect of weight loss on coronary circulation and adiponectin levels in obese women. Int J Cardiol 134: 414–416.
36. Xiang AH, Kawakubo M, Trigo E, Kjos SL, Buchanan TA (2010) Declining beta-cell compensation for insulin resistance in Hispanic women with recent gestational diabetes mellitus: association with changes in weight, adiponectin, and C-reactive protein. Diabetes Care 33: 396–401.
37. Yamauchi T, Kamon J, Waki H, Terauchi Y, Kubota N, et al. (2001) The fat-derived hormone adiponectin reverses insulin resistance associated with both lipoatrophy and obesity. Nat Med 7: 941–946.
38. Friebe D, Neef M, Kratzsch J, Erbs S, Dittrich K, et al. (2011) Leucocytes are a major source of circulating nicotinamide phosphoribosyltransferase (NAMPT)/pre-B cell colony (PBEF)/visfatin linking obesity and inflammation in humans. Diabetologia 54: 1200–1211.
39. Retnakaran R, Youn BS, Liu Y, Hanley AJ, Lee NS, et al. (2008) Correlation of circulating full-length visfatin (PBEF/NAMPT) with metabolic parameters in subjects with and without diabetes: a cross-sectional study. Clin Endocrinol (Oxf) 69: 885–893.
40. Korner A, Garten A, Bluher M, Tauscher R, Kratzsch J, et al. (2007) Molecular characteristics of serum visfatin and differential detection by immunoassays. J Clin Endocrinol Metab 92: 4783–4791.
41. Dahl TB, Haukeland JW, Yndestad A, Ranheim T, Gladhaug IP, et al. (2010) Intracellular nicotinamide phosphoribosyltransferase protects against hepatocyte apoptosis and is down-regulated in nonalcoholic fatty liver disease. J Clin Endocrinol Metab 95: 3039–3047.
42. Lee BW, Chun SW, Kim SH, Lee Y, Kang ES, et al. (2011) Lithospermic acid B protects beta-cells from cytokine-induced apoptosis by alleviating apoptotic pathways and activating anti-apoptotic pathways of Nrf2-HO-1 and Sirt1. Toxicol Appl Pharmacol 252: 47–54.
43. Sarkar SA, Kutlu B, Velmurugan K, Kizaka-Kondoh S, Lee CE, et al. (2009) Cytokine-mediated induction of anti-apoptotic genes that are linked to nuclear factor kappa-B (NF-kappaB) signalling in human islets and in a mouse beta cell line. Diabetologia 52: 1092–1101.
44. Drucker DJ (2003) Glucagon-like peptide-1 and the islet beta-cell: augmentation of cell proliferation and inhibition of apoptosis. Endocrinology 144: 5145–5148.
45. Imai S (2011) Dissecting systemic control of metabolism and aging in the NAD World: the importance of SIRT1 and NAMPT-mediated NAD biosynthesis. FEBS Lett 585: 1657–1662.
46. Bordone L, Motta MC, Picard F, Robinson A, Jhala US, et al. (2006) Sirt1 regulates insulin secretion by repressing UCP2 in pancreatic beta cells. PLoS Biol 4: e31.
47. Moynihan KA, Grimm AA, Plueger MM, Bernal-Mizrachi E, Ford E, et al. (2005) Increased dosage of mammalian Sir2 in pancreatic beta cells enhances glucose-stimulated insulin secretion in mice. Cell Metab 2: 105–117.
48. Ramsey KM, Mills KF, Satoh A, Imai S (2008) Age-associated loss of Sirt1-mediated enhancement of glucose-stimulated insulin secretion in beta cell-specific Sirt1-overexpressing (BESTO) mice. Aging Cell 7: 78–88.

3.2 Manganese mediated magnetic resonance imaging signals correlate with functional β-cell mass during diabetes progression

Anke Meyer[1], Katharina Stolz[1], Wolfgang Dreher[2], Jennifer Bergemann[1], Vani Holebasavanahalli Thimmashetty[2], Navina Lüschen[1], Zahra Azizi[1], Vrushali Khobragade[1], Kathrin Maedler[1*] and Ekkehard Kuestermann[2*]

1 Centre for Biomolecular Interactions Bremen, University of Bremen, Germany; **2** In-vivo MR, University of Bremen, Germany

*KM & EK contributed equally to this study

My contribution:

Animal handling and preparation during MRI experiments

β-cell mass performance and analysis for STZ-experiment

Anke Meyer,[1] Katharina Stolz,[1] Wolfgang Dreher,[2] Jennifer Bergemann,[1] Vani Holebasavanahalli Thimmashetty,[2] Navina Lueschen,[1] Zahra Azizi,[1] Vrushali Khobragade,[1] Kathrin Maedler,[1] and Ekkehard Kuestermann[2]

Manganese-Mediated MRI Signals Correlate With Functional β-Cell Mass During Diabetes Progression

DOI: 10.2337/db14-0864

Diabetes diagnostic therapy and research would strongly benefit from noninvasive accurate imaging of the functional β-cells in the pancreas. Here, we developed an analysis of functional β-cell mass (BCM) by measuring manganese (Mn^{2+}) uptake kinetics into glucose-stimulated β-cells by T1-weighted in vivo Mn^{2+}-mediated MRI (MnMRI) in C57Bl/6J mice. Weekly MRI analysis during the diabetes progression in mice fed a high-fat/high-sucrose diet (HFD) showed increased Mn^{2+}-signals in the pancreas of the HFD-fed mice during the compensation phase, when glucose tolerance and glucose-stimulated insulin secretion (GSIS) were improved and BCM was increased compared with normal diet–fed mice. The increased signal was only transient; from the 4th week on, MRI signals decreased significantly in the HFD group, and the reduced MRI signal in HFD mice persisted over the whole 12-week experimental period, which again correlated with both impaired glucose tolerance and GSIS, although BCM remained unchanged. Rapid and significantly decreased MRI signals were confirmed in diabetic mice after streptozotocin (STZ) injection. No long-term effects of Mn^{2+} on glucose tolerance were observed. Our optimized MnMRI protocol fulfills the requirements of noninvasive MRI analysis and detects already small changes in the functional BCM.

Both type 1 and type 2 diabetes are characterized by a loss and/or dysfunction of β-cells (1–5). As long as physiological insulin secretion is maintained by the β-cell, treatment toward the preservation of normoglycemia is easier to achieve. Thus, it is important to detect β-cell failure at a very early stage of the disease or even during the β-cell compensation phase. β-Cell compensation to maintain normoglycemia can be achieved in two ways: by increasing mass or increasing function (or both). Functional β-cell compensation can occur until up to a 65% β-cell loss; only at further β-cell mass (BCM) reduction was insulin secretion found to decline in patients (6). This analysis from autopsy pancreases highlights that the absolute BCM measure in an individual may not provide sufficient information on the status of diabetes progression and that the analysis of the functional BCM is essential for the evaluation of the diabetes risk.

Today, monitoring of functional BCM is achieved by measuring insulin and C-peptide secretion during a glucose as well as arginine tolerance test (7–9). Retrospective studies using human pancreata from autopsy show a strong correlation of fasting blood glucose levels with BCM and a reduction in BCM already before the diagnosis in subjects with impaired fasting glucose levels (1,10). The ideal time of diagnosis is the onset of diabetes at a stage when the functional BCM has just changed.

The noninvasive measurement of functional BCM has enormous potential for diagnostics but is rather challenging to achieve, partly because a ligand for specific β-cell labeling is currently not available (11–14). It is not possible to measure the actual mass of functional β-cells in vivo (15). MRI using manganese (Mn^{2+}) shows such monitoring of β-cell functionality in cell culture (16). Similar to Ca^{2+}, Mn^{2+} is taken up by glucose-activated β-cells, resulting in a robust signal increase in glucose-stimulated rodent β-cell lines and in islets (16,17). The uptake of Mn^{2+} is controlled by voltage-gated Ca^{2+} channels (18), and Mn^{2+} accumulates in the cytoplasm, primarily in the perinuclear region (19). Mn^{2+} uptake is glucose dependent and can be

[1]Centre for Biomolecular Interactions Bremen, University of Bremen, Bremen, Germany
[2]In-vivo-MR, University of Bremen, Bremen, Germany
Corresponding author: Kathrin Maedler, kmaedler@uni-bremen.de.
Received 30 May 2014 and accepted 13 January 2015.
This article contains Supplementary Data online at http://diabetes.diabetesjournals.org/lookup/suppl/doi:10.2337/db14-0864/-/DC1.
K.M. and E.K. contributed equally to this study.

Diabetes Publish Ahead of Print, published online March 24, 2015

used in vivo to assess the functionality of both grafted and endogenous pancreatic islets. Mn^{2+} behaves like calcium and will therefore enter metabolically active β-cells (16). $MnCl_2$-enhanced signals also reflect functional β-cells in vivo; pancreatic MRI signals of mice with streptozotocin (STZ)-induced diabetes were decreased in the case of both high- and low-dose STZ compared with nondiabetic control animals (20) and in BDC2.5 T-cell receptor transgenic nonobese diabetic mice even before the diabetes onset could be measured in the blood (21). Individual islets can be detected by MRI in $MnCl_2$-injected exteriorized pancreases, exactly correlating with immunohistochemistry performed in parallel (22).

First correlations could be made in humans by a single mangafodipir infusion; MRI data analysis could clearly and significantly distinguish between people without diabetes and patients with type 2 diabetes without differences in MRI signals in other tissues (23).

Mn^{2+} can be used not only in vitro to characterize isolated islet potency but also, more importantly, in vivo to assess the functionality of both grafted and endogenous pancreatic islets (16,24), since Mn^{2+} is also an excellent MRI agent owing to its effect on the longitudinal relaxation (T1) and was used as one of the first MRI contrast agents (25).

As with other contrast agents, Mn^{2+} has limitations mainly linked to its lack of cell specificity and its potential cytotoxicity. Chronic exposure to high concentrations of Mn^{2+} lead to extrapyramidal dysfunction resembling the dystonic movements associated with Parkinson disease, called manganism (26–28). Based on previous studies in mice, 20–35 mg/kg doses $MnCl_2$ were used for pancreas MRI in rodents (20,22). Although LD_{50} levels of 38 mg/kg i.v. injections in mice were reported (29), concentrations up to 175 mg/kg were injected to reach a sufficient Mn^{2+} concentration in the brain (30), which also led to systemic toxicity such as loss of temperature regulation, and Mn^{2+}-based signals changes in the brain were still measured for >4 days after Mn^{2+} infusion (30).

The present study aimed at developing a strategy to monitor the functional BCM by measuring Mn^{2+} uptake into β-cells by T1-weighted contrast in vivo Mn^{2+}-mediated MRI (MnMRI). By analyzing the Mn^{2+}-dependent MRI signal kinetics, we were able to identify early changes of functional BCM during β-cell compensation and failure in two diabetic mouse models in vivo.

RESEARCH DESIGN AND METHODS

Animals

C57Bl/6J mice were fed a high-fat/high-sucrose diet (HFD) ("Surwit" [31]) for 12 weeks as previously described (32) or injected with one single high dose of STZ (150 mg/kg i.p.) freshly dissolved in 0.1 mol/L citrate buffer (pH 4.5) (33). All animals were housed in a temperature-controlled room with a 12-h light, 12-h dark cycle and were allowed free access to food and water in compliance with Section 8 of the German animal protection law, the Guide for the Care and Use of Laboratory Animals, and the Bremen Senate in agreement with the National Institutes of Health Animal Care Guidelines (34). Blood glucose (measured with a glucometer) and weight were monitored during the experiments.

Intraperitoneal Glucose Tolerance Test

Glucose tolerance was monitored by intraperitoneal glucose tolerance tests (ipGTTs) in mice. For ipGTTs, mice were fasted 12 h overnight and injected with glucose (40%; B. Braun, Melsungen, Germany) at a dose of 1 g/kg body wt i.p. Blood samples were obtained at time points 0, 15, 30, 60, 90, and 120 min for glucose measurements using a glucometer. For detection of the effect of Mn^{2+} on glucose tolerance, 25 mg/kg $MnCl_2$ or vehicle control was injected once weekly in two consecutive experiments and ipGTT measured before and immediately after injection and at days 1 and 3.

Glucose-Stimulated Insulin Secretion

In Vivo Glucose-Stimulated Insulin Secretion

At time points 0 and 30 min after 2 g/kg body wt i.p. glucose injection, blood samples were collected for measurement of serum insulin levels. Insulin was determined with a mouse insulin ELISA kit (ALPCO Diagnostics, Salem, NH).

In Vitro Glucose-Stimulated Insulin Secretion

After the serial Mn^{2+} injections and MRI measurements, pancreata of normal diet (ND) and HFD animals were perfused with a Liberase TM (cat. no. 05401119001; Roche, Mannheim, Germany) solution according to the manufacturer's instructions and digested at 37°C, followed by washing and gradient purification of the islets using a 50:50 mixture of Histopaque1077 and -1119 (Sigma-Aldrich, Munich, Germany) as previously described (35,36). For acute insulin release in response to glucose, islets were washed and preincubated (30 min) in Krebs-Ringer bicarbonate buffer (KRBB) containing 2.8 mmol/L glucose and 0.5% BSA. The KRBB was then replaced by KRBB containing 2.8 mmol/L glucose for 1 h (basal), followed by an additional 1 h incubation in KRBB containing 16.7 mmol/L glucose (stimulated). Stimulatory index was calculated as stimulated divided by basal secretion.

Morphometric and β-Cell Mass Analysis

Pancreatic tissues were processed as previously described (32,37). Mouse pancreata were dissected and fixed in 4% formaldehyde at 4°C for 12 h before embedding in paraffin. For Ki67 and insulin staining, 2-μm sections were deparaffinized, rehydrated, and incubated overnight at 4°C with anti-Ki67 and the next day with anti-insulin (both Dako, Hamburg, Germany), followed by fluorescein isothiocyanate– or Cy3-conjugated secondary antibodies (Jackson ImmunoResearch Laboratories, West Grove, PA). Slides were mounted with glycerol gelatin (Sigma) or with Vectashield with DAPI (Vector Laboratories). For BCM measurement, 10 sections (spanning the width of the pancreas) per mouse were analyzed. Pancreatic

tissue area and insulin-positive area as well as nuclear size and nuclear distance were determined by computer-assisted measurements using a Nikon MEA53200 microscope (Nikon GmbH, Düsseldorf, Germany), and images were acquired using NIS-Elements software (Nikon). BCM was obtained by multiplying the ratio of insulin-positive tissue area to whole pancreatic tissue area by the weight of the pancreas as previously described (32).

MRI

For MnMRI, mice were fasted overnight and anesthetized with 1.0–2.0% isoflurane in 250 mL/min O_2, received a tail vein catheter, and were positioned in supine position on a warmed animal bed. Breathing was monitored with a pressure sensor at the chest. Just before positioning inside the magnet, mice received 2 g/kg glucose i.p., and two to four baseline images were acquired before $MnCl_2$ (8 mg/kg i.v.) was injected via a tail vein catheter. (For protocol, see Fig. 1*A*.) The experiments were performed on a 7 Tesla MR system (BioSpec 70/20 USR with AVIII; Bruker, Ettlingen, Germany) using a quadrature volume coil (72-mm inner diameter) for both radiofrequency transmission and signal reception. The scan repetition time was at least 6 s to ensure full relaxation and thus to avoid any breathing rate–dependent T1

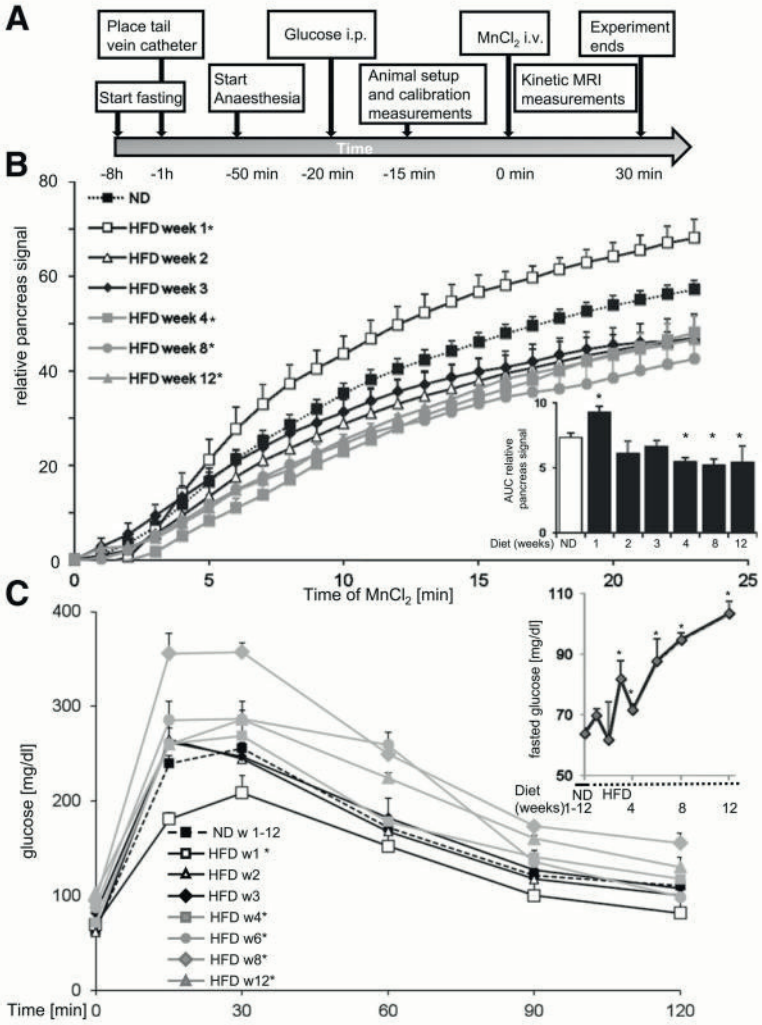

Figure 1—MRI measurements during HFD feeding of C57Bl/6J mice. *A*: Experimental work flow of the MnMRI measurement. *B*: Relative pancreas signals by MnMRI normalized to final liver signals after 23 min of $MnCl_2$ injection from age-matched ND (n = 19) and HFD mice over 12 weeks (n = 3, 6, 4, 3, 3, and 3 for HFD at 1, 2, 3, 4, 8, and 12 weeks, respectively; all mice 12 weeks old at the beginning of the feeding and analysis). Reported signal intensities reflect the signal changes after subtraction of the mean baseline signal taken from the first three to four images prior to intravenous Mn^{2+} injection. Before averaging of individual time courses, data were linearly interpolated and regridded to 1-min intervals referenced to t = 0 for Mn^{2+} injection. AUC integrations are done for the time interval of 0–23 min. *C*: ipGTT and fasting glucose levels (insert) from age-matched ND (n = 33) and HFD mice over 12 weeks (n = 3 for each data point at 1, 2, 3, 4, 8, and 12 weeks). w, week. *P < 0.05 compared with ND control.

effects (38). Time course experiments were acquired using a 3D Snapshot-FLASH sequence with inversion recovery preparation (39) with the following parameters: time of inversion (TI) = 700 ms, FLASH-type signal readout: echo time = 0.9 ms (thus insensitive to T2 relaxation), repetition time = 1.98 ms, excitation pulse = 10°, bandwidth = 500 kHz, matrix = 192 × 96 × 16, field of view = 70 × 35 × 16 mm, nominal image resolution = 365 × 365 × 1,000 μm, centric phase encoding, time of acquisition = 190 ms (38,40). For reference purposes, one proton-density image was acquired using the same 3D Snapshot-FLASH method but omitting the inversion preparation. During the experiments, all measurement parameters were kept constant (personnel, injection system, Mn^{2+} charge, narcotic setup).

Image Analysis

After standard image reconstruction on the Bruker system, the image data were converted from the Bruker to standard NIfTI data format using a home-written software (coded in Matlab 2008b, using "Tools for NIfTI and ANALYZE image" by Jimmy Chen, Matlab File Exchange [http://www.mathworks.de/matlabcentral/fileexchange/8797-tools-for-nifti-and-analyze-image]). These three-dimensional data sets were then subjected to a rigid body motion correction and concatenated to a single four-dimensional data set using SPM8 (Wellcome Department of Imaging Neuroscience, University College London [http://www.fil.ion.ucl.ac.uk/spm/]) for further analysis. The time course data of pancreatic and hepatic tissues were derived from manually drawn regions of interest (ROIs) (38,40). A reduction in breathing rate was often observed directly after bolus $MnCl_2$ administration, which normalized after ~3–5 min. ROIs were chosen after Mn^{2+} application. An organ-specific differentiation of MRI signals in the mouse abdomen is feasible, since each organ in the abdomen can be discriminated owing to their time- and signal amplitude–dependent response to the Mn^{2+} application. In the HFD studies, MRI signals were normalized to the 23-min liver signal in order to see the pancreas-specific kinetics. In the STZ studies, pancreatic MRI signals were normalized to the maximal signal of the corresponding ROI (proton-density image) because of the hepatic fibrosis induced by STZ injection.

Statistical Analysis

Stainings/MRI sets were evaluated in a randomized manner independently by the investigators (A.M., K.S., N.L., Z.A., V.K., and E.K.). The results presented are means ± SEM). The significance of difference between individual experiments was tested by Student *t* test. Significance was set at $P < 0.05$.

RESULTS

MRI Signals Correlate With β-Cell Compensation and Failure During 12 Weeks of HFD Feeding

For monitoring of β-cell function and mass during diabetes progression in the HFD mouse model, MnMRI (Figs. 1*A* and *B* and 2) together with ipGTT, insulin secretion during the ipGTT, and BCM (Figs. 1*C* and 3*A–C*) was analyzed. Figure 1*A* shows the experimental setting of the MnMRI measurements in the mice. Glucose was delivered intraperitoneally 25 min before intravenous $MnCl_2$ application to allow glucose-dependent Mn^{2+} uptake into the β-cells.

After Mn^{2+} injection, the signal increased in T1-weighted magnetic resonance images in a diet- and time-dependent manner (Fig. 1*B*); a time course of MnMRI revealed enlarged MRI signals after 1 week of HFD compared with in ND control mice. The increased signal was only transient, and decreased signals were measured with prolonged diet already after 2 weeks of the HFD. From the 4th week on, MRI signals decreased significantly in the HFD group, compared with ND mice, which had stable MRI signals during the course of the experiment. Such reduced MRI signals in HFD mice persisted over the whole 12-week experimental period, which is also reflected by the area-under-the-curve (AUC) calculation (Fig. 1*B*) of the MRI kinetics as well as by the continued MRI signal change from one single representative mouse over the 12 weeks of HFD (Supplementary Fig. 1*A*).

In order to compensate for inevitable variations of Mn^{2+} delivery to the tissues, we normalized pancreatic MRI signals to those of the liver. Reported signal intensities reflect the signal changes after subtraction of the mean baseline signal taken from the first three to four images prior to intravenous Mn^{2+} injection (Fig. 2). Before averaging of individual time courses, data were linearly interpolated and regridded to 1-min intervals referenced to $t = 0$ for Mn^{2+} injection.

Progressive Decline of Glucose Tolerance and β-Cell Function During 12 Weeks of HFD

The MnMRI signals in the HFD mice correlated well with both glucose tolerance and insulin secretion during the

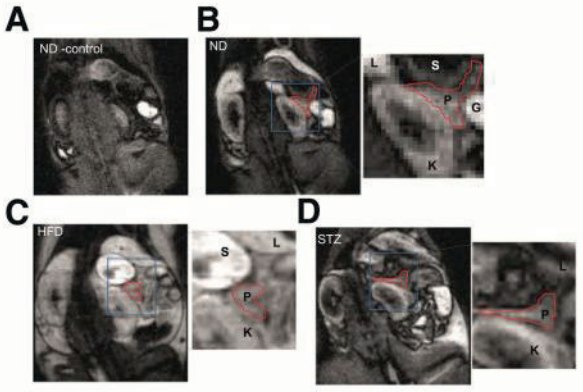

Figure 2—$Mn2^{+}$-based signals in the mouse abdomen. Representative ND MnMRI images and enlarged pancreas regions (right) from ND control mice before (*A*) and after (*B*) $MnCl_2$ injection and from HFD (*C*) and STZ (*D*) mice after $MnCl_2$ injection. G, gut; K, kidney; L, liver; P, pancreas; S, stomach. (A high-quality color representation of this figure is available in the online issue.)

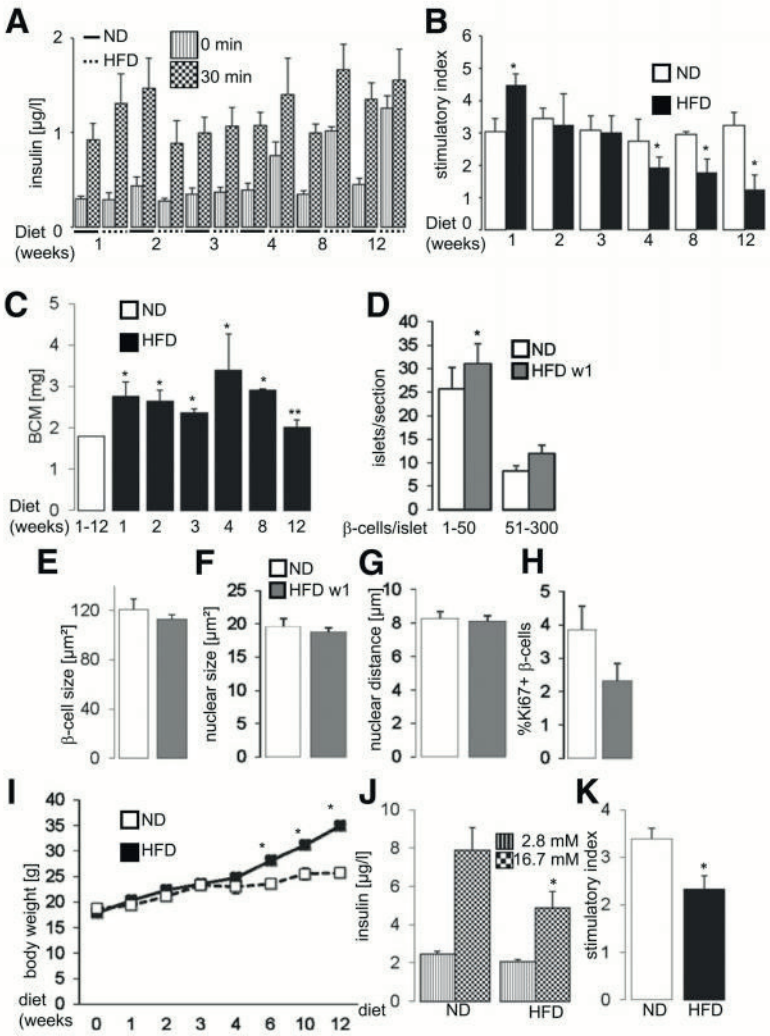

Figure 3—Progressive decline of glucose tolerance and β-cell function during 12 weeks of HFD. In vivo GSIS during the ipGTT (*A* and *B*) and β-cell mass (*C*) from ND and HFD mice fed over 12 weeks (n = 14 for ND; n = 3, 3, 3, 8, 8, and 8 for HFD at 1, 2, 3, 4, 8, and 12 weeks, respectively). *D*: Islet density was analyzed by counting all islets/section from ND and HFD mice and presenting them in two size groups with 1–50 and 51–300 β-cells/islet. *E*: Mean β-cell size was approximated by dividing total insulin-positive area by number of β-cells. Mean β-cell nuclear size (*F*), nuclear distance (*G*), and β-cell proliferation by double staining for Ki67 and insulin (*H*) were analyzed in a mean number of 155 islets/mouse from three mice/group. *I*: Mouse weight over the course of the diet. *J* and *K*: In vitro GSIS from isolated islets from $MnCl_2$-injected ND and HFD mice at the end of the 16-week experiment. Insulin secretion during 1-h incubation with 2.8 mmol/L (basal) and 16.7 mmol/L (stimulated) glucose. *K*: The insulin stimulatory index denotes the ratio of secreted insulin during 1-h incubation with 16.7 mmol/L and 2.8 mmol/L glucose, respectively. *P < 0.05 compared with ND control; **P < 0.05 compared with 8-week HFD data set.

course of HFD feeding (Figs. 1 and 3; Supplementary Fig. 1*A*). At 1 week after HFD, when MRI signals were increased, glucose tolerance was improved (Fig. 1*C*), together with increased glucose-stimulated insulin secretion (GSIS) (Fig. 3*A* and *B*), which confirms that the increased glucose-stimulated MnMRI signals indeed reflect the improved β-cell function. HFD feeding significantly impaired glucose tolerance and insulin secretion, with significantly higher glucose levels during the glucose tolerance test and higher fasting glucose (Fig. 1*C*) and reduced GSIS (Fig. 3*A* and *B*) after 4 weeks—the same time point when pancreatic MnMRI signals were reduced—compared with ND mice.

In contrast to the functional changes, BCM remained in the compensatory phase during the first 8 weeks of the HFD. Already after 1 week of HFD, BCM was 1.5-fold increased, while BCM was unchanged in ND controls during the 12 weeks (Fig. 3*C*). Again, the compensatory increase in BCM already after 1 week correlated with the improved function and the increased MRI signal. We did not expect such a fast mass adaptation and therefore analyzed single β-cell and islet size in detail. We observed

a significant increase in smaller islets consisting of 1–50 β-cells throughout the pancreas in the HFD mice for 1 week, compared with ND, while larger islets did not significantly increase (Fig. 3*D*). β-Cell size (Fig. 3*E*), β-cell nuclear size (Fig. 3*F*), and nuclear distance (Fig. 3*G*) as well as $Ki67^+$ β-cells (Fig. 3*H*) were similar in ND and HFD.

In contrast, from 4 weeks on, glucose tolerance and insulin secretion were impaired by the HFD, and MRI signals were reduced and BCM remained increased up to 8 weeks of diet, showing that the functional BCM and not the BCM alone is monitored by MnMRI. A drop in BCM back to the ND level was observed at 12 weeks (Fig. 3*C*); also here, glucose tolerance test (Fig. 1*C*) and GSIS (Fig. 3*A* and *B*) were lower than in control mice.

All mice fed with the HFD gained weight significantly after 6 weeks of feeding (1.4-fold increase compared with ND) (Fig. 3*I*). At the end of the experiments, in vitro GSIS was performed on isolated islets from the $MnCl_2$-injected mice under the ND and HFD (Fig. 3*J* and *K*). In line with our previous data (32,34), HFD significantly reduced GSIS compared with ND controls.

STZ-Induced β-Cell Destruction Correlates With the MnMRI Signal

A second model was tested for the MnMRI analysis of functional BCM. Three-month-old male C57Bl/6 mice were injected with a single dose of 150 mg/kg STZ or vehicle. On day 14, mice were analyzed by MRI (Fig. 4*A–C*; Supplementary Fig. 1*C*) and killed on the next day for BCM measurement (Fig. 4*E*). MRI signals were clearly reduced in the STZ mice (Fig. 4*A*), which was confirmed by the AUC analysis (Fig. 4*B*) (26% reduction). No changes in Mn^{2+} cellular uptake occurred during the first 10 min of $MnCl_2$ injection, although the majority of the β-cells were destroyed. But during the second phase of Mn^{2+} uptake from 10 to 30 min, we observed a 43% induction of the MRI signal in the control mice, while we could only detect a 9% signal enhancement in the STZ mice (Fig. 4*C*). Such 79% reduction of Mn^{2+} uptake also correlates with 73% loss in BCM in the STZ mice (Fig. 4*D*).

For each mouse, the relative pancreas signal at 30 min after bolus $MnCl_2$ infusion was monitored separately before and after STZ injection and its decrease differed between 30 and 75% (Supplementary Fig. 1*A*). In line with the MRI data, STZ increased glucose levels to >400 mg/dL after 14 days (Fig. 4*E*). In contrast to HFD feeding, where liver signals remained unchanged among the treatment groups, liver MRI signals were reduced in the STZ mice (Supplementary Fig. 1*B* and *C*). Pancreas MRI results were normalized to the maximal signal of the respective corresponding ROI (100%) (proton-density image).

No Long-term Effect of Mn^{2+} on Glucose Tolerance

For exclusion of a direct long-term effect of Mn^{2+} on glucose tolerance during the experiments, 25 mg/kg $MnCl_2$ or vehicle control was injected once weekly over 2 weeks and ipGTTs were performed immediately after the $MnCl_2$ injection (Fig. 5*A* and *C*) and 2 days later (Fig. 5*B* and *D*). After the 1st $MnCl_2$ injection, glucose concentrations were slightly increased at 15 and 60 min during the ipGTT (Fig. 5*A*)—an effect that disappeared after 2 days (Fig. 5*B*). Seven days after the first dose, mice

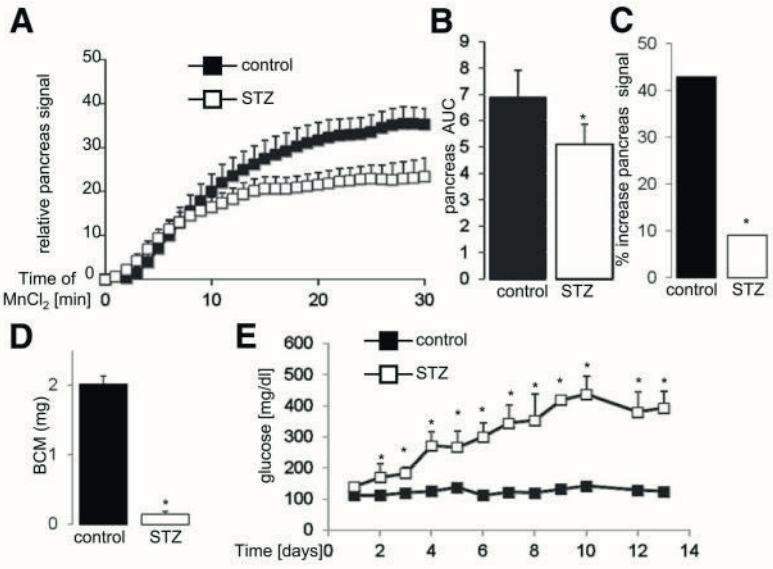

Figure 4—STZ-induced β-cell destruction correlates with the MnMRI signal. *A–C*: MRI analysis in C57Bl/6 mice injected with one single dose of 150 mg/kg STZ (n = 5) or control (n = 5). (*A*) MRI signals were normalized to the maximal signal of the corresponding ROI, the proton-density image during 30 min after $MnCl_2$ injection at day 14 after STZ treatment. *B* and *C*: AUC integrations are shown for the time interval of 0–23 min for the total measurement time (*B*) and for the second phase of Mn^{2+} uptake from 10 to 30 min (*C*). *D* and *E*: β-Cell mass analysis of isolated fixed pancreases at the end of the study (*D*) and random blood glucose levels during the 14 days of the experiment (*E*). *P < 0.05 compared with control.

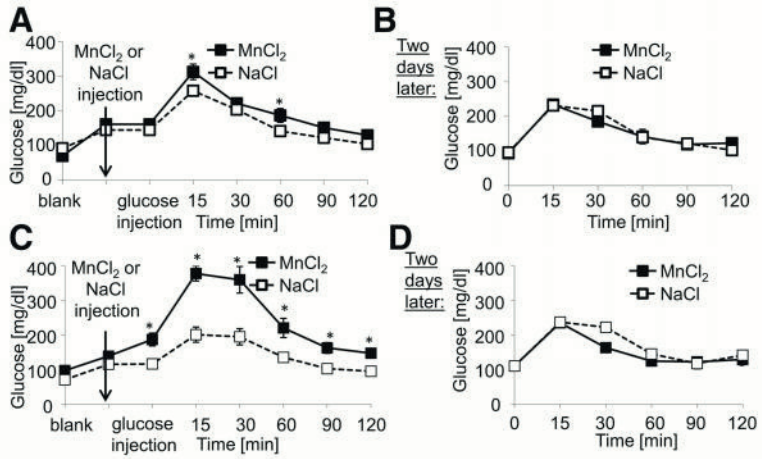

Figure 5—No long-term effect of Mn^{2+} on glucose tolerance. ipGTT with 1 g/kg glucose after the first injection (*A* and *B*) of 25 mg/kg $MnCl_2$ (n = 5) or solvent (NaCl) (n = 5) or the second injection (*C* and *D*) 1 week later in two independent experiments in normal diet fed C57Bl6/J mice. IpGTT was performed either directly after $MnCl_2$ injection (*A* and *C*) or 2 days later (*B* and *D*). *P < 0.05 compared with control.

received a second $MnCl_2$ injection, which showed again an impaired glucose tolerance (Fig. 5*C*), but this effect also washed off 2 days later (Fig. 5*D*). The results show that multiple $MnCl_2$ injections also had no long-term effects on glucose tolerance. We further monitored a possible Mn^{2+} accumulation in the brain but could not detect any MRI signal changes (Supplementary Fig. 1*E*).

DISCUSSION

In this study, we established in vivo imaging of functional BCM and show a strong correlation of MnMRI signals with a functional BCM during β-cell compensation as well as β-cell failure. Importantly, a sole association of MnMRI signals with conventionally determined BCM measurements was not observed; rather, MnMRI data displayed the functional BCM. This can be assumed from MnMRI comparisons with ipGTT, GSIS, and BCM during diabetes progression, when changes in glucose metabolism occur, and subsequently, the glucose-dependent uptake of Mn^{2+} is affected in parallel resulting in enhanced MnMRI signals as long as β-cells compensate successfully for the higher demand of insulin during HFD feeding and display adequate GSIS, which normalize glucose levels. In contrast, when GSIS was impaired and glucose levels rose, MnMRI levels were reduced in the HFD mice, even when a higher BCM was still present and declined further with more severe loss of β-cell function. In the STZ model, a more severe model of β-cell loss where loss of function together with a reduction of BCM occurred rapidly after high-dose STZ injection, MnMRI signals were significantly reduced. Initially, we expected that the MRI signals would change linearly and proportional to the BCM, but in none of the tested models did such linearity occur. Definitely, the BCM method is still the most accurate but invasive method to quantify insulin-producing cells. Our aim was to present a noninvasive alternative to the classical BCM measurement, which also allows studying BCM changes longitudinally, but this method has its limitations with respect to absolute accuracy, and we could not reach sensitivity to a single islet level.

While glucose dependent cellular Mn^{2+} uptake correlated with insulin secretion, we still observed glucose stimulated MnMRI signals after 12 weeks of HFD feeding, which were naturally reduced when compared with the ND group, but in contrast, glucose stimulated insulin secretion did not occur at all after 12 weeks. It is obvious, that basal insulin secretion raises in response to the insulin resistance, especially when free fatty acid levels are chronically elevated (32) and cause a chronic and glucose independent insulin secretion from the β-cells (41,42). In contrast, Mn^{2+} uptake is not elevated under physiological glucose concentrations at insulin resistance.

We could already see β-cell mass compensation after 1 week, a short time of the diet, together with improved function when basal insulin secretion was not increased yet. While improved function was only seen at week 1, it remained stable until week 4. After longer feeding times, basal insulin secretion was highly increased, as shown before, while GSIS is blunted in HFD mice (43), which resulted in an impaired stimulatory index.

It appears that there are different mechanisms of β-cell adaptation at young and old age as well as in the response to HFD feeding. While β-cell proliferation measured by BrdU incorporation is 10 times higher in 2-week-old than in 4-month-old mice, it is also increased after 2 weeks of HFD feeding but not after 14 weeks (43). This indicates that β-cells can proliferate at a young age (44), but at older age, β-cell compensation is unlikely to be mediated by proliferation. β-Cell hypertrophy is another mechanism reported for β-cell compensation (45). Here,

we started the HFD feeding at the age of 12 weeks and observed rapid adaptation in BCM already after 1 week of HFD, which could not be explained by increased proliferation or hypertrophy and was, rather, the result of an increased number of islets in the HFD (Fig. 3*D* and *H*). This possibility needs to be further investigated to avoid misinterpretation, as this was not the focus of our current study.

MRI kinetics display a rapid signal increase within 5 min after $MnCl_2$ injection. AUC analyses were used to calculate the signal differences during the 30 min of analysis and showed clear differences in signal intensities of the region of the pancreas, irrespective of normalization to liver signals or proton-density image. For exclusion of a general and unspecific uptake of $MnCl_2$, signals were measured in muscle during 30 min in response to $MnCl_2$; only a negligible signal decrease was observed, which was expected owing to lack of calcium uptake in the nonactive skeletal muscle (46).

In the HFD experiments, we normalized pancreatic to hepatic signal, since with its high blood flow, intravenously injected $MnCl_2$ quickly accumulates in the liver. This makes the normalization to the liver the best option. Although this is still not optimal because changes in the liver signal occurred in the different mice, so liver signals were individual and could not be correlated with any measure: neither to the selected liver ROI nor to the week of feeding in the two different ND and HFD groups.

During obesity and diabetes progression, liver and pancreas tissue accumulated fat droplets after a time period of 12 weeks, which prevented accurate measurement of the ROIs and was therefore excluded from the study. After week 12, it was not possible to mark pancreatic ROIs without the risk of including the fat signals or voxels, which are influenced by the partial volume effect in all mice and would inhibit accurate data analysis under the established experimental conditions during a longitudinal study.

In STZ experiments, the liver is highly affected by alkylation; a significant reduction of the MnMRI signal intensity in the liver was measured and shown in contrast to findings by Antkowiak et al. (20), where no liver signal changes were assumed. At the end, both our study and that by Antkowiak et al. study show an STZ-based MRI signal reduction under glucose stimulation. Hepatic damage evaluated by increased expression of alanine aminotransferase and morphologic analysis shows large necrotic areas in the liver in STZ-injected rats (47). We suspect that the STZ uptake via GLUT2 transporter of the liver is the reason for hepatic damage (48). Therefore, an alternative MnMRI signal normalization strategy in the pancreas was chosen in the STZ experiments. Signals were referenced to the maximal signal of the corresponding ROI in the proton-density image. Proton-density images were acquired without the inversion recovery pulse to see the maximal signal of the ROI, arising from all protons in the ROI (100%), which is constant over the course of measurement.

It has to be pointed out that with the described method, it is not possible to visualize individual islets, which form clusters of roughly 40–300 μm in diameter (49–51). In theory, the partial volume effect is especially strong when imaging the small β-cell organelles by MnMRI because small single spots appear much brighter in smaller measured voxels. Nevertheless, those small structures fall far below the achievable actual spatial resolution of the MnMRI, especially with our kinetic approach, which is limited to measure time and thus resolution. With increased measuring time, individual islets of Langerhans could be detected by ex vivo MnMRI (22), but even ex vivo, an accurate determination of the islet volume is not possible. The goal of the current study was to detect not individual islets but the correlation of MnMRI signals with β-cell function and mass during β-cell compensation and diabetes progression. Therefore, we set up serial measurements enabling the differentiation between kinetics and final signal amplitude.

Mn^{2+} kinetics follows the glucose-induced Ca^{2+} entry in a better way than a single time point. This can especially be observed by the differences in the HFD and STZ models; while a significant Mn^{2+}-signal decrease in the pancreas was already observed after 5 min in the HFD mice, it occurred only after 10 min in the STZ model. Nevertheless, in our setting of 30-min Mn^{2+} kinetic measurement at 50 min after glucose, a clear plateau phase was not reached yet, while a plateau phase was already reported 15 min after glucose and Mn^{2+} injection (20) and a maximal signal was observed at 1 h (52), which is in accordance with our studies.

We decided on the 30-min experimental setting after Mn^{2+} and 20–50 min after glucose because we did not expect large changes in β-cell Ca^{2+}-channel activity at 50 min after glucose injection. In this longitudinal study, we kept the experimental settings constant for the animals' welfare, which also allowed shorter anesthesia duration for the mice.

One risk under Mn^{2+} exposure is the development of detrimental side effects (manganism), which occur at higher and chronic doses of $MnCl_2$ (LD_{50} 38 mg/kg) (29,53), while in our study, 8 mg/kg was used for the MRI measures in one single bolus injection. No Mn^{2+} enhancement was detectable in the brain, which would be necessary to develop the diseases described. Also, serial Mn^{2+} injections did not lead to a magnetic resonance–detectable accumulation of Mn^{2+} in the brain. A high Mn^{2+} accumulation in a small number of cells cannot be ruled out if their volume is much smaller than the voxel volume of the image taken in these experiments.

Although Mn^{2+} caused a static impairment of glucose tolerance in mice, glucose homeostasis was not durably affected by Mn^{2+} injections.

Other endocrine as well as acinar cells in the pancreas express calcium channels; we consider the glucose-stimulated Mn^{2+} uptake to be rather specific for β-cells, but further in vitro studies on a single cell level are necessary to prove this.

α-Cells carry ATP-sensitive K^+ channels (K_{ATP}) similar to β-cells (54) as well as Ca^{2+}-channels (55,56). K_{ATP} channels play similar roles in both cell types; the difference is that the K_{ATP} channel activity in α-cells is very low. Glucose would lead to closure of the channels and membrane depolarization; however, membrane depolarization in α-cells results in lower Ca^{2+} entry versus in β-cells (57,58). The paracrine effect of insulin on the α-cells does not involve electrical activity, and α-cells are rather electrically active at hypoglycemia (below 5 mmol/L glucose).

Somatostatin-releasing δ-cells are the 3rd largest cell population in islets and also express voltage-gated L-type Ca^{2+}-channels. While increase of glucose results in the stimulation of somatostatin secretion, it had no effects on intracellular Ca^{2+} levels (59), membrane potential, or electrical activity (60) in in vitro studies. Therefore, we also do not expect large amounts of Mn^{2+} entry into δ-cells in response to glucose.

Amylase secretion by acinar cells is also regulated by Ca^{2+}-channels, and Mn^{2+} was shown to increase Amylase secretion in vitro in Ca^{2+}- and Mg^{2+}-free solution; in contrast, under physiological conditions, Mn^{2+} does not induce amylase increase and thus is not expected to give a signal in acinar cells (61); acinar cells show a robust mangafodipir-MRI signal at low glucose (62). By monitoring the difference in the MRI signal from low to high glucose in the mice, we expect a rather β-cell–specific change, as shown previously (52).

Measurements of functional BCM remain a challenge owing to the small size of pancreatic islets, their poor contrast compared with the surrounding tissues, and their position in the body. However, the present study has proven that noninvasive MRI is a reliable tool to detect small changes in the functionality of β-cells in vivo and exhibits the potential for early noninvasive detection of changes in functional BCM. Our approach carries further potential for multifaceted longitudinal studies to monitor functional BCM adaptation during diabetes progression as well as for the evaluation of therapies for diabetes as an alternative to classical BCM analysis. The optimized protocol of T1-weighted MRI of the mouse abdomen fulfills the requirements of least invasive MR imaging.

Acknowledgments. The authors thank Benjamin Pawlik and Amod Godbole (University of Bremen) for help with the MRI analysis and the Maedler laboratory, especially Amin Ardestani and Federico Paroni (University of Bremen), for helpful suggestions.

Funding. This work was supported by the FP7 program In Vivo Imaging of Beta cell Receptors by Applied Nano Technology (VIBRANT; FP7-228933-2), the European Research Council, the Diabetes Competence Network supported by the German Federal Ministry of Science, and University of Bremen research funds.

Duality of Interest. No potential conflicts of interest relevant to this article were reported.

Authors Contributions. A.M., K.M., and E.K. designed, performed, and analyzed research. K.S., W.D., J.B., V.H.T., N.L., Z.A., and V.K. performed experiments. A.M., K.M., and E.K. wrote the manuscript. K.M. is the guarantor of this work and, as such, had full access to all the data in the study and takes responsibility for the integrity of the data and the accuracy of the data analysis.

References

1. Butler AE, Janson J, Bonner-Weir S, Ritzel R, Rizza RA, Butler PC. Beta-cell deficit and increased beta-cell apoptosis in humans with type 2 diabetes. Diabetes 2003;52:102–110
2. Kurrer MO, Pakala SV, Hanson HL, Katz JD. Beta cell apoptosis in T cell-mediated autoimmune diabetes. Proc Natl Acad Sci U S A 1997;94:213–218
3. Mathis D, Vence L, Benoist C. beta-Cell death during progression to diabetes. Nature 2001;414:792–798
4. Nolan CJ, Prentki M. The islet beta-cell: fuel responsive and vulnerable. Trends Endocrinol Metab 2008;19:285–291
5. Rhodes CJ. Type 2 diabetes-a matter of beta-cell life and death? Science 2005;307:380–384
6. Meier JJ, Breuer TG, Bonadonna RC, et al. Pancreatic diabetes manifests when beta cell area declines by approximately 65% in humans. Diabetologia 2012;55:1346–1354
7. Polonsky KS, Rubenstein AH. C-peptide as a measure of the secretion and hepatic extraction of insulin. Pitfalls and limitations. Diabetes 1984;33:486–494
8. Sjostrand M, Carlson K, Arnqvist HJ, et al. Assessment of beta-cell function in young patients with type 2 diabetes: arginine-stimulated insulin secretion may reflect beta-cell reserve. J Intern Med 2014;275:39–48
9. Palmer JP, Fleming GA, Greenbaum CJ, et al. C-peptide is the appropriate outcome measure for type 1 diabetes clinical trials to preserve beta-cell function: report of an ADA workshop, 21-22 October 2001. Diabetes 2004;53:250–264
10. Ritzel RA, Butler AE, Rizza RA, Veldhuis JD, Butler PC. Relationship between beta-cell mass and fasting blood glucose concentration in humans. Diabetes Care 2006;29:717–718
11. Malaisse WJ, Maedler K. Imaging of the β-cells of the islets of Langerhans. Diabetes Res Clin Pract 2012;98:11–18
12. Gotthardt M. A therapeutic insight in beta-cell imaging? Diabetes 2011;60:381–382
13. Wang P, Yoo B, Yang J, et al. GLP-1R-targeting magnetic nanoparticles for pancreatic islet imaging. Diabetes 2014;63:1465–1474
14. Andralojc K, Srinivas M, Brom M, et al. Obstacles on the way to the clinical visualisation of beta cells: looking for the Aeneas of molecular imaging to navigate between Scylla and Charybdis. Diabetologia 2012;55:1247–1257
15. Leibiger IB, Caicedo A, Berggren PO. Non-invasive in vivo imaging of pancreatic β-cell function and survival - a perspective. Acta Physiol (Oxf) 2012;204:178–185
16. Gimi B, Leoni L, Oberholzer J, et al. Functional MR microimaging of pancreatic beta-cell activation. Cell Transplant 2006;15:195–203
17. Nagata M, Kagawa T, Koutou D, Matsushita T, Yamazaki Y, Murase K. Measurement of manganese content in various organs in rats with or without glucose stimulation. Radiological Phys Technol 2011;4:7–12
18. Leoni L, Serai SD, Haque ME, Magin RL, Roman BB. Functional MRI characterization of isolated human islet activation. NMR Biomed 2010;23:1158–1165
19. Leoni L, Dhyani A, La Riviere P, Vogt S, Lai B, Roman BB. β-Cell subcellular localization of glucose-stimulated Mn uptake by X-ray fluorescence microscopy: implications for pancreatic MRI. Contrast Media Mol Imaging 2011;6:474–481
20. Antkowiak PF, Tersey SA, Carter JD, et al. Noninvasive assessment of pancreatic beta-cell function in vivo with manganese-enhanced magnetic resonance imaging. Am J Physiol Endocrinol Metab 2009;296:E573–E578
21. Antkowiak PF, Stevens BK, Nunemaker CS, McDuffie M, Epstein FH. Manganese-enhanced magnetic resonance imaging detects declining pancreatic β-cell mass in a cyclophosphamide-accelerated mouse model of type 1 diabetes. Diabetes 2013;62:44–48
22. Lamprianou S, Immonen R, Nabuurs C, et al. High-resolution magnetic resonance imaging quantitatively detects individual pancreatic islets. Diabetes 2011;60:2853–2860

23. Botsikas D, Terraz S, Vinet L, et al. Pancreatic magnetic resonance imaging after manganese injection distinguishes type 2 diabetic and normoglycemic patients. Islets 2012;4:243–248
24. Leoni L, Roman BB. MR imaging of pancreatic islets: tracking isolation, transplantation and function. Curr Pharm Des 2010;16:1582–1594
25. Mendonça-Dias MH, Gaggelli E, Lauterbur PC. Paramagnetic contrast agents in nuclear magnetic resonance medical imaging. Semin Nucl Med 1983; 13:364–376
26. Gorell JM, Johnson CC, Rybicki BA, et al. Occupational exposure to manganese, copper, lead, iron, mercury and zinc and the risk of Parkinson's disease. Neurotoxicology 1999;20:239–247
27. Olanow CW. Manganese-induced parkinsonism and Parkinson's disease. Ann N Y Acad Sci 2004;1012:209–223
28. Roth JA, Garrick MD. Iron interactions and other biological reactions mediating the physiological and toxic actions of manganese. Biochem Pharmacol 2003;66:1–13
29. Silva AC, Lee JH, Aoki I, Koretsky AP. Manganese-enhanced magnetic resonance imaging (MEMRI): methodological and practical considerations. NMR Biomed 2004;17:532–543
30. Lee JH, Silva AC, Merkle H, Koretsky AP. Manganese-enhanced magnetic resonance imaging of mouse brain after systemic administration of MnCl2: dose-dependent and temporal evolution of T1 contrast. Magn Reson Med 2005;53: 640–648
31. Surwit RS, Kuhn CM, Cochrane C, McCubbin JA, Feinglos MN. Diet-induced type II diabetes in C57BL/6J mice. Diabetes 1988;37:1163–1167
32. Sauter NS, Schulthess FT, Galasso R, Castellani LW, Maedler K. The anti-inflammatory cytokine interleukin-1 receptor antagonist protects from high-fat diet-induced hyperglycemia. Endocrinology 2008;149:2208–2218
33. Wang Z, Dohle C, Friemann J, Green BS, Gleichmann H. Prevention of high- and low-dose STZ-induced diabetes with D-glucose and 5-thio-D-glucose. Diabetes 1993;42:420–428
34. Owyang AM, Maedler K, Gross L, et al. XOMA 052, an anti-IL-1beta monoclonal antibody, improves glucose control and beta-cell function in the diet-induced obesity mouse model. Endocrinology 2010;151:2515–2527
35. Ardestani A, Paroni F, Azizi Z, et al. MST1 is a key regulator of beta cell apoptosis and dysfunction in diabetes. Nat Med 2014;20:385–397
36. Schulthess FT, Paroni F, Sauter NS, et al. CXCL10 impairs beta cell function and viability in diabetes through TLR4 signaling. Cell Metab 2009;9:125–139
37. Shu L, Sauter NS, Schulthess FT, Matveyenko AV, Oberholzer J, Maedler K. Transcription factor 7-like 2 regulates beta-cell survival and function in human pancreatic islets. Diabetes 2008;57:645–653
38. Kustermann E, Meyer A, Godbole A, Dreher W, Maedler K. (2011) Investigating the Pancreatic Function: Robust 3D MR imaging of Mouse Abdomen. In: 19th Annual Meeting & Exhibition International Society for Magnetic Resonance in Medicine, Montreal, Canada
39. Haase A, Matthaei D, Bartkowski R, Dühmke E, Leibfritz D. Inversion recovery snapshot FLASH MR imaging. J Comput Assist Tomogr 1989;13:1036–1040
40. Meyer A, Kuestermann E, Stolz K, Bergemann J, Dreher W, Maedler K. Non-invasive in-vivo analysis of beta cell function and mass by MRI. Diabetologia 2012;55:210
41. Crespin SR, Greenough WB 3rd, Steinberg D. Stimulation of insulin secretion by infusion of free fatty acids. J Clin Invest 1969;48:1934–1943
42. Wiederkehr A, Wollheim CB. Minireview: implication of mitochondria in insulin secretion and action. Endocrinology 2006;147:2643–2649
43. Roat R, Rao V, Doliba NM, et al. Alterations of pancreatic islet structure, metabolism and gene expression in diet-induced obese C57BL/6J mice. PLoS ONE 2014;9:e86815
44. Maedler K, Schumann DM, Schulthess F, et al. Aging correlates with decreased beta-cell proliferative capacity and enhanced sensitivity to apoptosis: a potential role for Fas and pancreatic duodenal homeobox-1. Diabetes 2006;55: 2455–2462
45. Sachdeva MM, Claiborn KC, Khoo C, et al. Pdx1 (MODY4) regulates pancreatic beta cell susceptibility to ER stress. Proc Natl Acad Sci U S A 2009;106: 19090–19095
46. Berchtold MW, Brinkmeier H, Müntener M. Calcium ion in skeletal muscle: its crucial role for muscle function, plasticity, and disease. Physiol Rev 2000;80: 1215–1265
47. Simões C, Domingues P, Ferreira R, et al. Remodeling of liver phospholipidomic profile in streptozotocin-induced diabetic rats. Arch Biochem Biophys 2013;538:95–102
48. Ogawa A, Kurita K, Ikezawa Y, et al. Functional localization of glucose transporter 2 in rat liver. J Histochem Cytochem 1996;44:1231–1236
49. Bosco D, Armanet M, Morel P, et al. Unique arrangement of alpha- and beta-cells in human islets of Langerhans. Diabetes 2010;59:1202–1210
50. Carter JD, Dula SB, Corbin KL, Wu R, Nunemaker CS. A practical guide to rodent islet isolation and assessment. Biol Proced Online 2009;11:3–31
51. Jo J, Hara M, Ahlgren U, Sorenson R, Periwal V. Mathematical models of pancreatic islet size distributions. Islets 2012;4:10–19
52. Antkowiak PF, Vandsburger MH, Epstein FH. Quantitative pancreatic β cell MRI using manganese-enhanced Look-Locker imaging and two-site water exchange analysis. Magn Reson Med 2012;67:1730–1739
53. Boretius S, Frahm J. Manganese-enhanced magnetic resonance imaging. Methods Mol Biol 2011;771:531–568
54. Bokvist K, Olsen HL, Høy M, et al. Characterisation of sulphonylurea and ATP-regulated K+ channels in rat pancreatic A-cells. Pflugers Arch 1999;438: 428–436
55. De Marinis YZ, Salehi A, Ward CE, et al. GLP-1 inhibits and adrenaline stimulates glucagon release by differential modulation of N- and L-type Ca2+ channel-dependent exocytosis. Cell Metab 2010;11:543–553
56. Gromada J, Bokvist K, Ding WG, et al. Adrenaline stimulates glucagon secretion in pancreatic A-cells by increasing the Ca2+ current and the number of granules close to the L-type Ca2+ channels. J Gen Physiol 1997;110:217–228
57. Rorsman P, Salehi SA, Abdulkader F, Braun M, MacDonald PE. K(ATP)-channels and glucose-regulated glucagon secretion. Trends Endocrinol Metab 2008;19:277–284
58. Rorsman P, Braun M, Zhang Q. Regulation of calcium in pancreatic α- and β-cells in health and disease. Cell Calcium 2012;51:300–308
59. Berts A, Liu YJ, Gylfe E, Hellman B. Oscillatory Ca2+ signaling in somatostatin-producing cells from the human pancreas. Metabolism 1997; 46:366–369
60. Braun M, Ramracheya R, Amisten S, et al. Somatostatin release, electrical activity, membrane currents and exocytosis in human pancreatic delta cells. Diabetologia 2009;52:1566–1578
61. Petersen OH, Ueda N. Pancreatic acinar cells: the role of calcium in stimulus-secretion coupling. J Physiol 1976;254:583–606
62. Sahani D, Prasad SR, Maher M, Warshaw AL, Hahn PF, Saini S. Functioning acinar cell pancreatic carcinoma: diagnosis on mangafodipir trisodium (Mn-DPDP)-enhanced MRI. J Comput Assist Tomogr 2002;26:126–128

3.3 Siglec-7 is down-regulated in inflamed islets and activated peripheral blood mononuclear cells; restores β-cell function and survival

Gitanjali Dharmadhikari[1], Katharina Stolz[1], Eelco de Koning[2], Julie Kerr-Conte[3], Francois Pattou[3], Sørge Kelm[1], and Kathrin Maedler[1]

1 Centre for Biomolecular Interactions Bremen, University of Bremen, Germany; **2** Leiden University Medical Center, Department of Nephrology, Leiden and University Medical Center Utrecht, Hubrecht Institute, Utrecht, The Netherlands; **3** Thérapie Cellulaire du Diabète, INSERM /Université de Lille, France

My contribution:

Performance and analysis of mouse *in vivo* experiments

Performance and analysis of mouse islet isolation and *in vitro* experiments

Performance and analysis of FACS stained mouse islet fractions

Abstract

Chronic inflammation is consequential to the etiology of both T1D and T2D. Cytokine and chemokine production by infiltrating macrophages and by β-cells themselves in a diabetic milieu contributes to their destruction in inflamed islets and thus to progression of diabetes. In order to find potential targets for inhibition of this deleterious response of islets, the investigation of underlying mechanisms for triggering inflammation is essential. The expression of a novel family of adhesion molecules called Sialic acid-binding immunoglobulin-like lectins (Siglecs) in pancreatic islets was observed in a cell type specific manner. Siglec-7, expressed on the β-cells, was down-regulated in diabetes. Over-expression of Siglec-7 in cultured isolated islets prevented β-cell dysfunction and apoptosis under chronic diabetic stimuli and also in diabetic islets. The protective effect of Siglec-7 was mediated by the inhibition of the NF-κB pathway and the subsequent decrease in cytokine secretion. Also, activated immune cells showed loss of Siglec-7 expression. Ultimately, restoration of Siglec-7 in stressed islets caused a reduction in the number of recruited migrating monocytes. Siglec-7 expression on β-cells contributes to the inhibition of pro-inflammatory activation of these cells in diabetes. Restoration of Siglec-7 expression or signaling may be a potential therapeutic strategy to preserve β-cell function and mass in the manifestation of diabetes. This strategy would not only rescue the β- cells, but also inhibit systemic inflammation observed in T2D.

Introduction

Diabetes mellitus is a syndrome of disordered glucose metabolism, usually due to a combination of hereditary and environmental causes, resulting in hyperglycemia. The ability of the β-cells to secrete adequate amounts of insulin to maintain normoglycemia depends on their function and mass. In both, Type 1 diabetes mellitus (T1D) and Type 2 diabetes mellitus (T2D), the major mechanism leading to decreased β-cell mass is increased β-cell apoptosis. T1D results from an absolute insulin deficiency due to the autoimmune destruction of the

insulin producing β-cells [1]. β-cell destruction occurs through immune mediated processes such as mononuclear cell infiltration in the pancreatic islets and interaction between antigen presenting cells and T cells, which leads to high local concentrations of inflammatory cytokines, chemokines, reactive oxygen species (ROS) and other inflammatory products, and subsequently to β-cell apoptosis. T2D is characterized by chronic insulin resistance and a progressive decline in β-cell function and mass. Obesity is strongly associated with the development of insulin resistance [2], and is the main risk factor for the development of T2D. A chronic, low-grade inflammatory state is present in obesity, with adipose tissue macrophage infiltration and pro-inflammatory activity of macrophages [3]. Epidemiological studies suggest that low-grade inflammation precedes and predicts the development of T2D [4]. Cytokines and chemokines are produced and secreted not only by activated infiltrating macrophages, but also by adipocytes and pancreatic β-cells themselves. Chronic elevated glucose and free fatty acid levels occurring in diabetes trigger pro-inflammatory responses in several tissues like adipose tissue, muscle, liver, immune cells and also the islets [5]. Proinflammatory cytokines can cause insulin resistance [6], impair β-cell function [7], and anti-inflammatory mediators may reverse both [8, 9], implying that inflammation may be directly involved in the pathogenesis of T2D. Hence, activation of the innate immune system and triggering of local as well as systemic inflammation are hallmarks of both T1D and T2D.

In the event of immune system activation, the signaling and activation of immune cells is brought by secreted stimulators as well as via cell-cell interactions. Different cell surface receptors and adhesion molecules play a role in the immune system activation. One such family of adhesion and signaling molecules are Sialic acid-binding immunoglobulin-like lectins (Siglecs) [10]. Siglecs are I-type lectins which recognize and interact via immunoglobulin (Ig)-like domains with sialylated glycan residues on same cell surface (*cis*-interaction) or on neighboring cell surface, extracellular matrix protein or secreted glycoproteins (*trans*-interactions). The siglecs can be divided into two groups: an

evolutionarily conserved subgroup (Siglecs-1, -2, -4 and -15) and a rapidly evolving CD33/Siglec- 3-related subgroup (Siglecs-3, -5 to -11 and -14, -16 in primates) [11]. Only Siglec-4 (myelinassociated glycoprotein, MAG) expressed on glial cells and placental Siglec-6 are siglecs present on non-hematopoetic cells. All other siglecs are expressed on the hematopoietic and immune cells, in a very cell-type specific manner. Every siglec recognizes specific sialic acid linkages, thus hinting towards their unique function [12]. Typically, cytoplasmic motifs of siglecs show presence of one or more immunoreceptor tyrosine-based inhibitory motifs (ITIMs). These ITIMs recruit tyrosine phosphatases and eventually can inhibit activatory signals of other receptors. These cell-cell signaling interactions play a role in the immune system [13]. To verify the presence and function of siglecs in the infiltrating immune cells in islets, we investigated expression levels of siglecs in the pancreas. Surprisingly, these investigations have brought to surface the presence of siglecs in noninflammatory cells in pancreatic tissue, opening a whole new perspective for the role of siglecs in general. Here, we show cell type specific siglec expression in the human endocrine pancreas. Because of its specific presence on β-cells, we focused our experimentation on Siglec-7. Cloned for the first time in 1999 [14], Siglec-7 is a CD-33 related siglec constitutively expressed on all natural killer (NK) cells, monocytes and also on a subset of T cells [15]. Structurally, it is characterized by 3 immunoglobulin-like extracellular domains (one NH 2-terminal V-type and two C2-type), a trans-membrane region and a cytoplasmic tail containing two tyrosine residues located in immunoreceptor tyrosine-based inhibitory motifs. Siglec-7 acts as an inhibitory receptor in human NK cells after engagement by antibodies [14] or binding with sialic acid-containing ligands [16]. Upon phosphorylation, it can recruit the SH2 domain-bearing protein tyrosine phosphatase (PTP) SHP-1 [14]. Anti-Siglec-7 Abs also inhibits the proliferation of myeloid cells [17]. Also, Siglec-7 inhibits the FcRI-mediated serotonin release from RBL cells following crosslinking. The ITIMs are essential for this inhibitory function, and facilitate tyrosine phosphorylation and recruitment of SHP-1 and

SHP-2 phosphatases [18]. Siglec-7 is also expressed on a subset of T-cells and negatively regulates T-cell receptor (TCR) signaling [19]. Thus, Siglec-7 can be considered as an inhibitory receptor, participating in the regulation of cell function and survival. The present study identifies the role of cell adhesion molecules, siglecs, in the manifestation and progression of T2D. We investigated, whether inhibitory signals by Siglec-7 can restore β-cell survival and function in a diabetic milieu and whether Siglec-7 expression can influence immune cell migration.

Methods

Islet culture. Human islets were isolated from ten pancreata of healthy and 3 diabetic organ donors at the University of Lille or University of Leiden and cultured in CMRL-1066 medium (Invitrogen) as described previously [20]. Islets from SigF-/- mice and their WT and heterozygous littermates were isolated as described previously [1]. Pancreata were perifused with a Liberase TM (#05401119001, Roche, Mannheim, Germany) solution according to the manufacturer's instructions and digested at 37°C, followed by washing and handpicking. Mouse islets were cultured in RPMI-1640 medium supplemented with 100 units/ml penicillin, 100 mg/ml streptomycin, 10% fetal bovine serum, 1 mM sodium pyruvate, 2 mM L-Glutamine, 0.25 µg/ml Fungizone® Antimycotic (Gibco) and 0.1 mg/ml Gentamycinsulfat (Gemini). Briefly, islets were cultured on extracellular matrix coated dishes derived from bovine corneal endothelial cells (Novamed Ltd., Jerusalem, Israel) for 2 days, allowing the cells to attach to the dishes and spread [21]. They were exposed to 5.5, 22.2 or 33.3 mM glucose, with or without 0.5 mM palmitate (dissolved as described previously [22]) or the mixture of 2 ng/ml recombinant human IL-1β (R&D Systems, Minneapolis, MN) +1,000 U/ml recombinant human IFN-γ (PeProTech, Rocky Hill, NJ, USA) for 72h. For depletion of macrophages mouse islets were cultured in suspension with 0,5 mg/ml clodronate or PBS containing liposomes for 48 h, washed and plated for further experiments afterwards.

Animal studies. Siglec-F-knockout mice were kindly provided by Ajit Varki. For MLD-STZ experiments, 8 week old Siglec-F-/- mice on a B6 genetic background and their heterozygous Siglec-F+/- and WT littermates were injected i.p. with streptozotocin (STZ; 50 mg/kg; Sigma) freshly dissolved in 50mM sodium citrate buffer (pH 4.5) for 5 consecutive days (referred to as multiple low dose/MLD-STZ). Random blood was obtained from the tail vein of non-fasted mice and glucose was measured using a Glucometer (Freestyle; TheraSense Inc., Alameda, CA). All animals were housed in a temperature-controlled room with a 12-hour light/dark cycle and were allowed free access to food and water in agreement to NIH animal care guidelines of the §8 German animal protection law and approved by the Bremen Senate. For intraperitoneal glucose tolerance test (ipGTTs), mice were fasted 12h overnight and injected i.p. with glucose (40%; B.Braun, Melsungen, Germany) at a dose of 1 g/kg body weight. Blood samples were obtained at time points 0, 15, 30, 60, 90, and 120 min for glucose measurements using a Glucometer. For glucose stimulated insulin secretion mice were fasted for 12h overnight and blood samples were collected retrobulbar at timepoints 0 and 15 min for measurement of serum insulin levels. Insulin secretion was measured before (0min) and after (15min) i.p. injection of glucose (2 g/kg) and measured using ultrasensitive mouse Elisa kit (ALPCO Diagnostics, Salem, NH).

Transfection. At 2 days post-isolation and culture on extracellular matrix coated dishes, isolated islets were transfected using Ca2+-KRH medium (KCl 4.74 mM, KH2PO4 1.19 mM, MgCl26H2O 1.19 mM, NaCl 119 mM, CaCl2 2.54 mM, NaHCO3 25 mM, HEPES 10 mM). After 1h incubation lipoplexes (Lipofectamine2000, Invitrogen, Carlsbad, CA, USA)/DNA ratio 2.5:1, 5 µg CMV-Siglec-7 (Life technologies) or LacZ/GFP control plasmid DNA/100 islets or 100 nM siRNA to Siglec-7 (ON-TARGETplus SMARTpool against human *Siglec-7*, (Dharmacon, Lafayette CO, USA) and scramble siRNA (Dharmacon) were added to transfect

the cells as described previously [23, 24]. After additional 6h incubation, CMRL 1066 medium containing 20% FCS and L-Glutamine were added to the transfected islets. Transfection efficiency was determined using RT PCR.

Glucose stimulated insulin secretion. Islets used to perform glucose-stimulated insulin secretion experiments were kept in culture medium on matrix-coated plates. For acute insulin release in response to glucose, islets were washed and pre-incubated (30 min) in Kreb's Ringer bicarbonate buffer (KRB) containing 2.8 mM glucose and 0.5% BSA. KRB was then replaced by KRB 2.8 mM glucose for 1 h (basal), followed by an additional 1 h in KRB 16.7 mM glucose (stimulated). Islets were extracted with 0.18 N HCl in 70% ethanol for determination of insulin content. Islet insulin was determined using mouse insulin ELISA (ALPCO, Salem, NH, USA).

RNA extraction and RT-PCR analysis. Total RNA was isolated from cultured Human and mouse islets as described previously [20]. For gene expression analysis of siglecs, semi-quantitative Real Time-PCR was performed in the StepOne Plus Real Time PCR system (Applied Biosystems, Darmstadt, Germany) using Power SYBR Green PCR Master Mix (Applied Biosystems, Darmstadt,Germany). cDNA based on RNA from human pancreatic tissues were analyzed for the genes cyclophilin, glucagon, SAT2, insulin and SN1. Amplification of the endogenous housekeeping gene cyclophilin as well as the genes glucagon, SAT2, insulin and SN1 consisted of an initial denaturation step at 95°C for 10 min, followed by 40 PCR cycles of denaturation by 95°C for 30 s, primer annealing by 60°C for 20 s, and elongation by 72°C for 10 s. All Siglecs were amplified carrying out the touchdown PCR with annealing temperatures from 57°C-53°C in each 5 cycles. Primers used for this RT-PCR were:

(Siglec-7)

5'AAGAAGCCACCAACAATGAG3'/5'CAGTTAGACAAGAGGAATAAGTTC3';

(Siglec-3) 5'TGGTGTGACTACGGAGAG3'/5'ATGAAGAAGATGAGGCAGAG3'

(Siglec-10) 5'CATTATGCCACGCTCAAC3'/5'TCTTCAACCTCTTACTCTACC3';

(insulin) 5'CTACCTAGTGTGCGGGGAAC3'/5'GCTGGTAGAGGGAGCAGATG3';

(glucagon) 5'CATTCACAGGGCACATTCAC3'/5'CAGCTTGGCCTTCCAAATAA3';

(SN1) 5'TACGACGTGCTATCCAGCAG3'/5'CCAGGATTTTAGGGGTGGAT3';

(SAT2) 5'AGTTGCCTTTGGTGATCCAG3'/5'CAGGACACGGAACCTGAAAT3' and

(PPIA) 5'TACGGGTCCTGGCATCTTGT3'/5'CCATTTGTGTTGGGTCCAGC3'.

For analysis of PBMCS and isolated islets, we used the Applied Biosystems StepOne Real-Time PCR system (Applied Biosystems, Carlsbad, CA, USA) with a commercial kit (TaqMan(R) PCR Master Mix; Applied Biosystems). TaqMan(R) Primers used: Siglec-7 (Hs00255574_m1); Siglec-3 (Hs00233544_m1); ST8SIA1 (Hs00268157_m1); PPIA (Hs99999904_m1); CD25 (Hs00907779_m1); Neu3 (Hs00198406_m1); Siglec-E (Mm01205915_g1); Siglec-F (Mm00523987_m1); CD68 (Mm03047343); CD11b (Mm00434455_m1); F4/80 (Mm00802529_m1); IL1β (Mm00434228_m1); IL6 (Mm00446190_m1); Ins1 (Mm04207513_g1); Ins2 (Mm00731595_gH); Pdx1 (Mm00435565_m1); β-Actin (Mm00607939_s1).

Western Blot analysis. At the end of the incubation periods, islets were washed in ice-cold PBS and lysed in 40 µl lysis buffer RIPA (20 mM Tris acetate, 0.27 M sucrose, 1 mM EDTA, 1 mM EGTA, 50mM NaF, 1% Triton X-100, 5 mM sodium pyrophosphate and 10 mM β-glycerophosphate) by repeated rounds of freezing and thawing on ice. Prior to use, the lysis buffer was supplemented with Proteaseand Phosphatase-inhibitors (Pierce, Rockford, IL, USA). Protein concentration was measured using BCA assay (Pierce, Rockford, IL, USA). Equivalent amounts of protein from each treatment group were run on a NuPAGE 4-12% Bis-Tris gel (Invitrogen) and electrically transferred onto PVDF membranes. Membranes were incubated with rabbit anti- p-IκBα; rabbit anti- p-p65 rabbit anti-β-actin (Cell Signaling Technology, Danvers. MA, USA) antibodies, followed by horseradishperoxidase-linked anti-

rabbit IgG. Membrane was developed using a chemiluminescence assay system (Pierce) and analyzed using DocIT®LS image acquisition 6.6a (UVP BioImaging Systems, Upland, CA, USA). Densitometric analysis of the blots was carried out using Vision Works LS Image Acquisition and Analysis software Version 6.8 (UVP BioImaging Systems, Upland, CA, USA). The gray scale values were normalized on the housekeeping genes as loading controls, and the fold change against control condition was plotted.

Immunocytochemistry. Pancreas from 5 healthy controls and from 5 patients with T2DM were obtained from the National Disease Research Interchange (NDRI), approval for the studies were granted by the Ethical Commission of Bremen University. The tissues were fixed in 4% paraformaldehyde overnight and embedded in paraffin. Islets cultured in suspension were washed with PBS and were fixed in Bouin's (Sigma, Hamburg, Germany) solution for 15 min, resuspended in 2% melted agarose in phosphate buffered saline (PBS), followed by short centrifugation and paraffin embedding. Both, islet agarose pellets and human tissue samples were washed overnight in 70% ethanol followed by dewatering in ethanol and xylol and paraffin embedding using Leica TP1020 tissue processor (Leica, Microsystems, Wetzlar, Germany). 4μm sections were cut using a microtome and mounted on slides. For immunohistochemical analysis of pancreatic and islet sections, they were deparaffinized and rehydrated by washing twice in toluene for 10 min, respectively, in 100%, 95% and 70% ethanol for 3 min, and then in water for 5 min. Slides were then exposed to antigen-retrieval using Antigen Unmasking Solution (Vector Laboratories, Inc. Burlingame, CA) prewarmed in a microwave at 600 Watt for 3 cycles each 5 min. and 1 min break in between each cycle. The sections were then cooled to room temperature and permeablized in soaking buffer (0.4% Triton X-100 in TBS) for 30 min. After this, to minimize unspecific binding of antibodies, slides were incubated in blocking buffer containing 0.2% Tween 20, 3% IgG-free Bovine serum albumin (BSA), and 0.5% Triton X-100 or 1 h RT. For Fc-chimera staining, Human Fc receptor blocking reagent (MACS #130-059-901) was used for 15-20 min room temperature.

As a negative control for staining with Fc chimera, slides were treated with 10mU/ml *V. cholerae* sialidase (Roche) for 2h at 37°C. Primary antibodies were diluted (1:50 or 1:100) in the antibody dilution buffer (0,2% Tween 20, 3% IgG-free BSA in TBS) as recommended and incubated with the slides for either 1 h room temperature or overnight at 4°C. Antibodies used were: polyclonal rabbit anti-Siglec-7 (Abcam, Cambridge, UK); rabbit anti-human CD22 (Abcam, Cambridge, UK); rabbit anti-human Sialoadhesin (Abcam, Cambridge, UK); monoclonal mouse anti- Siglec-7 (kindly provided by Prof. Paul Crocker), polyclonal sheep anti-Siglec-3,-5,-8,-7 and -10 (kindly provided by Prof. Paul Crocker); Siglec-7 Fc-chimera (kindly provided by Prof. Sørge Kelm); GD3 (R24; Abcam); guinea pig anti-insulin and mouse anti-glucagon. Secondary antibodies were against the primary antibody species and were either FITC- , Cy3- or AMCAconjugated antibodies (Dako, Hamburg, Germany). For bright field staining, the secondary antibodies conjugated to enzyme alkaline phosphatase were used, followed by development with BCPI/NBT substrate (Sigma, Steinheim, Germany) for 15 min at room temperature. After the staining procedures, slides were mounted with Vectashield with 4'6-diamidino-2-phenylindole (DAPI) (Vector Labs) or Glycerogelatin. Fluorescence was analyzed using a Nikon MEA53200 (Nikon GmbH, Dusseldorf, Germany) microscope and images were acquired using NISElements software (Nikon). Intensity and saturation of the staining was measured using Adobe Photoshop© Extended analysis software after an adapted model used by Pham et al [25]. Briefly, the insulin positive area in the green channel was manually marked and the selection was saved. By loading this selection onto the red channel image, the area positive for Siglec-7 or GD3 was assigned and measurements were recorded. The mean gray scale values were termed as the saturation and the integrated density values considered as intensities. For detection of β-cell apoptosis and proliferation, insulin and TUNEL (In Situ Cell Death Detection Kit -AP; Roche Diagnostics, Mannheim, Germany) or Ki67 staining (Mouse anti-Ki67 (7B11) prediluted, Invitrogen, Camarillo, CA, USA) were performed as described previously [26]. Dishes were analyzed using Nikon

MEA53200 (Nikon GmbH, Dusseldorf, Germany) microscope and images were acquired using NIS-Elements software (Nikon).

Cytokine quantification. The cell culture supernatants stored at -20°C were evaluated in a cytokine multiplex array system called Meso Scale Discovery® (Gaithersburg, MD, USA) using a kit (Human Pro-inflammatory II 4-plex assay) read at the Sector Imager 6000® as per manufacturer's instructions. The platform uses electrochemiluminescence technology, in which multiple specific capture antibodies are coated at corresponding spots on an electric wired microplate. The detection antibody is conjugated to a tag which is excited with emission beams in the electric field applied by the reading instrument. Co-reactants present in the "read buffer" amplify these electric signals [27]. Using a standard curve these signals are quantified and expressed as absolute concentrations.

PBMC isolation. The isolation of PBMCs from buffy coats was adapted from Repnik U et.al.[28]. Briefly**,** buffy coats were obtained from the Central Institute for Transfusion Medicine, Hamburg (Germany) and WBCs were Purified using a Ficoll gradient (GE healthcare, Uppsala, Sweden), a subsequent hyperosmotic Percoll gradient (GE healthcare, Uppsala, Sweden) led to separation of monocytes from lymphocytes and a third iso-osmotic Percoll gradient to monocytes from platelets and dead cells. The pellet obtained after this gradient is the monocyte-enriched fraction, which we refer to as PBMCs. According to the forward and side scatter plots, this fraction contains about 55-80% monocytes along with 45-20% of lymphocytes.

Flow cytometry. The PBMC fraction was cultured in RPMI supplemented with 10% FCS, 2 mM L-Glutamine and 100 U/ml Penicillin-Streptomycin for 12 hours with or without 22.2 mM glucose and 0.5 mM Palmitate. Mouse islets from Siglec-F-/- and their corresponding controls or WTB6 mice were treated with Accutase (PAA, Cat.-No: L11-007) to reach a single cell state. They were seeded on extracellular-matrix coated dishes and allowed to recover for 24h. For flow cytometry of PBMCs and islet cells, they were fixed in freshly-

prepared 1% paraformaldehyde for 10 min at RT. After washing, PBMCs were incubated in polyclonal rabbit anti-Siglec-7 Ab (Abcam) followed by incubation with FITC/Alexa 488 labeled donkey anti-rabbit secondary antibody (Dako, Hamburg, Germany). Rabbit IgG was used as isotype control. For CD25 and CD14 labeling, the PE conjugated anti-CD25 Antibody (Beckman and Coulter A0 7774) and PE-Cy5 conjugated anti-CD14 (Beckman and Coulter A0 7765) were incubated for 30 min at 37°C. Islet cells were incubated with monoclonal rat-anti Siglec-F (BD Pharmingen) or polyclonal goat anti-Siglec-E (R&D systems) antibodies, followed by FITC-labeled secondary antibodies from donkey (Dako, Hamburg, Germany). The fractions analyzed by FACS were: unstained, control with only secondary, single labeled Siglec-E and Siglec-F, or Siglec-7, CD14 and CD25 and a triple stained fraction. Statistical analysis has been performed on the cell populations in all the different quadrants of the dot plots of CD14 vs. Siglec-7 and CD25 vs. Siglec-7 in the triple stained samples, and the data represented in the graphs signify quantifications of the co-stained populations.

Statistical analysis. Samples were evaluated in a randomized manner by G.D, who was blinded to the treatment conditions. Data are presented as means +/- SE and were analyzed by Student's *t*- tests.

Results

Siglecs are differentially expressed in human pancreatic islets

Siglecs are classically expressed in the cells of the hematopoietic system and regulate the inflammatory cell response. Since many pattern recognition receptors and cytokine receptors are highly expressed on β-cells, we assessed expression levels of the 10 classical siglecs in the human pancreas. Immunofluorescent labeling of siglecs, insulin and glucagon revealed the presence of siglecs predominantly in the endocrine pancreas. The evolutionarily conserved siglecs Siglec-1 (Sialoadhesin) and Siglec-2 (CD22); as well as Siglec-7 and -10 were expressed exclusively in the β-cells (Fig.1A-D) and Siglec-3,-5, and -8 were expressed solely by the α-cells (Fig.1E-G). In contrast, Siglec-4, -6 and -9 were not expressed in the pancreatic islets. The cellular localization was confirmed by carrying out Confocal Laser Scanning Microscopy (data not shown). Cell surface expression of Siglec-7 in islets was confirmed by flow cytometric analysis of dispersed islets (Supp. Fig. 1A). In addition to this, the presence of Siglec-7 was tested using two different polyclonal antibodies and a monoclonal antibody (data not shown), which validated our observations in human pancreas sections.

Siglec-7 and -3 are oppositely regulated in type 2 diabetes

In order to understand the role of siglec expression in the endocrine pancreas, we investigated whether siglecs are regulated in T2D. Semi-quantitative real time PCR analysis was performed on cDNAs obtained from non-diabetic and diabetic human pancreas from autopsy. In addition to housekeeping genes, expression levels of siglecs were normalized on cell specific markers of β- and α-cells i.e. insulin and glucagon, to account for the changes in their mass in diabetic individuals. In addition, pancreatic siglec expression was normalized to the β- and α-cell specific glutamate receptors SN1 and SAT2, whose expression is unregulated in diabetes [29]. Siglec-7 expressed on β-cells was drastically decreased in diabetic individuals when normalized on expression levels of cyclophylin (PPIA), insulin and SN1 (Fig.2A; reduced by 94%, 85%, 94%) respectively in individuals with T2D). Also, Siglec-10 was

significantly downregulated in T2D as compared to cyclophylin (PPIA) and SN1 and showed similar tendency when normalized on insulin (Supp.Fig.1B). On the other hand, the α-cell specific Siglec-3 showed substantial increase in diabetes upon normalization with cyclophylin (PPIA), glucagon and SAT2 (Fig.2A; induced to 5.15-, 4.29-, 5.52-fold, respectively in individuals with T2D, vs. non-diabetic controls). A decrease in insulin mRNA was confirmed in T2D (Fig.2B), while glucagon mRNA showed an increase in T2D (Fig.2C) and β- and α-cell specific SN1 and SAT2 remained unchanged in T2D (Fig.2D, E). The down-regulation of β-cell siglecs was confirmed in freshly isolated human islets from organ donors with T2D and controls. Siglec-7 showed 87% reduction vs non-diabetic control islets (Fig.2F) and Siglec-10 showed a similar decrease (Suppl.Fig.1C). Because of the β-cell specific expression and significant regulation in diabetes, we focused our research on the presence and implication of Siglec-7 in the progression of diabetes. Siglecs bind to different linkages of the terminal sialic acid to its underlying glycan with varying affinities [30]. Siglec-7 has a binding preference for α2,8-linked disialic acid, which leads to downstream signaling via its cytoplasmic inhibitory motifs [31]. In contrast to Siglec-7, the sialyl-transferase responsible for α2-8 linkage formation, St8Sia1 showed a tendency of up-regulation in the diabetic islets (Fig.2G), suggestive of a compensatory mechanism. The membrane-associated sialic acid-cleaving enzyme sialidase Neu3 (Fig.2H), which may unmask Siglec-7 residues and thus induce Siglec-7 mediated inhibition of cell death [16], was significantly down-regulated in T2D islets, which is a further deleterious signal in the inflammation-initiation cascade. GD3 is one of the endogenous ligands for Siglec-7 which displays 2,8-linked disialic acids [32]. High levels of GD3 reverse the Siglec-7 protective functions in cell survival [16]. Its constitutive expression was detected in β-cells in human pancreas sections by immunofluorescent labeling. As compared to non-diabetic individuals GD3 was more strongly expressed in patients with T2D. Quantification of the staining showed a 1.50-fold and 3.27-fold increase in intensity and saturation respectively in non-diabetic controls vs. patients with T2D (Fig.2I, J).

The loss in Siglec-7 expression was confirmed in the same sections from autopsy and showed a 60% and 63% decrease in intensity and saturation respectively in patients with T2D vs. non-diabetic controls (Fig.2K, L). We further confirmed the opposite regulation of Siglec-7 ligands by another biochemical approach. Chimeric proteins consisting of the IgG like V-set domain attached to an Fc-region were constructed, expressed and purified from the Cholec1 cell line [33]. They were used as probes to detect the presence of their binding partners. As a negative control, slides treated with sialidase were probed, in which there was no detection of ligands. Bright field staining of the chimeras revealed the presence of Siglec-7 ligands in both α- and β-cells (Fig.2M), which was increased in pancreatic sections of patients with T2D. These findings hint towards a disruption of Siglec-7 engagement in diabetic islets, and the cells attempt to counteract this by up-regulating its ligands.

Siglec-7 over-expression improves β-cell survival and function

In order to understand the physiological impact of decreased Siglec-7 expression in diabetes, we used an *in vitro* model of human islets exposed to a diabetic milieu of elevated glucose (22.2-33.3 mM) (HG) and free fatty acid (0.5 mM palmitate)(Pal) levels or the cytokine mixture of IL-1β and IFNγ (IL/IF) and subsequently investigated whether re-expression of Siglec-7 can restore β-cell function and survival under diabetogenic conditions. Siglec-7 was restored by liposome-mediated transfection of human islets isolated from non-diabetic and diabetic (T2D) organ donors. Plasmid over-expression of Siglec-7 was analysed using flow cytometry following over-expression in HEK293T cells (Supp.Fig.1D). β-cell function (Fig.3A-D) and survival (Fig.3E-F) were impaired by all diabetogenic culture conditions (Fig.3A,C,D) as well as in islets isolated from patients with T2D (3B,D,F). In contrast, Siglec-7 over-expression improved β-cell function and survival at all diabetic conditions (3A-F) in healthy non diabetic islets as well as in islets isolated from T2D organ donors, where Siglec-7 over-expression completely normalized β-cell function and survival in these islets (Fig. 3B, D and F). Treatment of diabetic islets with a diabetic milieu did not further impair

the β-cells. In line with our observation in the diabetic pancreas, diabetogenic conditions *in vitro* led to a loss in Siglec-7 expression (Fig.3G). Down-regulation of Siglec-7 by siRNA shows that a loss of Siglec-7 alone impairs β-cell function *in vitro* (Fig.3H, I; 60% reduction in GSIS, as compared to scramble transfected control islets). Furthermore, the deleterious effects of glucolipotoxicity and cytokines impair insulin secretion in β-cells; loss of Siglec-7 adds to it as seen by a tendency of lower stimulatory indices in cytokine treated islets. This down-regulation may directly influence β-cell survival and function under these conditions. We checked for possible mechanisms by which Siglec-7 can bring about inhibition of destruction of β-cells.

Siglec-7 over-expression inhibits NF-κB activation and cytokine production

Islets exposed to elevated glucose and palmitate or cytokines are triggered to secrete pro-inflammatory cytokines. As Siglec-7 is an inhibitory cell adhesion molecule on immune cells [34], we hypothesized that the protective role of Siglec-7 was mediated via the inhibition of inflammation. Expression and secretion of both IL-1β and IL-6 were induced by exposure of islets to elevated glucose and palmitate as well as by the cytokine mixture; this was strongly inhibited on islets over-expressing Siglec-7 (Fig. 4A-D). In order to identify the underlying signaling cascades of Siglec-7 mediated β-cell protection, downstream inflammatory pathways were investigated. Western blot analysis of isolated islets treated with elevated glucose and palmitate and the cytokine mixture revealed the activation of the NF-κB pathway, as observed by the induction of phosphorylation of IκB-α and p65 phosphorylation at Ser536, both core components leading to NF-κB activation (Fig.4E,F). This induction could at least be partially prevented by over expression of Siglec-7 shown by subsequent decrease in IκB-α phosphorylation (Fig.4E, H, I). p65 phosphorylation at Ser536 merely enhances its transcription factor activity and is known to be independent of IκB-α [35]. Nevertheless, also the induction of p65 phosphorylation upon cytokine treatment was inhibited upon Siglec-7 over-expression (Fig.4F, J, K). These observations consolidated the immunosuppressive role

of Siglec-7 in the prevention of triggering islet inflammation observed in diabetes. Since also PBMCs showed induction of phosphorylation of IκB-α and p65 phosphorylation at Ser536 in response to elevated glucose and palmitate and the cytokine mixture IL/IF (Fig.4G), we subsequently analyzed Siglec-7 expression in PBMCs under a diabetogenic milieu.

Loss of Siglec-7 is a hallmark of LPS and Gluc/Pal mediated monocyte activation.

Since Siglec-7 is classically expressed by cells of the immune system, we investigated whether diabetogenic conditions would also affect Siglec-7 expression in enriched monocytes. The monocyte-enriched fraction of peripheral blood mononuclear cells (PBMCs) was isolated from human buffy coats using sequential Ficoll-Percoll gradients and exposed to control media, Lipopolysaccharide (LPS, 20 μg/ml) as known activator of the immune cells or the mixture of 22.2 mM glucose and 0.5 mM palmitate. The activated state of these cells was analyzed at 2h and 12h after treatment by real time PCR analysis of the expression of CD25 and the cytokine IL-6. The activation of the canonical NF-κB pathway in PBMCs after the chronic treatments was seen by western blot analysis of the cell lysates (Fig.4G). LPS elucidated rapid (after 2h) and sustained (after 12h) activation of immune cells, as seen by the induction of IL-6 expression after 2h exposure (Fig.5A, B; ~22-fold/~390-fold at 2 and 12h as compared to control). Elevated glucose/palmitate induced a similar activation pattern in monocytes but to a lesser extent (Fig.5A, B; ~4-fold/~50-fold at 2 and 12h as compared to control). Both LPS and glucose/palmitate induced the expression of CD25 after 2h and, similar to IL-6, CD25 expression was much higher induced after 12h, with LPS showing a stronger effect (Fig.5C, D; ~45-fold, ~3-fold at LPS and Gluc/Pal respectively, as compared to control). In parallel, Siglec-7 m-RNA expression was down-regulated already after 2h treatment with LPS and glucose/palmitate (Fig.5E, F; 45% reduction as compared to control). While LPS-induced Siglec-7 down-regulation was only transient, glucose/palmitate induced a sustained Siglec-7 down-regulation (Fig.5F; 47% reduction as compared to control), suggesting the chronic nature of activation of these cells under conditions of

glucolipotoxicity. In line with our findings that Neu3 is decreased in islets in T2D, there was marked down-regulation of Neu3 gene expression in the activated PBMCs at both acute and chronic treatments (Fig.5G, H). For confirming the changes in mRNA, we carried out flow cytometric analysis of the treated PBMCs (Fig.5I). The mean fluorescence intensity of Siglec-7 staining of cells treated with LPS and glucose/palmitate was decreased by 21.38% and 28.49%, respectively, as compared to control (Fig.5J), along with increased expression of CD25 (Supp.Fig.3). To assess the Siglec-7 expression in activated cell population, cell surface expression of CD25 and CD14 was checked along with Siglec-7. By plotting the intensity of Siglec-7 vs intensity of either CD14 or CD25, followed by quadrant analysis, we determined the Siglec-7 intensity in these cells. The CD25 and Siglec-7 population increases upon exposure to LPS or Gluc/Pal, and the Siglec-7 expression in these cells decreased. On the other hand CD14+ Sig7+ cells showed a decline in these conditions, with Siglec-7 staying stably expressed in these cells. Thus, loss of Siglec-7 expression was observed only in activated PBMCs, indicating the decreased immune-suppression in these conditions (supplementary figure 2).

Immune cell migration into inflamed islets is inhibited by Siglec-7

Increased infiltration of macrophages has been observed in islets in T2D [36]. To elaborate on the immune-regulatory role of Siglec-7, we evaluated the migration of monocytes *in vitro* in response to conditioned media obtained from isolated human islets, which had been exposed to diabetogenic conditions. For this, we established an *in vitro* migration assay wherein leukocytes isolated from human buffy coats were allowed to migrate over a period of 4h through a 1µm pore size membrane to the lower compartment containing the conditioned islet media. The membranes were mounted in fluorescein diacetate solution, which rendered the live cells fluorescent upon excitation and enabled quantification by fluorescence microscopy (Fig.5M). Induced migration of immune cells was observed under conditions of elevated glucose/palmitate (Fig.5K, 9.61-fold as compared to control), which demonstrates the

triggering of inflammation in islets upon chronic exposure to elevated glucose/palmitate. Conditioned media from islets overexpressing Siglec-7 majorly inhibited cell migration of immune cells (Fig.5K, 74% reduction as compared to glucose/palmitate-treated, LacZ-transfected control islets). We also analysed the migratory response of the cells towards isolated islets obtained from patients with T2D. Islet supernatants from T2D islets induced significantly higher migration of the immune cells (Fig. 5L, ~ 2.2-fold induction as compared to non-diabetic islet supernatants, $p<0.05$) which could also be blocked by restoring Siglec-7 expression in these islets (Fig. 5L 54%, reduction as compared to lacz-transfected control T2D islets, $p<0.05$). Treatment with glucose and palmitate could not further induce the migration in diabetic islets, but Siglec-7 over-expressing islets showed a decreased tendency of immune cell migration (data not shown). These findings elaborate on the anti-inflammatory role and the inhibition of immune cell stimulation by Siglec-7 in β-cells.

Siglec-F does not affect diabetes progression in mice

Next we sought to understand whether Siglecs play a role in diabetes in vivo and investigated expression patterns of Siglec orthologues in mouse islets. FACS staining of isolated and dispersed islet cells displayed only a very low percentage of Siglec-F positive cells (Fig. 6A), which was specific, since a signal reduction was observed in Siglec-F knockout mice. Similarly only a very small population of Siglec-E expressing cells was found (Fig. 6B). Because of the small amount of Siglec-E and –F positive cells we wondered, which islet cells express the Siglecs and whether the low signal comes from resident macrophages within the islets. Isolated wildtype islets were treated with clodronate containing liposomes to deplete the macrophages, which reduced CD68, F4/80 as well as CD11b expression significantly (Fig 6C). Along with reduction of the macrophage markers, also Siglec-E was strongly and significantly reduced and Siglec-F wasn`t even detectable after macrophage depletion (Fig. 6E), while β-cell markers remained unchanged (Fig. 6D). As expected, also cytokine expression was affected by clodronate treatment. While IL-6 did not change, IL-1β was

significantly reduced compared to PBS control, indicating resident macrophages as the main source of IL-1β release (Fig. 6E). We also tested Siglec-G and –H expression, but were not able to detect them in islets.

Because inner-islet inflammation plays a causative role in diabetes progression, we further investigated the role of Siglec-F in the multiple low dose streptozotocin (STZ) model of diabetes. 8-week old male Siglec-$F^{-/-}$ mice and their heterozygous and wildtype littermates were injected with 50 mg/kg STZ on 5 consecutive days to induce diabetes. STZ injected mice showed higher random blood glucose levels (Fig. 6F), reduced glucose tolerance (Fig. 6G), as well as impaired insulin secretion (Fig. 6H), but no differences between the different genotypes were detectable (Fig. 6F, G, H). To further confirm no effect of Siglec-F on diabetes progression, we isolated wildtype, Sig-$F^{+/-}$ and Sig-$F^{-/-}$ islets and treated them with high glucose/palmitate or a cytokine mixture for 72h. Also in vitro, diabetogenic conditions reduced insulin secretion in all genotypes to the same extent (Fig. 6J).

Discussion

The present study investigated the role of sialic acid-binding immunoglobulin-like lectins (Siglecs), a novel, and still-expanding family of cell adhesion molecules, in islet inflammation observed in T2D. Siglecs, previously known to be majorly expressed in the hematopoietic cells, are also expressed, in a cell type specific manner, in the endocrine pancreas. Of the evolutionarily evolving CD-33 related siglecs which were investigated, Siglec-7 and -10 were expressed solely in the β-cells, whereas Siglec-3, -5 and -8 were expressed only in the α-cells. Although Siglec-7 shares around 84% sequence homology with Siglec-9 [37], its presence was undetectable in the endocrine pancreas as assessed by real-time PCR and immunohistochemical analyses. The β-cell specific Siglec-7 and -10 were markedly down-regulated in pancreas of individuals with T2D. In contrast, Siglec-3 was significantly up-regulated in α-cells in T2D.

Owing to the significant, drastic regulation of Siglec-7 in diabetes, we focused our research on its role in the β-cells. A marked decrease in the surface expression of Siglec-7 is the foremost marker of the aberrant NK-cell dysregulation in patients with chronic HIV-1 viremia [38]. Similarly, we saw down-regulation of Siglec-7 in β-cells, in T2D. Thus, we hypothesized that the loss of Siglec-7 in the β-cells contributed to their dysfunction and apoptosis. Indeed, restoring surface Siglec-7 expression protected the β-cells from deleterious effects of a diabetic milieu. Siglec-7 could not only maintain glucose stimulated insulin secretion even under diabetogenic conditions, but also inhibit β-cell apoptosis. This rescue of function and survival was also evident in *in vitro* studies of freshly isolated T2D islets. Additionally, depletion of Siglec-7 in healthy isolated control islets impaired β-cell function. Hence, we could conclude that loss of Siglec-7 in the β-cells contributed to their destruction observed in T2D. Siglec-3 also has cytoplasmic ITIMs, but its functional significance in α-cells needs to be further investigated. Also, it is one C2-set domain shorter than Siglec-7, and might vary its interactions within the islets. Siglec-7 has an unusual binding preference for α-2,8-linked disialic acids and weaker interactions with branched α-2,6 sialyl residues [31]. Subsequently, we immunohistochemically investigated the presence of these binding partners in the human pancreas using Siglec-7 Fc-chimeras, and found them to be expressed in islets. Interaction partners were present in both α- and β-cells, indicating possibility of intra-islet *trans* interactions of Siglec-7 with its ligands on both these cell types. An endogenous ligand of Siglec-7, ganglioside GD3, was strongly up-regulated in diabetes. The disialoganglioside GD3 is an acidic glycosphingolipid, generated downstream of the ceramide-driven ganglioside biosynthesis, by sialylation of its immediate precursor GM3 by the GD3 synthase (α-2,8-sialyltransferase or ST8Sia I or SAT II) [39]. In freshly isolated islets obtained from autopsy of patients with T2D, we could detect a tendency of increase in ST8SiaI expression, which supported our observed up-regulation of GD3 in diabetic individuals. GD3 activates Fas and ceramide mediated apoptosis, directly targets mitochondria and disrupts

mitochondrial trans-membrane potential [40], leading to the release of apoptotic factors such as cytochrome c, production of ROS and activation of AIF and caspase-9 [41]. Its induced expression in diabetes, thus, hints not only towards feedback up-regulation of ligand upon loss of Siglec-7 expression, but also gives an indirect proof of activation of the pro-apoptotic signaling like that of the Fas receptor, previously reported in the context of glucotoxicity as well as immune mediated β-cell destruction in islets [42, 43]. Increased levels of GD3 in serum have also been implicated in inflammatory processes such as atherosclerosis [44] and lipopolysaccharide triggered inflammation in brain, wherein the microglial cells are activated and secrete GD3 leading to apoptosis of oligodendrocytes [45]. Parallels can be drawn between cytokines (e.g. IL-1β) and GD3, as both at low concentrations, stimulate cell proliferation while at high concentration triggers apoptosis [7, 46]. Also, GD3 expression has been observed specifically in the islets of a T1D mouse model i.e. NOD mice, whereas its precursor GM3 is expressed in the wild type islets [47]. Hence, increased GD3 expression reiterates the pro-apoptotic inflamed state of islets in T2D. While we observed increased GD3 synthase, the membrane-associated sialidase, specific for ganglioside, NEU3 [48] was decreased in islets isolated from individuals with T2D. NEU3 cleaves off the surface sialic acid residues, which can unmask Siglec-7 and induce its inhibitory signaling cascade [16]. This unmasking may be diminished in T2D, as observed by significantly lower levels of NEU3 consequently leasing to increased Siglec-7 ligand expression in diabetic islets. Tissue specific effects of NEU3 were observed previously; mice overexpressing NEU3 mainly in muscles develop severe insulin-resistant diabetes [49], but, hepatic NEU3 over-expression improves insulin sensitivity and glucose tolerance through modification of ganglioside composition and Peroxisome Proliferator-activated Receptor gamma (PPAR-γ) signaling [50]. In islets, PPAR-γ activation restores β-cell function under conditions of hyperglycemia and cytokine stress [51] and also regulates β-cell transcription factors PDX-1 and Nkx6.1[52]. Decreased NEU3 expression in T2D islets may thus lead to reduced PPAR-γ signaling, and

hence might contribute to β-cell dysfunction under diabetogenic conditions. Activated and insulin resistant immune cells have been observed in obesity [53]. Also, chronic exposure to FFAs leads to activation of monocytes, along with upregulation of toll-like receptors TLR2 and TLR4 [54], which leads to impaired glucose metabolism on the level of insulin sensitive as well as insulin producing cells. As Siglec-7 is endogenously expressed mainly by natural killer cells and monocytes and balances the immune response, the observed loss of Siglec-7 in PBMCs was a hallmark of activated monocytes under diabetogenic conditions. Acute exposure to LPS as well as elevated glucose and palmitate was sufficient to inhibit Siglec-7 expression. In spite of that, chronic exposure to LPS led to restoration of the messenger RNA, but maintained reduced cell surface expression of Siglec-7. Glucose and palmitate chronically kept both the mRNA and protein levels down, proving their chronic effect on the activation of the immune cells under circumstances when also IL-6 was induced. CD25, an atypical marker for activated macrophages [55] was induced after chronic treatment with the diabetic milieu, reiterating the activation of these cells. The down-regulation of Siglec-7 in activated PBMCs goes in hand with the decreased expression in islets under conditions of inflammation, which highlights its anti-inflammatory role in both these cell types. Ultimately, we investigated the effect of restoration of the siglecs in the islets on the actual infiltration of the immune cells. Maintaining Siglec-7 expression in stressed islets under glucolipotoxic conditions could inhibit the recruitment and migration of the immune cells. The increased number of macrophages per islet observed *in vivo* in diabetes [36] could, for the first time, be confirmed *in vitro* using a leukocyte migration assay, which also be prevented by restoring Siglec-7 expression in these islets. Hence, Siglec-7 expression in islets is essential for maintaining an anti-inflammatory environment in islets, which prevents subsequent immune system activation.

Because mouse animal studies play an important role in the research for the development and cure of Diabetes mellitus we investigated the role of CD33-related Siglec orthologues in mice.

FACS analysis showed only very low numbers of Siglec-E and -F positive cells within the islets. This expression pattern outlines Siglec expression in α- or β-cells, which display higher percentages in cell number within the islets. Because Siglecs are known to be expressed on cells of the immune system this signal could arise from intraislet resident macrophages. This was approved by depleting macrophages by clodronate liposomes, which reduced well established macrophage markers and Siglec-E and -F within the islet, while β-cell markers remained unchanged. This points to resident macrophages as the source for Siglec expression in mouse islets. Mouse and human islet cells differ in their morphology [56] and their transcriptome [57], which could lead to interspecies discrepancies like we found here. This makes the mouse an inappropriate model for investigating the effect of Siglecs directly in the α- or β-cells. But its expression in the immune system could still modulate the inflammatory response during the progression of diabetes. Therefore we used a wholebody Siglec-F knockout mouse model and their corresponding littermate controls to induce diabetes via STZ injection. As expected, all STZ injected mice showed increased random blood sugar levels as well as reduced glucose tolerance and insulin secretion, but the knockout of Siglec-F showed no visible effect on diabetes progression. So we can hypothesize that Siglec-F modulation of the immune system, like it is known for eosinophilic inflammation [58] does not work similar in the development of STZ-induced Diabetes mellitus. This does not completely exclude a role of Siglec-F, but makes it minor compared to the important role in humans.

Summarizing the findings, we detected the presence of a novel family of cell adhesion molecules-Siglecs, expressed in the endocrine cells of the pancreas in human. One of its β-cell specific members, Siglec-7 was lost in diabetes. Restoration of Siglec-7 in these cells could protect them from the harmful effects of diabetic milieu, and help preserve β-cell function and survival under these conditions by inhibition of pro-inflammatory cytokine secretion by suppressing NF-κB activity. Not only was this immunemodulatory function evident in the cytokine profile of the β-cells, but also the PBMCs showed loss of Siglec-7 expression upon

activation. Taken together, Siglec-7 plays a substantial role in the maintenance of immune-suppressive anti-inflammatory microenvironment, which is lost in diabetes, and may contribute to the manifestation and progression of this metabolic syndrome (Suppl.Fig.4). Thus, preserving Siglec-7 expression and function on β-cells as well as immune cells may be a novel therapeutic strategy which could help target both, the sensitization and pro-inflammatory activation of the immune system as well as the islets, thereby being beneficial to effectively halt the deterioration of islets in T2D.

Acknowledgements

This work was supported by the European Research Council (ERC), the JDRF, the German Research Foundation (DFG, Emmy Noether Programm MA4172/1-1) and the BMBF (Competence Network diabetes). We would like to thank Prof. Paul Crocker for fruitful discussion and advice and providing us the sheep anti-siglec antibodies. We thank Jennifer Bergemann for excellent technical assistance; Katharina Zyromski and Payal Shah for help with the analyses. Special thanks to Dr Anna-Leena Krämer and Prof. Andreas Dotzauer for helping with the FACS analysis. Human islets were provided through the JDRF award 31-2008-413 (ECIT Islet for Basic Research program) and by the integrated islet distribution program (IIDP). Human pancreatic sections were provided from the National Disease Research Interchange (NDRI), supported by the NIH.

Figure legends

Figure 1. Siglecs are differentially expressed in the human Islets of Langerhans.

Triple immunostaining for insulin (blue), glucagon (green) and siglecs (red) was carried out on human pancreatic sections obtained at autopsy of healthy nondiabetic controls and patients with T2DM, all with documented fasting plasma glucose >150 mg/dl. **(A)** Siglecs 1, **(B)** -2, **(C)** -7and **(D)** -10 were expressed in β-cells. **(E)** Siglecs 3, **(F)** -5, **(G)** -8 were expressed

solely in α-cells. Representative analyses from 5 pancreases from patients with T2D and 5 controls are shown.

Figure 2. **Siglec-7 and -3 are oppositely regulated in type 2 diabetes**

Semi quantitative real time PCR analysis was performed on cDNAs obtained from non-diabetic (n=9) and diabetic human pancreas (n=5) from autopsy. **(A)** Siglec-7 expression was normalized on cyclophilin (PPIA), insulin (ins) and SN1; whereas Siglec-3 expression was normalized on cyclophylin, glucagon (gluc) and SAT2. **(BE)** Insulin; Glucagon; SN1 and SAT2 were normalized on cyclophylin. **(F-H)** Real time PCR analysis of isolated islets obtained from autopsy of T2D patients (n=5) were compared to that of nondiabetic individuals (n=3) of **(F)** Siglec-7; **(G)** St8Sia1 and **(H)** Neu3 **(I,J)** Immunohistochemical analysis was carried out on human pancreatic sections obtained at autopsy of healthy non-diabetic controls (n=3) and patients with T2DM (n=3) for **(I)** GD3 and **(K)** Siglec-7; **(J,L)** staining saturation and intensity were quantified using Photoshop; each data point represents saturation and intensity of the protein signal of islets from 3 donors, 2 sections per donor, average 7 islets per section. **(M)** Bright field staining using Siglec-7 Fcchimeras; along with glucagon (red) and insulin (green) of pancreas sections obtained from autopsies of healthy non-diabetic controls (n=3) and patients with T2DM (n=3); along with control slides treated with sialidase treatment. (*$p<0.05$ to 5.5 mM glucose control).

Figure 3. Siglec-7 over-expression improves β-cell survival and function

Freshly isolated human islets of nondiabetic individuals as well as from patients with T2D were cultured on extracellular matrix-coated dishes and exposed to elevated glucose (22.2 or 33.3 mM) (HG) with or without palmitate (HGPal), palmitate alone (Pal) or the cytokine mixture IL-1β (2 ng/ml) and IFNγ (1,000 U/ml) (IL/IF) for 72 h with or without over-expression by lipofectamine-mediated Siglec-7 plasmid transfection. Glucose stimulated insulin secretion assays were performed after the 72h culture period. **(A,B)** Basal (2.8 mM)

and glucose stimulated (16.7mM) insulin secretion was expressed as percent change of control condition basal insulin levels. **(C,D)** Stimulatory index denotes the amount of glucose stimulated (16.7 mM glucose) divided by the amount of basal insulin secretion. Fold changes in stimulatory indices of treated islets were plotted, compared to stimulatory index of control islets **(E,F)** Apoptosis was analyzed by the TUNEL assay in dishes. Islets were triple-stained for insulin and counterstained for DAPI (not shown). Results are means ± SE of the percentage of TUNEL-positive β-cells. The average number of β-cells counted was 8124 for each treatment group in 3 separate experiments from 3 separate dishes per treatment from 3 different organ donors. **(G)** Isolated human islets were treated with 22.2 mM glucose and 0.5 mM palmitate; or the cytokine mixture IL/IF, followed by immunohistochemical analysis of paraffin-embedded islet sections. Representative images show glucagon (green), Siglec-7 (red) and DAPI (blue). **(A-D)** Data are shown from parallel experiments as mean □ SE from 3 islet isolations from 3 different donors. For control islets; *p<0.05 to 5.5 mM glucose treated LacZ transfected islets, **p<0.05 to diabetic stimuli treated LacZ transfected islets For T2D analysis, #p<0.05 to 5.5 mM glucose treated LacZ transfected nondiabetic control islets.

Figure 4. Siglec-7 inhibits NF-κB activation and cytokine secretion.

Human pancreatic islets were cultured on extracellular matrix-coated dishes and exposed to elevated glucose (22.2 mM) and palmitate (Gluc/Pal) or the cytokine mixture IL-1β (2 ng/ml) and IFNγ (1,000 U/ml) (IL/IF) for 72 h with or without overexpression by lipofectamine-mediated Siglec-7 plasmid transfection. **(A-D)** The cytokine profiles of the supernatants of transfected and treated islets were assessed using protein microarray ELISAs. Western blot analysis was performed after Siglec-7 over-expression in islets and 72h treatment with **(E)** 22.2mM glucose and palmitate or **(F)** IL1β and IFNγ; and analyzed for p-p65, p-IKBα and actin. **(G)** PBMCs purified from buffy coats were exposed to 22.2mM glucose and palmitate or IL1β and IFNγ for 12h followed by western blotting. The blots were probed for p65, p-IκBα and actin. **(H-K)** Densitometry was carried on blots, protein of interest i.e. p- IκBα and

p-p65, normalized on housekeeping, and plotted as fold change of islets at control condition. The graphs and blots are representative of 3-4 independent experiments. *p<0.05 to 5.5 mM glucose treated LacZ transfected control islets, **p<0.05 to diabetic stimuli treated LacZ transfected control islets.

Figure 5. Immune cell migration into inflamed islets is inhibited by Siglec-7.

PBMCs purified from buffy coats of blood donors (n=6) were treated with Lipo polysaccharide (LPS) or elevated glucose and palmitate (Gluc/Pal) for **(A,C,E,G)** 2h or **(B,D,F,H)** 12h. Real time PCR analysis of these treated cells was carried out for **(A-B)** IL6, **(C-D)** CD25, **(E,F)** Siglec-7 and **(G,H)** Neu-3. Cell surface expression of Siglec-7 in the treated PBMCs was determined using flow cytometry. **(I)** Histograms for intensity of Siglec-7 (FL1 filter) was plotted and overlayed to observe the effect of these treatments. **(J)** Histograms were quantified and Siglec-7 expression was plotted as % mean fluorescent intensity as compared to untreated control fraction. The migration of leukocytes (n=3 buffy coat donors) in response to conditioned media obtained from transfected and treated islets (n=3) separate dishes from 3 independent experiments from 3 donors), was quantified after 4h using an *in vitro* migration assay. **(K)** The fold induction of migration as compared to untreated control islet supernatants was plotted. **(L)** Migration of mononuclear cells (n=3) with respect to cultured islets from diabetic donors (n=3), with or without Siglec-7 over-expression, was plotted as fold change of migrated cells compared to untreated control islets of a nondiabetic individual. **(M)** The images are representative of fluorescent microscopic analysis of live cells migrating through membranes observed in green. For PBMC treatments; *p<0.05 to 11.1mM glucose treated monocyte fraction. For migration assay, *p<0.05 to monocyte fraction treated with 5.5 mM glucose, LacZ transfected control islets, **p<0.05 to monocyte fraction treated with Gluc/Pal, LacZ transfected control islets.

Figure 6. Siglec-F is not expressed by mouse islet cells.

Isolated mouse islets were dispersed by Accutase treatment till a single cell state and plated on extracellular matrix-coated dishes. After one day of recovery time cells were scraped off, fixed and stained for FACS analysis. Data show one representative of three experiments, numbers indicate the percentage of stained cells **(A, B)**. WTB6 mouse islets were isolated, cultured in suspension (con) and then treated with Clodronate containing liposomes (Clo) or PBS containing liposomes (PBS) for 48h. RNA was isolated, reverse transcribed and analyzed for the indicated genes by qRT-PCR **(C, D,E)**. Eight-week-old male Siglec-F-knockout (SigF-/-) mice and their littermate wildtype (WT) and heterozygous (SigF+/-) controls where injected with 50mg/kg streptozotocin (STZ) or citric buffer (control) on 5 consecutive days (n = 12-15). Random blood glucose was measured **(F)**, glucose tolerance test **(G)** and in vivo glucose stimulated insulin secretion **(H, I)** were performed after 20 days. Stimulatory index show the amount of glucose stimulated divided by the amount of basal insulin secretion **(I)**. Isolated mouse islets of all three genotypes were plated on extracellular matrix-coated dishes and exposed to 22.2 mM glucose with palmitate (0.5 mM) or the cytokine mixture IL-1β (2 ng/ml) and IFNγ (1,000 U/ml) for 72 h. Glucose stimulated insulin secretion assay was performed **(J)**. All data are shown as mean +/-SE representing 3 independent experiments, *$p<0.05$ to PBS liposome control.

Supplementary Figure 1: **(A)** Islets were dispersed using accutase and cultured overnight for recovery. These dispersed cells were stained with Siglec-7 and analyzed by flow cytometry. Histograms indicate the intensity of FL1 for unstained, isotype control and Siglec-7 stained cells. **(B)** Semi quantitative real time PCR analysis was performed on cDNAs obtained from non-diabetic (n=9) and diabetic human pancreas (n=6) from autopsy. Siglec-10 expression was normalized on cyclophilin (PPIA), insulin and SN1 **(C)** Real time PCR analysis for Siglec-10 of isolated islets obtained from autopsy of T2D patients (n=3) were compared to that of nondiabetic individuals (n=3). **(D)** HEK293T cells were transfected with LacZ or

Siglec-7 plasmids were stained for Siglec-7 and analyzed using flow cytometry. (*p<0.05 to 5.5 mM glucose control)

Supplementary Figure 2: (A) PBMCs purified from buffy coats of blood donors (n=6) were treated with elevated glucose and palmitate for 12h. They were triple stained for Siglec-7, CD-14 and CD-25 and analyzed using flow cytometry. Their intensities were plotted against each other, and the quadrants were analyzed for number of positive cell and signal intensities. **(B)**The % cells co-labeled for CD25 and Siglec-7 were quantified, and also the **(C)** % mean fluorescent intensities of Siglec-7 in these cells was plotted. **(D)** % cells co-labeled for CD14 and Siglec-7 were quantified, and the **(E)** % mean fluorescent intensities of Siglec-7 in these cells were plotted. *p<0.05 to 11.1mM glucose treated monocyte fraction.

Supplementary Figure 3: Cell surface expression of CD25 in elevated glucose and palmitate treated PBMCs (n=6) after 12h was determined using flow cytometry. Histograms for intensity of CD25 (FL2 filter) were plotted and overlayed to observe the effect of these treatments. *p<0.05 to 11.1mM glucose treated monocyte fraction.

Supplementary Figure 4: This model illustrates the role of Siglec-7 as investigated in this paper. In healthy individuals, Siglec-7 helps to maintain a prosurvival anti-inflammatory signaling in monocytes as well as β-cells. In diabetes however, chronic elevated glucose along with palmitate and cytokines cause loss of Siglec-7 in these cells. This leads to triggering of apoptotic and proinflammatory signals, activation of macrophages and ultimately to β-cell death.

References

1. Tisch, R. and H. McDevitt, *Insulin-dependent diabetes mellitus.* Cell, 1996. **85**(3): p. 291-7.
2. Mokdad, A.H., et al., *Prevalence of obesity, diabetes, and obesity-related health risk actors, 2001.* JAMA, 2003. **289**(1): p. 76-9.
3. Neels, J.G. and J.M. Olefsky, *Inflamed fat: what starts the fire?* J Clin Invest, 2006. **116**(1): p. 33-5.
4. Festa, A., et al., *Elevated levels of acute-phase proteins and plasminogen activator inhibitor-1 predict the development of type 2 diabetes: the insulin resistance atherosclerosis study.* Diabetes, 2002. **51**(4): p. 1131-7.
5. Donath, M.Y., et al., *Inflammation in obesity and diabetes: islet dysfunction and therapeutic opportunity.* Cell Metab, 2013. **17**(6): p. 860-72.
6. Hotamisligil, G.S., N.S. Shargill, and B.M. Spiegelman, *Adipose expression of tumor necrosis factor-alpha: direct role in obesity-linked insulin resistance.* Science, 1993. **259**(5091): p. 87-91.
7. Maedler, K., et al., *Glucose-induced beta-cell production of interleukin-I1beta contributes to glucotoxicity in human pancreatic islets.* J.Clin.Invest, 2002. **110**: p. 851-860.
8. Larsen, C.M., et al., *Interleukin-1-receptor antagonist in type 2 diabetes mellitus.* N Engl J Med, 2007. **356**(15): p. 1517-26.
9. Yuan, M., et al., *Reversal of obesity- and diet-induced insulin resistance with salicylates or targeted disruption of Ikkbeta.* Science, 2001. **293**(5535): p. 1673-7.
10. Crocker, P.R., et al., *Siglecs: a family of sialic-acid binding lectins.* Glycobiology, 1998. **8**(2): p. v.
11. Jandus, C., H.U. Simon, and S. von Gunten, *Targeting siglecs--a novel pharmacological strategy for immuno- and glycotherapy.* Biochem Pharmacol, 2011. **82**(4): p. 323-32.
12. Crocker, P.R. and A. Varki, *Siglecs in the immune system.* Immunology, 2001. **103**(2): p. 137-45.
13. Crocker, P.R., J.C. Paulson, and A. Varki, *Siglecs and their roles in the immune system.* Nat Rev Immunol, 2007. **7**(4): p. 255-66.
14. Falco, M., et al., *Identification and molecular cloning of p75/AIRM1, a novel member of the sialoadhesin family that functions as an inhibitory receptor in human natural killer cells.* J Exp Med, 1999. **190**(6): p. 793-802.
15. Nicoll, G., et al., *Identification and characterization of a novel siglec, siglec-7, expressed by human natural killer cells and monocytes.* J Biol Chem, 1999. **274**(48): p. 34089-95.
16. Nicoll, G., et al., *Ganglioside GD3 expression on target cells can modulate NK cell cytotoxicity via siglec-7-dependent and -independent mechanisms.* Eur J Immunol, 2003. **33**(6): p. 1642-8.
17. Vitale, C., et al., *Engagement of p75/AIRM1 or CD33 inhibits the proliferation of normal or leukemic myeloid cells.* Proc Natl Acad Sci U S A, 1999. **96**(26): p. 15091-6.
18. Avril, T., et al., *The membrane-proximal immunoreceptor tyrosine-based inhibitory motif is critical for the inhibitory signaling mediated by Siglecs-7 and -9, CD33-related Siglecs expressed on human monocytes and NK cells.* J Immunol, 2004. **173**(11): p. 6841-9.
19. Ikehara, Y., S.K. Ikehara, and J.C. Paulson, *Negative regulation of T cell receptor signaling by Siglec-7 (p70/AIRM) and Siglec-9.* J Biol Chem, 2004. **279**(41): p. 43117-25.
20. Schulthess, F.T., et al., *CXCL10 impairs beta cell function and viability in diabetes through TLR4 signaling.* Cell Metab, 2009. **9**(2): p. 125-39.
21. Kaiser, N., et al., *Monolayer culture of adult rat pancreatic islets on extracellular matrix: modulation of B-cell function by chronic exposure to high glucose.* Endocrinology, 1991. **129**(4): p. 2067-2076.
22. Maedler, K., et al., *Distinct effects of saturated and monounsaturated fatty acids on beta-cell turnover and function.* Diabetes, 2001. **50**(1): p. 69-76.

23. Ardestani, A., et al., *Neutralizing IL-1{beta} induces {beta}-cell survival by maintaining PDX1 nuclear localization.* J Biol Chem, 2011.
24. Le Bacquer, O., et al., *TCF7L2 splice variants have distinct effects on {beta}-cell turnover and function.* Hum Mol Genet, 2011. **20**(10): p. 1906-15.
25. Pham, N.A., et al., *Quantitative image analysis of immunohistochemical stains using a CMYK color model.* Diagn Pathol, 2007. **2**: p. 8.
26. Shu, L., et al., *Transcription factor 7-like 2 regulates beta-cell survival and function in human pancreatic islets.* Diabetes, 2008. **57**(3): p. 645-53.
27. Leng, S.X., et al., *ELISA and multiplex technologies for cytokine measurement in inflammation and aging research.* J Gerontol A Biol Sci Med Sci, 2008. **63**(8): p. 879-84.
28. Repnik, U., M. Knezevic, and M. Jeras, *Simple and cost-effective isolation of monocytes from buffy coats.* J Immunol Methods, 2003. **278**(1-2): p. 283-92.
29. Gammelsaeter, R., et al., *Complementary expression of SN1 and SAT2 in the islets of Langerhans suggests concerted action of glutamine transport in the regulation of insulin secretion.* Biochem Biophys Res Commun, 2009. **381**(3): p. 378-82.
30. Blixt, O., et al., *Sialoside specificity of the siglec family assessed using novel multivalent probes: identification of potent inhibitors of myelinassociated glycoprotein.* J Biol Chem, 2003. **278**(33): p. 31007-19.
31. Yamaji, T., et al., *A small region of the natural killer cell receptor, Siglec-7, is responsible for its preferred binding to alpha 2,8-disialyl and branched alpha 2,6-sialyl residues. A comparison with Siglec-9.* J Biol Chem, 2002. **277**(8): p. 6324-32.
32. Rapoport, E., et al., *Ganglioside binding pattern of CD33-related siglecs.* Bioorg Med Chem Lett, 2003. **13**(4): p. 675-8.
33. Bock, N. and S. Kelm, *Binding and inhibition assays for Siglecs.* Methods Mol Biol, 2006. **347**: p. 359-75.
34. Angata, T. and A. Varki, *Siglec-7: a sialic acid-binding lectin of the immunoglobulin superfamily.* Glycobiology, 2000. **10**(4): p. 431-8.
35. Sasaki, C.Y., et al., *Phosphorylation of RelA/p65 on serine 536 defines an I{kappa}B{alpha}-independent NF-{kappa}B pathway.* J Biol Chem, 2005. **280**(41): p. 34538-47.
36. Ehses, J.A., et al., *Increased number of islet-associated macrophages in type 2 diabetes.* Diabetes, 2007. **56**(9): p. 2356-70.
37. Zhang, J.Q., et al., *Siglec-9, a novel sialic acid binding member of the immunoglobulin superfamily expressed broadly on human blood leukocytes.* J Biol Chem, 2000. **275**(29): p. 22121-6.
38. Brunetta, E., et al., *The decreased expression of Siglec-7 represents an early marker of dysfunctional natural killer-cell subsets associated with high levels of HIV-1 viremia.* Blood, 2009. **114**(18): p. 3822-30.
39. Malisan, F. and R. Testi, *GD3 in cellular ageing and apoptosis.* Exp Gerontol, 2002. **37**(10-11): p. 1273-82.
40. De Maria, R., et al., *Requirement for GD3 ganglioside in CD95- and ceramide-induced apoptosis.* Science, 1997. **277**(5332): p. 1652-5.
41. Malisan, F. and R. Testi, *GD3 ganglioside and apoptosis.* Biochim Biophys Acta, 2002. **1585**(2-3): p. 179-87.
42. Maedler, K., et al., *Glucose induces beta-cell apoptosis via upregulation of the Fas-receptor in human islets.* Diabetes, 2001. **50**: p. 1683-1690.
43. Loweth, A.C., et al., *Human islets of Langerhans express Fas ligand and undergo apoptosis in response to interleukin-1beta and Fas ligation.* Diabetes, 1998. **47**(5): p. 727-732.
44. Prokazova, N.V. and L.D. Bergelson, *Gangliosides and atherosclerosis.* Lipids, 1994. **29**(1): p. 1-5.

45. Simon, B.M., et al., *Disialoganglioside GD3 is released by microglia and induces oligodendrocyte apoptosis.* Cell Death Differ, 2002. **9**(7): p. 758-67.
46. Bhunia, A.K., G. Schwarzmann, and S. Chatterjee, *GD3 recruits reactive oxygen species to induce cell proliferation and apoptosis in human aortic smooth muscle cells.* J Biol Chem, 2002. **277**(19): p. 16396-402.
47. Dotta, F., et al., *Pancreatic islet ganglioside expression in nonobese diabetic mice: comparison with C57BL/10 mice and changes after autoimmune beta-cell destruction.* Endocrinology, 1992. **130**(1): p. 37-42.
48. Miyagi, T., et al., *Molecular cloning and characterization of a plasma membrane-associated sialidase specific for gangliosides.* J Biol Chem, 1999. **274**(8): p. 5004-11.
49. Sasaki, A., et al., *Overexpression of plasma membrane-associated sialidase attenuates insulin signaling in transgenic mice.* J Biol Chem, 2003. **278**(30): p. 27896-902.
50. Yoshizumi, S., et al., *Increased hepatic expression of ganglioside-specific sialidase, NEU3, improves insulin sensitivity and glucose tolerance in mice.* Metabolism, 2007. **56**(3): p. 420-9.
51. Kono, T., et al., *PPAR-gamma activation restores pancreatic islet SERCA2 levels and prevents beta-cell dysfunction under conditions of hyperglycemic and cytokine stress.* Mol Endocrinol, 2012. **26**(2): p. 257-71.
52. Moibi, J.A., et al., *Peroxisome proliferator-activated receptor-gamma regulates expression of PDX-1 and NKX6.1 in INS-1 cells.* Diabetes, 2007. **56**(1): p. 88-95.
53. Viardot, A., et al., *Obesity is associated with activated and insulin resistant immune cells.* Diabetes Metab Res Rev, 2012. **28**(5): p. 447-54.
54. Dasu, M.R. and I. Jialal, *Free fatty acids in the presence of high glucose amplify monocyte inflammation via Toll-like receptors.* Am J Physiol Endocrinol Metab, 2011. **300**(1): p. E145-54.
55. Smith, P.D., et al., *Intestinal macrophages and response to microbial encroachment.* Mucosal Immunol, 2011. **4**(1): p. 31-
56. Dolenšek, J., Rupnik, M.S. & Stožer, *A. Structural similarities and differences between the human and the mouse pancreas* , Islets, 7:1, 2015, e1024405
57. Benner, C., et al., *The transcriptional landscape of mouse beta cells compared to human beta cells reveals notable species differences in long non-coding RNA and protein-coding gene expression.* BMC Genomics. 2014; 15(1): 620.
58. Zhang, M. et al. *Defining the in vivo function of Siglec-F, a CD33-related Siglec expressed on mouse eosinophils*. Blood, 2007 **109**, 4280-7

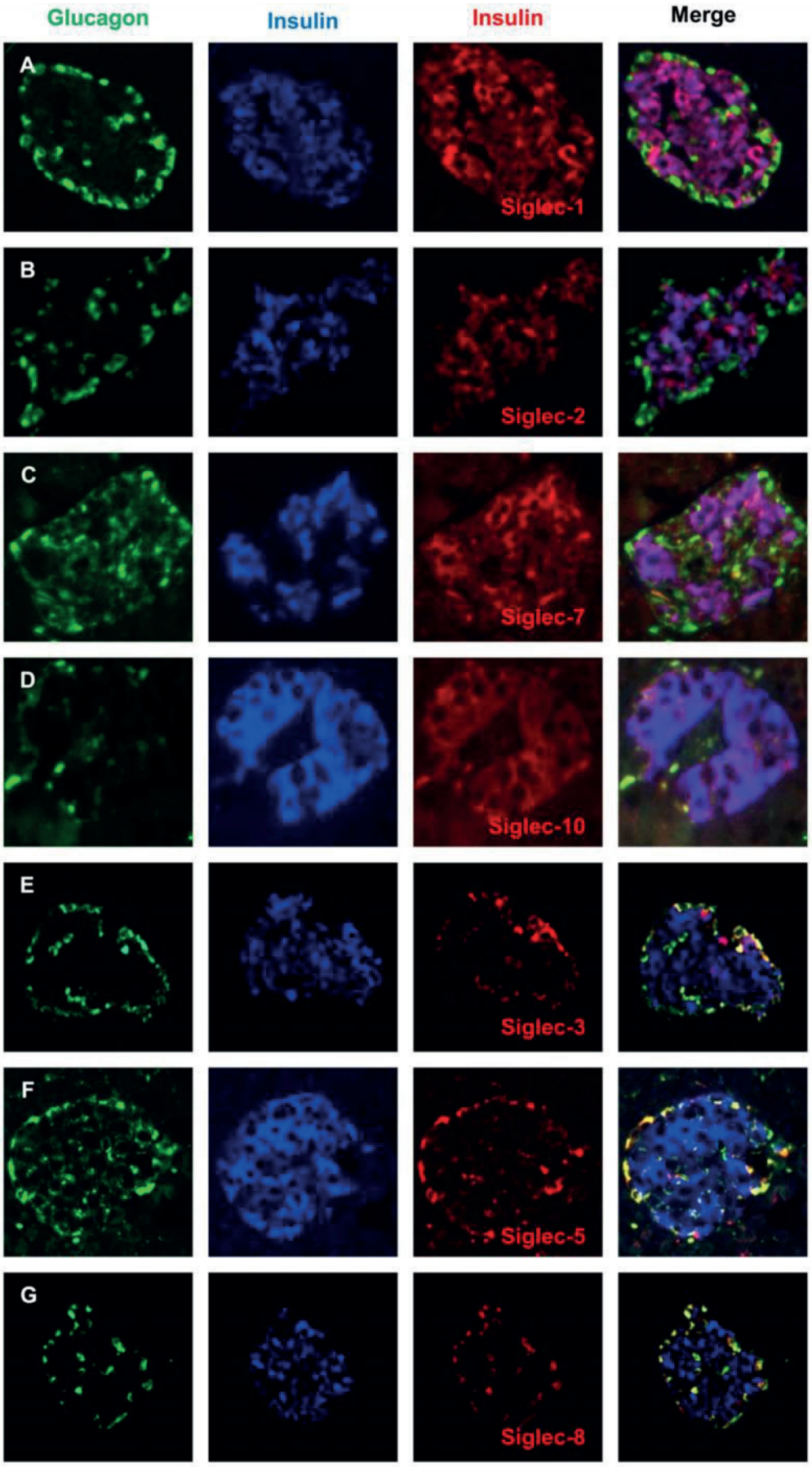
Glucagon
Insulin
Insulin
Merge
A
Siglec-1
B
Siglec-2
C
Siglec-7
D
Siglec-10
E
Siglec-3
F
Siglec-5
G
Siglec-8

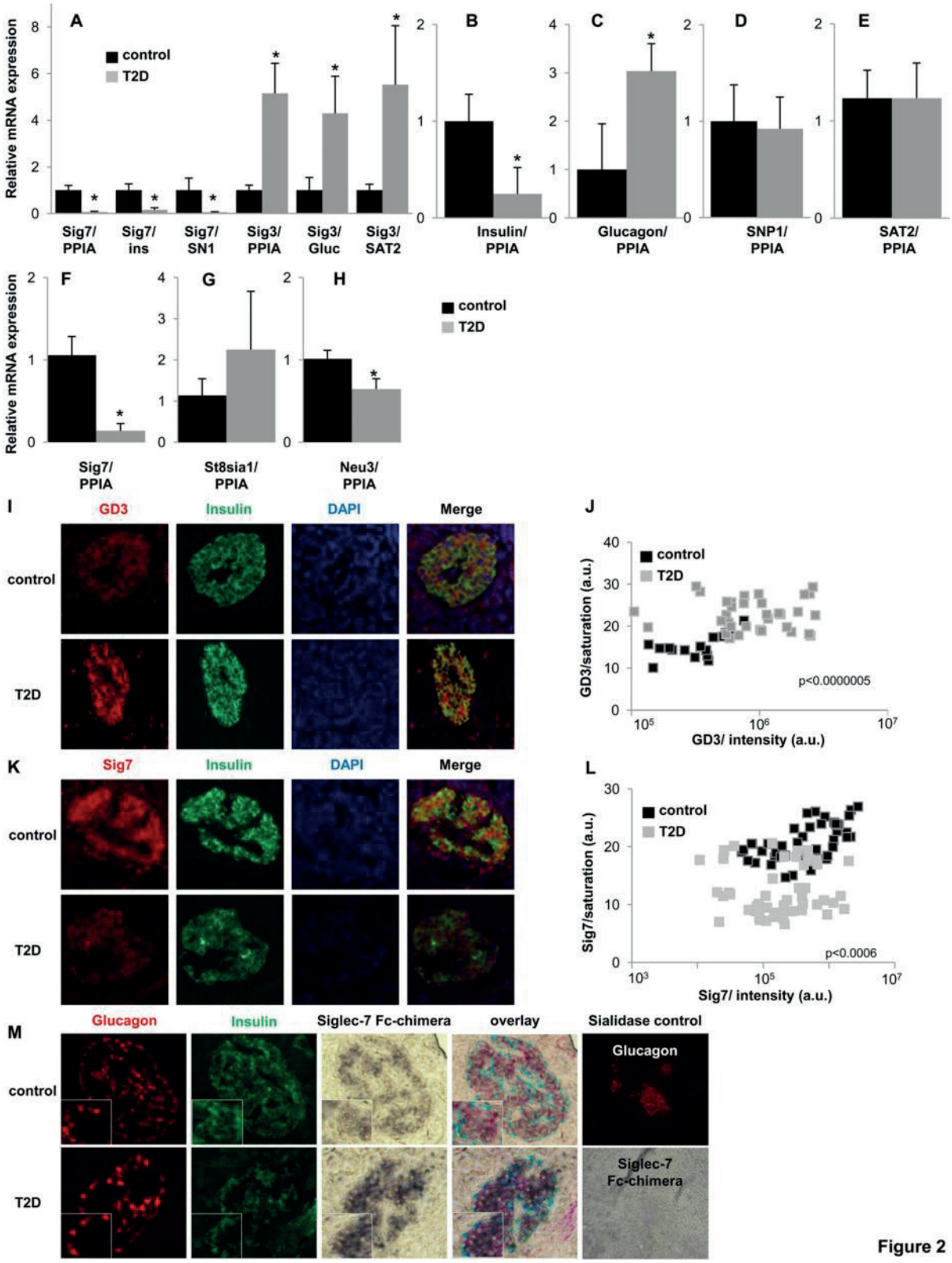
A
B
C
D
E
F
G
H
I
J
K
L
M
control
T2D
Relative mRNA expression
Sig7/ PPIA
Sig7/ ins
Sig7/ SN1
Sig3/ PPIA
Sig3/ Gluc
Sig3/ SAT2
Insulin/ PPIA
Glucagon/ PPIA
SNP1/ PPIA
SAT2/ PPIA
Sig7/ PPIA
St8sia1/ PPIA
Neu3/ PPIA
GD3
Insulin
DAPI
Merge
Sig7
GD3/saturation (a.u.)
GD3/ intensity (a.u.)
p<0.0000005
Sig7/saturation (a.u.)
Sig7/ intensity (a.u.)
p<0.0006
Glucagon
Siglec-7 Fc-chimera
overlay
Sialidase control

Figure 2

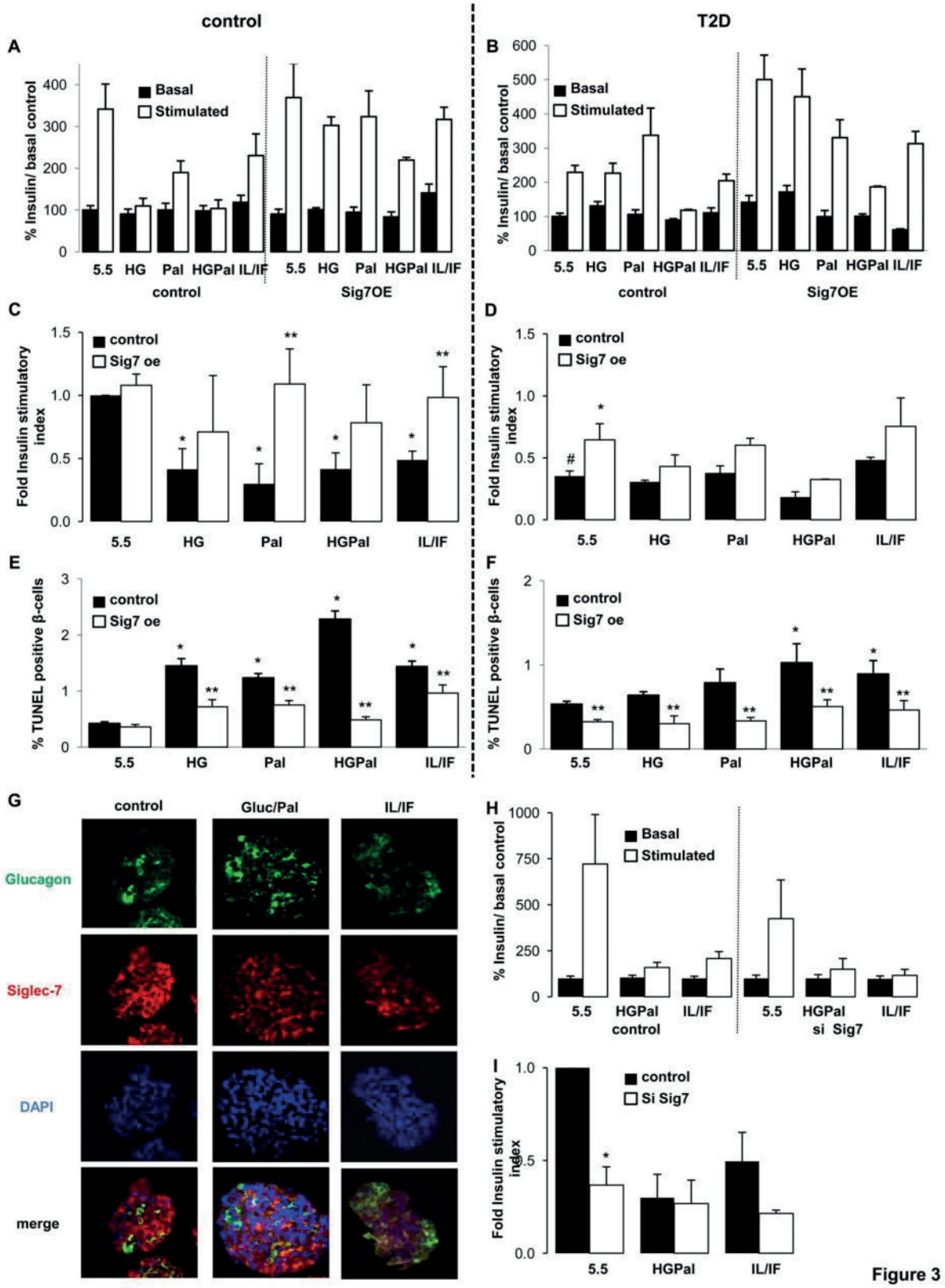
control
T2D
A
B
% Insulin/ basal control
Basal
Stimulated
5.5 HG Pal HGPal IL/IF
control
Sig7OE
C
D
Fold Insulin stimulatory index
control
Sig7 oe
E
F
% TUNEL positive β-cells
G
control
Gluc/Pal
IL/IF
Glucagon
Siglec-7
DAPI
merge
H
si Sig7
I
Si Sig7

Figure 3

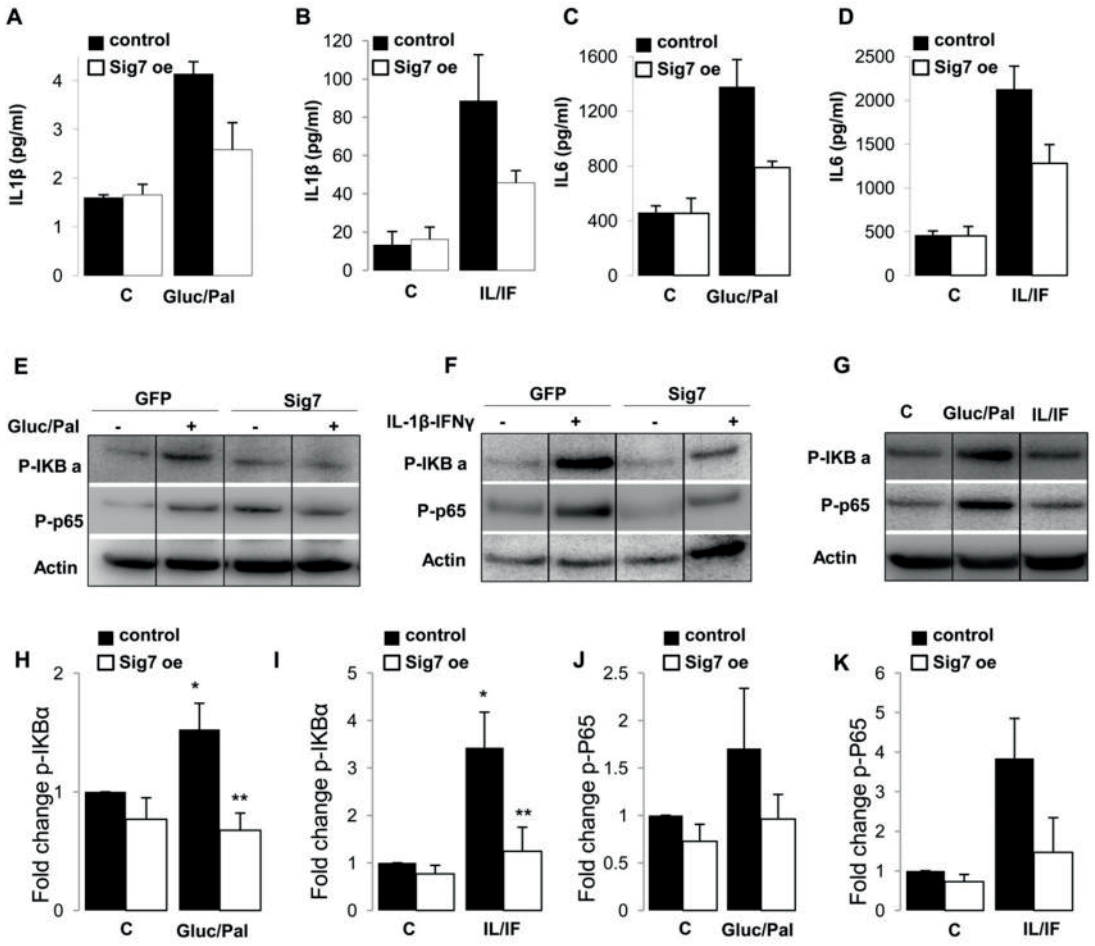
A
control
Sig7 oe
IL1β (pg/ml)
C
Gluc/Pal
B
control
Sig7 oe
IL1β (pg/ml)
C
IL/IF
C
control
Sig7 oe
IL6 (pg/ml)
C
Gluc/Pal
D
control
Sig7 oe
IL6 (pg/ml)
C
IL/IF
E
GFP
Sig7
Gluc/Pal
P-IKB a
P-p65
Actin
F
GFP
Sig7
IL-1β-IFNγ
P-IKB a
P-p65
Actin
G
C
Gluc/Pal
IL/IF
P-IKB a
P-p65
Actin
H
control
Sig7 oe
Fold change p-IKBα
C
Gluc/Pal
I
control
Sig7 oe
Fold change p-IKBα
C
IL/IF
J
control
Sig7 oe
Fold change p-P65
C
Gluc/Pal
K
control
Sig7 oe
Fold change p-P65
C
IL/IF

Figure 4

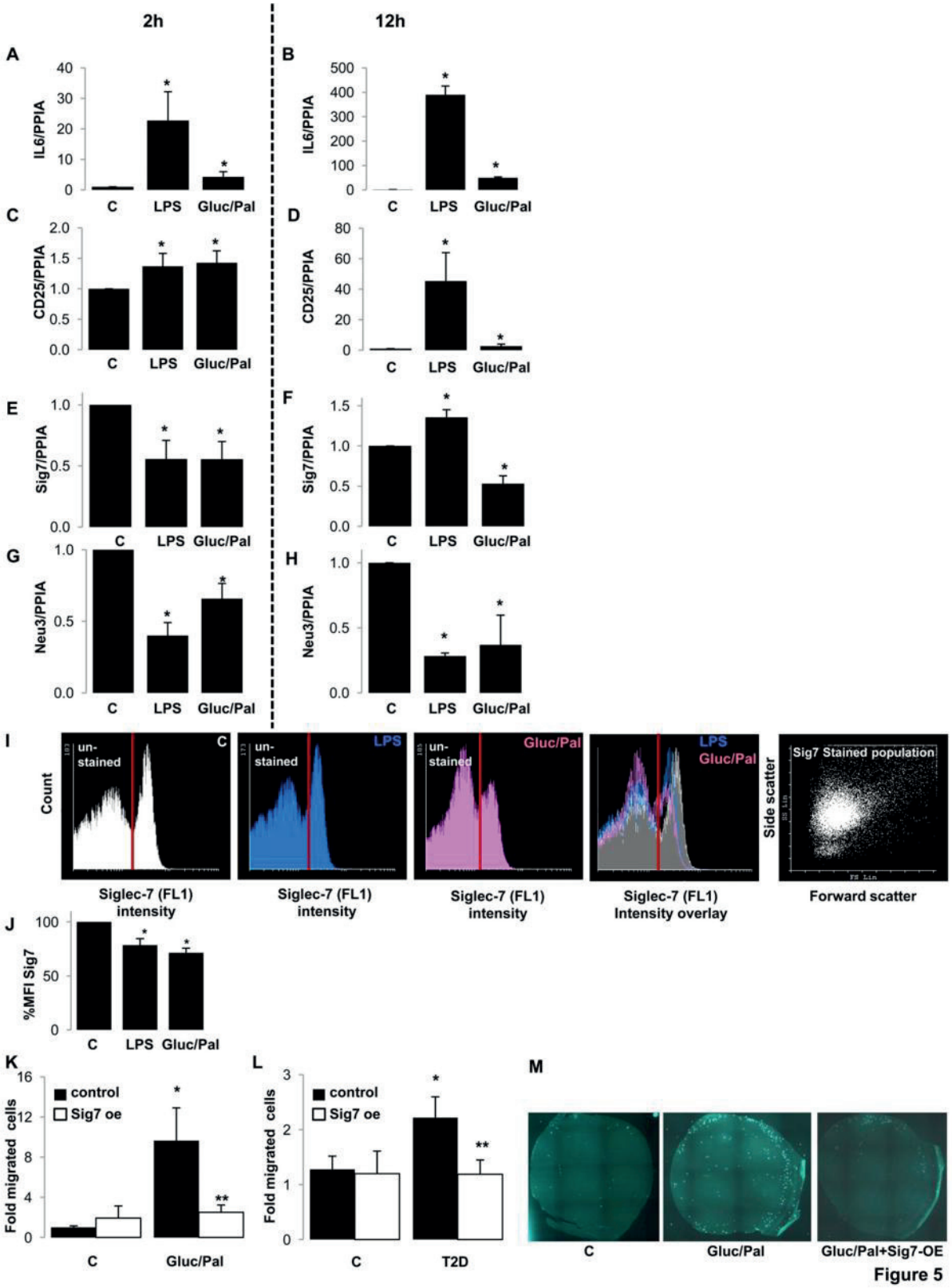
2h
12h
A
IL6/PPIA
C
LPS
Gluc/Pal
B
C
CD25/PPIA
D
E
Sig7/PPIA
F
G
Neu3/PPIA
H
I
un-stained
C
LPS
Gluc/Pal
Count
Siglec-7 (FL1) intensity
Siglec-7 (FL1) Intensity overlay
Side scatter
Sig7 Stained population
Forward scatter
J
%MFI Sig7
K
control
Sig7 oe
Fold migrated cells
L
T2D
M
Gluc/Pal+Sig7-OE

Figure 5

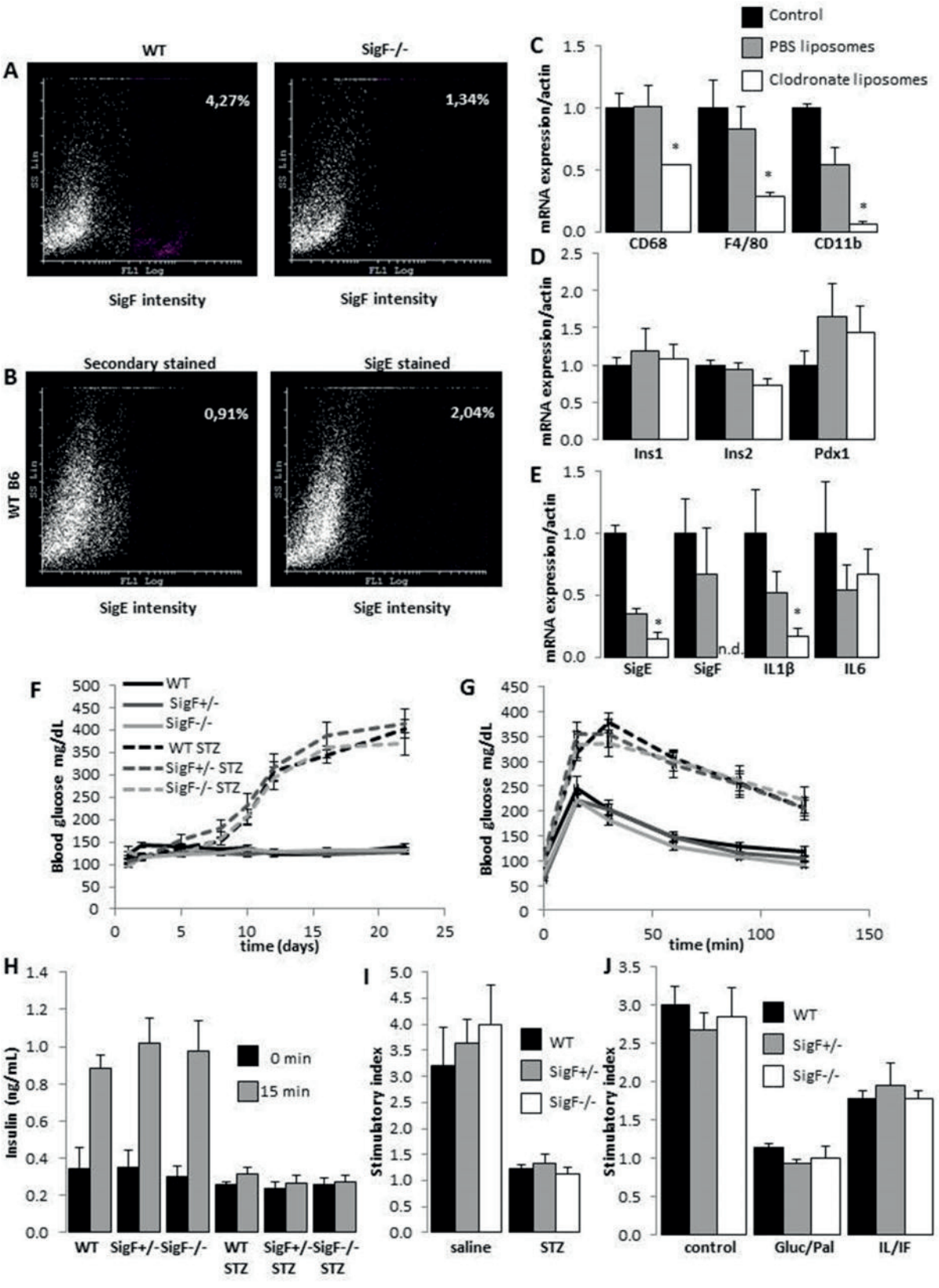
A
WT
SigF-/-
4,27%
1,34%
SS Lin
FL1 Log
SigF intensity
SigF intensity
B
Secondary stained
SigE stained
WT B6
0,91%
2,04%
SigE intensity
SigE intensity
C
Control
PBS liposomes
Clodronate liposomes
mRNA expression/actin
CD68
F4/80
CD11b
D
Ins1
Ins2
Pdx1
E
SigE
SigF
n.d.
IL1β
IL6
F
WT
SigF+/-
SigF-/-
WT STZ
SigF+/- STZ
SigF-/- STZ
Blood glucose mg/dL
time (days)
G
Blood glucose mg/dL
time (min)
H
Insulin (ng/mL)
0 min
15 min
WT
SigF+/-
SigF-/-
WT STZ
SigF+/- STZ
SigF-/- STZ
I
Stimulatory index
WT
SigF+/-
SigF-/-
saline
STZ
J
Stimulatory index
WT
SigF+/-
SigF-/-
control
Gluc/Pal
IL/IF

Supplementary figure 1

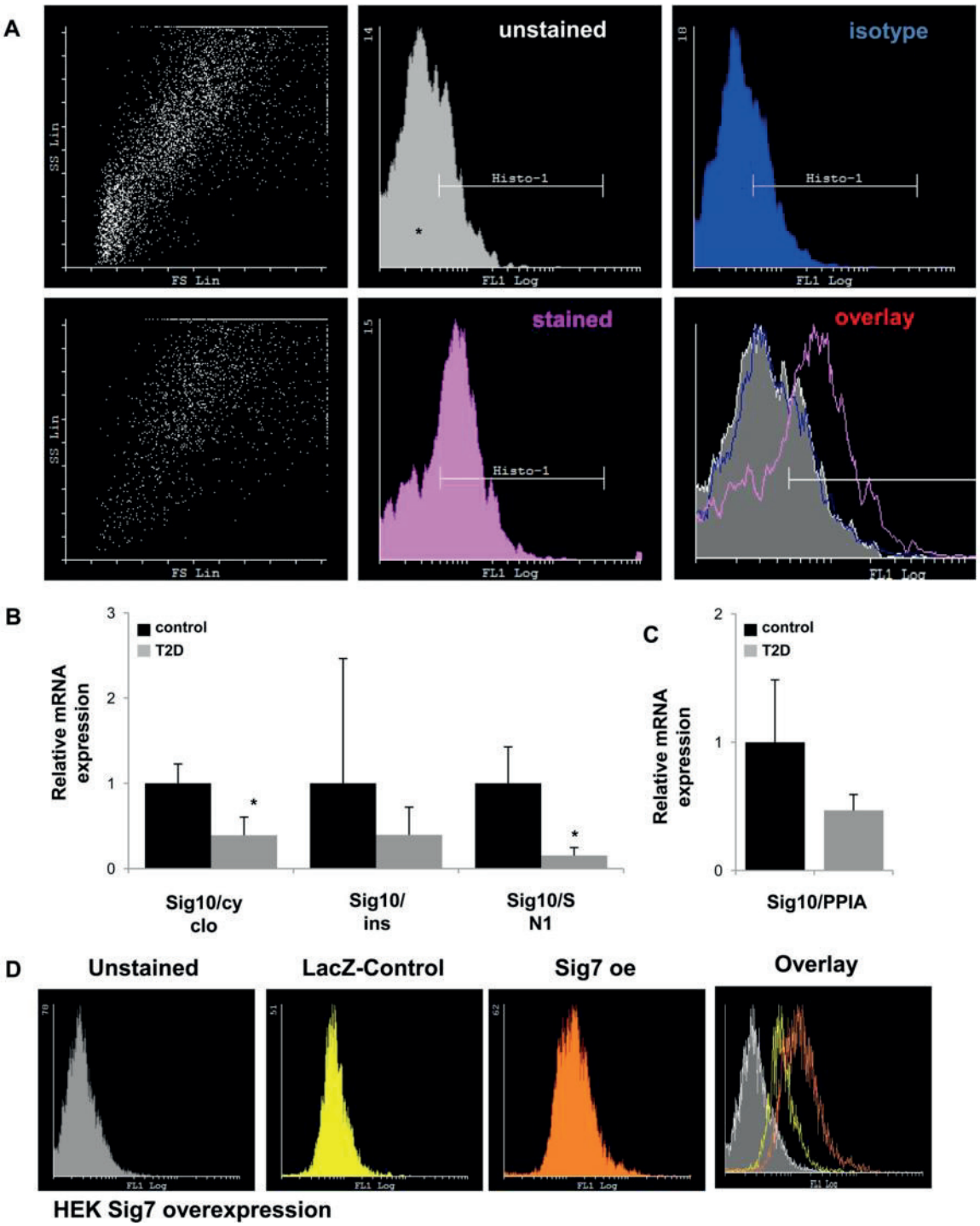

Supplementary figure 2

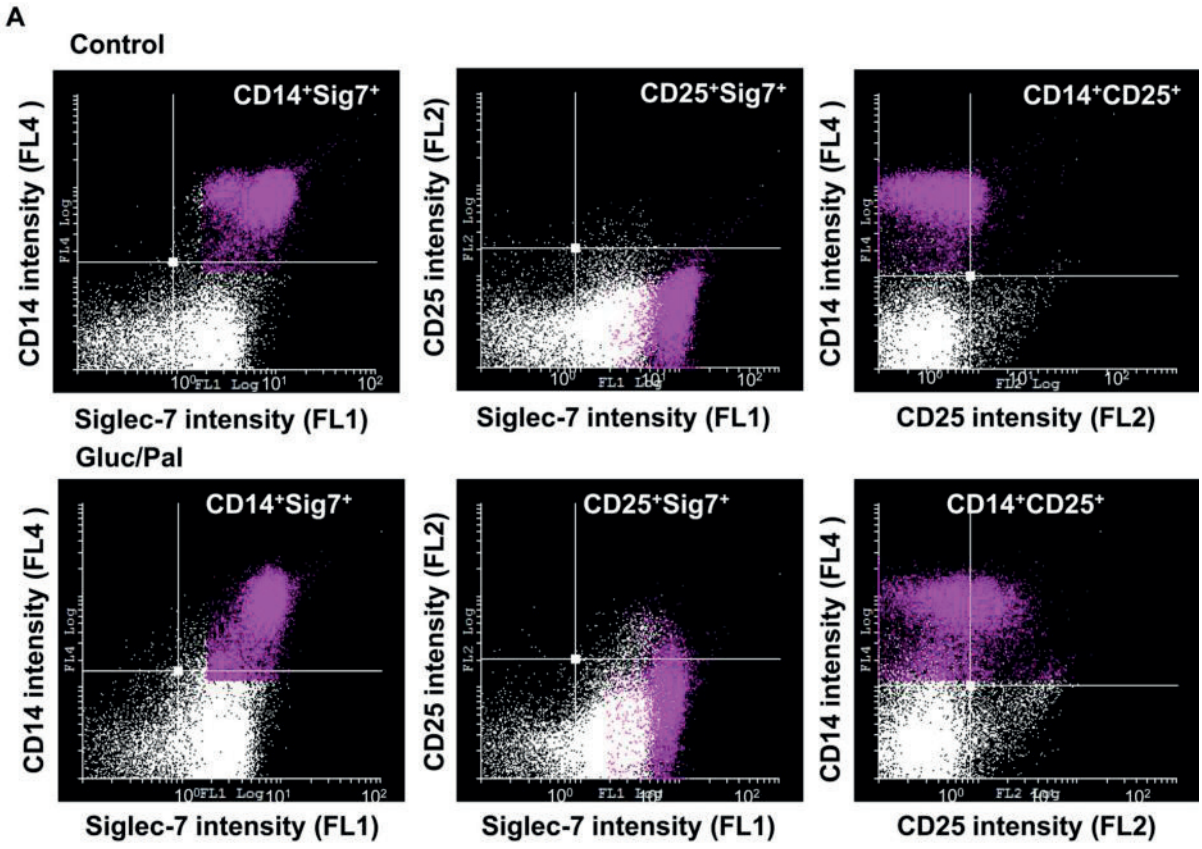

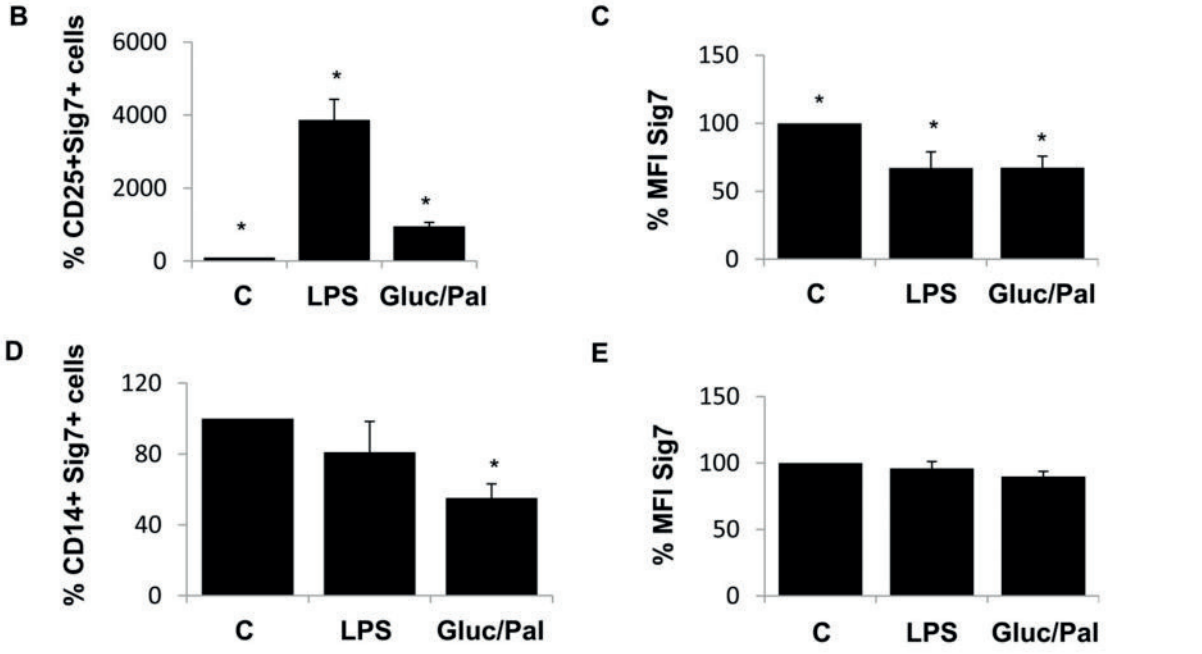

Supplementary figure 3

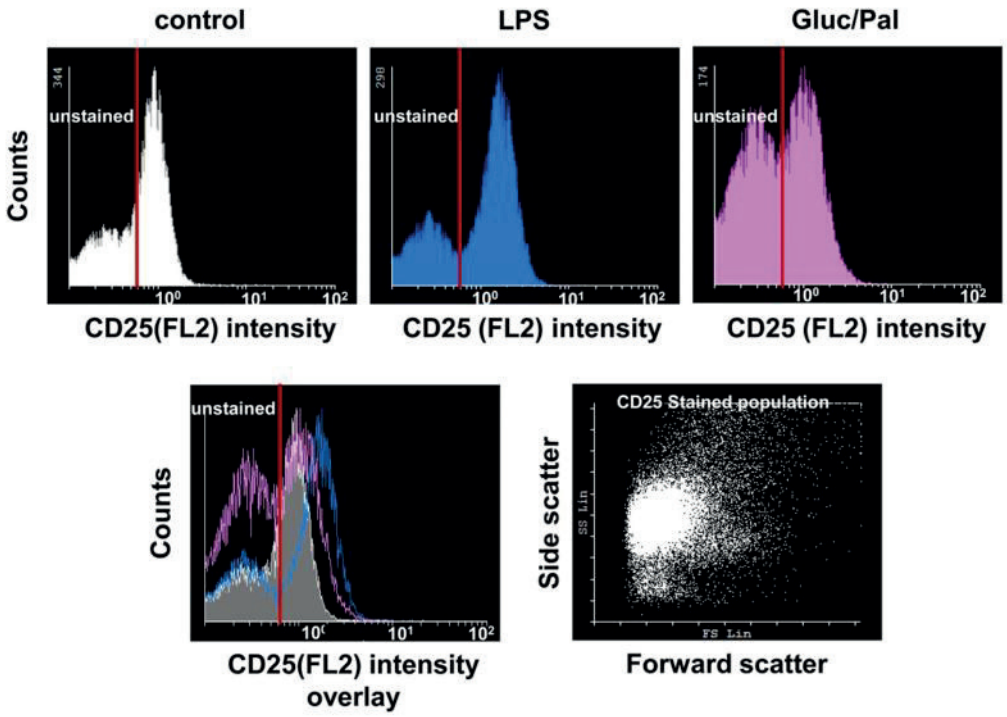

Supplementary figure 4

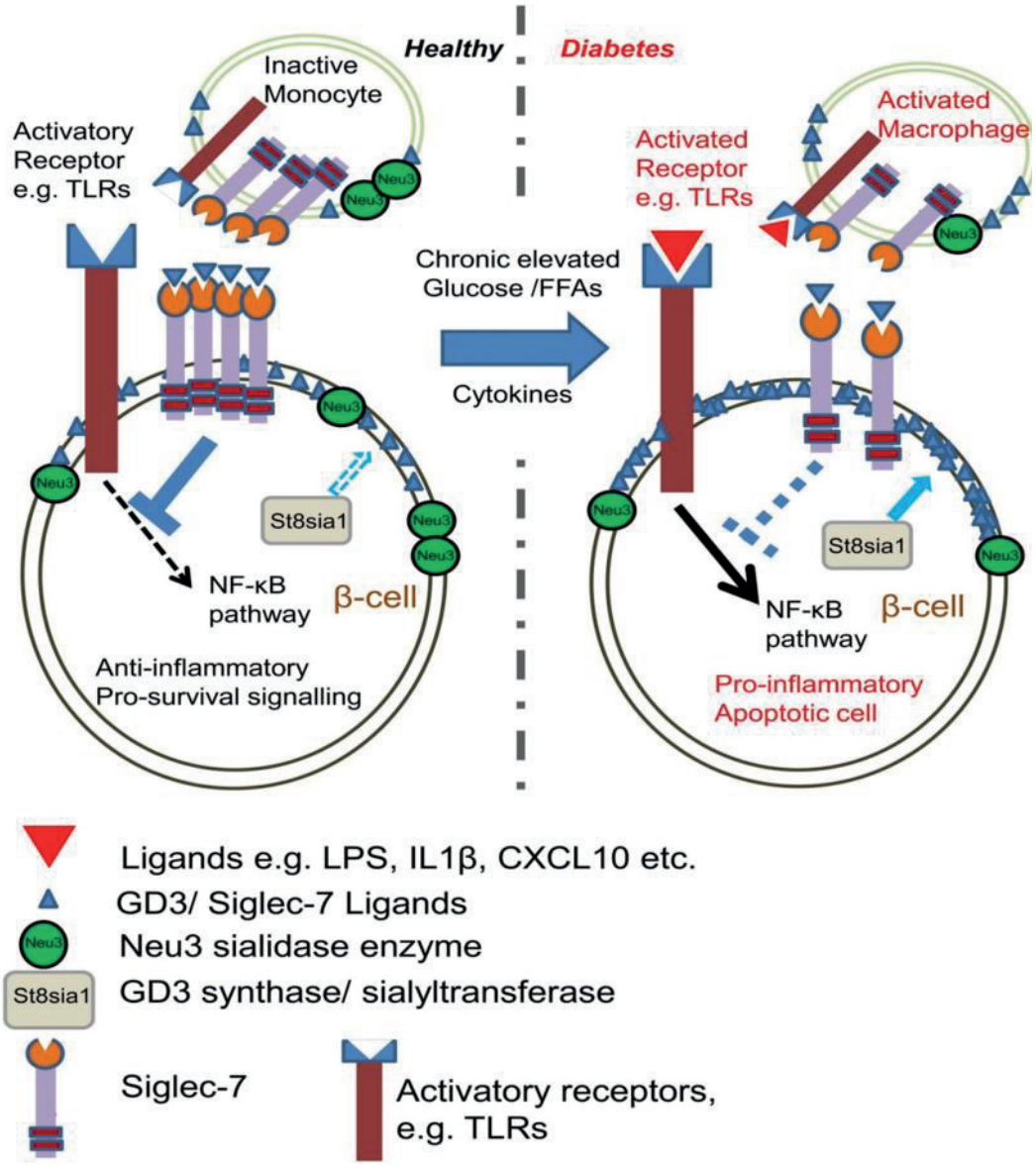

4. Discussion

Diabetes mellitus is a disease with worldwide increasing importance. Although the research of the last decades illuminated much about conditions and processes of diabetes progression, we are still not able to cure the disease. Till now the main therapy for severe diabetes is extra administration of exogenous insulin to overcome the β-cell failure, but the precise adjustment of blood glucose levels is complicated and includes regular blood sugar tests and insulin injections. Therefore research is still searching for new tools to cure diabetes. Most diabetic individuals suffer from T2D and the focus of this thesis lies on different aspects of this form. One focused on secreted factors of adipose tissue that are altered in case of obesity. A second study focused on *in vivo* β-cell imaging, a promising tool that would allow early diagnosis of diabetes and effective cure by changing lifestyle and drug administration. The third publication concentrates on Siglecs, a group of transmembrane proteins participating in immune cell regulation and β-cell survival. Due to the distinct areas of the publications they will be discussed here in individually.

4.1 The Adipocytokine Nampt and Its Product NMN Have No Effect on Beta-Cell Survival but Potentiate Glucose-Stimulated Insulin Secretion

Insulin resistance in peripheral tissues in combination with β-cell failure is the key factor for the development of T2D. One of the main factors for the development of insulin resistance in adipose tissue is obesity. Hypertrophy, hyperplasia and hypoxia lead to inflammation of adipocytes, resulting in altered secretion of adipocytokines. These adipocytokines in turn can display direct effect on β-cells, showing a possible mechanism of communication between adipocytes and the pancreatic islet cells. Secreted adipocytokines span a huge diversity of molecules, including well known cytokines. We were able to show the proapoptotic effects of the mixture of IFNγ, TNFα and IL1β in the INS-1E cell line, whereas the adipocytokines leptin, adiponectin, Nampt and its product NMN showed no effect on cell survival. None of the adipocytokines had any effect on apoptosis when treated in parallel with a cytokine mixture or free fatty acids. The effect of adiponectin goes along with previous results, which reported no visible effect of adiponectin on insulin secretion or β-cell survival[122]. But these findings run against other studies that showed modulating effects of adiponectin and leptin on apoptosis by significant reduction of cytokine or palmitic acid induced caspase 3 activity and partially inhibited DNA fragmentation in

INS-1E cells[123]. In contrast other studies showed a proapoptotic effect of leptin on β-cells[124] and this variety of contradictory results indicates the dependence on experimental design to evaluate the clear leptin effects[54].

To see if any detectable effects of this study are due to the enzymatic activity of Nampt we used also its enzymatic product NMN for treatments. Although Nampt has been reported to exhibit enzyme-independent antiapoptotic effects in hepatocytes[125] and macrophages[126], we were not able to detect any impact on INS-1E cells or human islet survival and apoptosis for Nampt or NMN. Cell proliferating and antiapoptotic effects were also found in MIN6 cells, but this study used a drastically elevated concentration of Nampt compared to physiological levels[59]. Along with the lacking effect on β-cell survival, neither Nampt nor NMN show influence on insulin secretion of isolated human islets in chronic control or diabetogenic conditions. Previous studies on isolated mouse islets reported a protective effect of NMN on insulin secretion, when treated with a cytokine mixture. The use of an alternative cytokine mixture in combination with species differences and reduced culture period could be a possible explanation for this different finding[127]. Along with the increased insulin secretion under NMN treatment, we found an acute effect on insulin secretion, if added to high glucose concentrations for Nampt as well as for NMN. In line with this it was shown, that Nampt null allele heterozygous mice display impaired glucose tolerance, which could be reversed by NMN administration[55,127], leading to the conclusion that the diminishing effects are due to lack of Nampt-mediated NAD synthesis.

iNampt levels in peripheral tissues were shown to be reduced in terms of T2D, and additional administration of NMN to HFD fed animals was able to reduce oxidative stress and inflammatory responses, ameliorates glucose intolerance and enhance hepatic insulin sensitivity[57]. In contrast, circulating eNampt levels are elevated in T2D[60]. Compared to other tissues pancreatic islets express very low amounts of iNampt and are therefore dependent on plasma NMN levels[55]. Increased release of eNampt by adipose tissue in terms of obesity could provide a mechanism to improve β-cell function.

NAD and its derivate compounds play an important role as coenzymes in cellular redox reactions and participate in important signaling pathways[128,129] and transcriptional regulation[130]. One family of these NAD-consuming enzymes are the sirtuins, that are involved in cellular homeostasis, glucose metabolism and stress

responses[131]. They also regulate cytokine production. Reduced NAD levels due to Nampt inhibition attenuate TNFα and IL6 production[132,133]. External administration of Nampt and its product NMN leads to upregulation of intracellular NAD levels in human islets in a short time period. A number of studies showed that Nampt inhibition leads to ATP depletion in cancer cells[134,135], giving a possible mechanism for Nampts effect on insulin secretion. Besides its direct beneficial effect on β-cells, eNampt was shown to enhance monocyte polarization towards a M2 phenotype[136], which display a health and growth promoting setting.

4.2 Manganese mediated magnetic resonance imaging signals correlate with functional β-cell mass during diabetes progression

Diabetes mellitus is characterized by the loss of functional β-cell mass. Analysis of autopsy pancreases showed already, that the β-cell mass alone cannot provide sufficient information about diabetes progression, because compensation of β-cells can be achieved by increasing mass or function or a combination of both. Till now functional β-cell mass is monitored by measuring insulin and C-peptide release during glucose or arginine tolerance tests[137,138]. Early diagnosed changes in β-cell mass would allow better treatment towards the preservation of normoglycemia. Noninvasive measurement of functional β-cell mass in living individuals has an enormous potential for diagnostics but failed till now because of the lack for a specific β-cell ligand[61,69].

Mn^{2+} is internalized into β-cells upon glucose stimulation and acts simultaneously as a T_1 contrast agent, allowing visualization *in vivo* by MRI. In this study we developed *in vivo* imaging of the functional β-cell mass in different mouse models and showed a strong correlation between Mn^{2+} signals and β-cell function. Mn^{2+} enters the cell via Ca^{2+} channels expressed on various cell types[139]. Glucose stimulation leads to activation of voltage gated Ca^{2+} channels in the β-cells, giving a specific tool for exclusive Mn^{2+} uptake into β-cells[83]. Mn^{2+} injection into the tail vein of anesthetized mice showed increasing pancreas signals over time in a diet dependent manner. While ND fed mice showed constant signals over the whole experimental time, HFD fed mice revealed significant upregulation of pancreatic Mn^{2+} signals after one week that declined directly again showing lower signals after two and three weeks compared to ND fed mice. However these decreased signals reached significance only from week four on and stayed lower than that of ND mice throughout the 12

weeks of experiment. This is supported by ipGTT and GSIS during diabetes progression, which both show an improvement during the first week of HFD and a subsequent impairment under longer HFD conditions. The rising Mn^{2+} signals in the pancreas during the first week, as well as the improved ipGTT and GSIS, represent the adaptation of β-cells for higher demands of insulin under HFD feeding[35,36]. Prolonged exposure to HFD leads to impaired ipGTT and GSIS, indicating the failure of the β-cells to compensate for higher insulin demands[140,141], also represented by reduced pancreatic Mn^{2+} signals. While functional analysis changed within weeks, β-cell mass was increased from week 1 on under HFD feeding and stayed at this elevated level for 8 weeks. Elevated β-cell mass is a known phenomenon in HFD treated mice, but were reported for longer time periods than 12 weeks[141,142]. In week 12 it drops to a level comparable to that of ND fed mice, demonstrating that pancreatic Mn^{2+} signals reflect functional β-cell mass and not β-cell mass alone. The dropping β-cell mass goes along with studies reporting decreased β-cell mass in autopsy samples in various populations (European, Asian, and North American) of T2 diabetic human individuals compared to healthy controls[31,143]. Measurement for longer than 12 weeks was not possible in the tested animals; due to the HFD they accumulated fat in and around the organs. Discrimination between fat and organ signals becomes more inaccurate, influencing final analysis. This limits its application potential in obese TD patients and therefore this method needs more optimization. To overcome individual differences of mice and injection efficiencies, all data were normalized to the liver signal, which represents the Mn^{2+} distribution in the blood stream.

Besides the HFD mouse model, we investigated also MRI signals in STZ-injected mice. Diabetes onset was induced by a single high dose of STZ[144] and two weeks later mice displayed blood glucose levels around 400 mg/dL. β-cell mass showed 13-fold reduction at this point, indicating the effective destruction of β-cells by STZ. Also pancreatic Mn^{2+} signals were significantly reduced, however the AUC analysis revealed only 26% reduction. Changing of analysis and comparing only the AUC between 10 and 30 min after Mn^{2+} injection results in better fitting of signal differences, resulting in approximately 80% reduced signals in STZ mice. STZ enters the cells via the GLUT2 transporter and leads to alkylation of DNA. This transporter is not exclusively expressed on β-cells, also hepatic cells take up glucose via GLUT2[145]. STZ application is therefore damaging also hepatic cells[146], which we can

see by decreased liver signals in STZ treated mice. Another report did not see liver signal alteration under STZ treatment, but still found reduced pancreatic Mn^{2+} signals upon STZ treatment[83]. Nevertheless, this makes the liver an inappropriate organ for signal normalization, therefore STZ data were normalized to the maximal signal of the corresponding region of interest in the proton density image.

Elevated levels of Mn^{2+} can result in toxic neurological effects that finally lead to Parkinson like disease, called manganism[147]. To monitor possible toxic side effects on insulin secretion by Mn^{2+} injection, mice were injected with $MnCl_2$ and glucose tolerance was tested. Directly after injection ipGTT was impaired in $MnCl_2$ injected mice compared to control mice, but this effect was gone after two days. Repeating the experiment one week later showed a stronger impairment of glucose tolerance, which was also gone two days later. Impairment of acute administration of $MnCl_2$ can be explained by Mn^{2+} entering the β-cells via voltage gated Ca^{2+} channels[148] and the resulting lower influx of Ca^{2+} ions, that are necessary for insulin exocytosis[13]. Although Mn^{2+} did not affect glucose metabolism, accumulation of Mn^{2+} in other tissues like brain, muscles or blood cannot be ruled out and needs further investigation. Another idea to overcome potential Mn^{2+} toxicity is the use of chelated Mn^{2+} that is approved for imaging the human liver or the use of lower Mn^{2+} concentrations, but this has to be investigated. Imaging β-cell mass *in vivo* exhibits different complications, starting with the clear identification of the pancreas in MRI images and the limitation to only a few slides for pancreas analysis, which have to represent the whole organ. Other complications are changes in vascularization of islets due to diabetes progression and therefore altered Mn^{2+} administration.

Although β-cells constitute only for a very small part of the total pancreas mass we proved non-invasive MRI as a reliable tool for detection of small changes in functional β-cell *in vivo*.

4.3 Siglec-7 is down-regulated in inflamed islets and activated peripheral blood mononuclear cells; restores β-cell function and survival

Siglecs are a still expanding group of transmembrane proteins that are known to be mainly expressed on cells of the hematopoietic system. They function as simple adhesion molecules or by the activation of their ITIM domains for intracellular signaling cascades. It is already known that they participate in inflammatory responses such as lung way inflammation; therefore we investigated their role in

T2D, which also shows inflammatory features. We found Siglecs to be expressed on islet cells and modulate β-cell survival and function in humans during diabetes progression.

Besides Siglec expression in humans, we also investigated Siglec expression in Siglec-F knockout and C57Bl/6J mice. Because FACS analyses revealed only very few Siglec-E and –F positive cells in dispersed islet fractions, it is unlikely that these expression is based on β-cells, which represent up to 80% of the cells[7]. δ-cells, ε-cells, PP-cells[3,5] or resident macrophages[149] represent a cell number in the range of the detected Siglec positive cells, from which macrophages are the most likely source of Siglec expression. Siglec-F expression was already detected in alveolar macrophages[115] and Siglec-E is expressed on monocytes[88], the precursors of macrophages. Therefore we depleted the macrophages by clodronate containing liposomes. Liposomes themselves are not toxic for cells and only phagocytic cells are able to swallow the liposomes with the containing agent. Clodronate is released intracellular and leads to irreversibly damage, resulting in apoptosis, specifically in macrophages[150]. Islets treated with PBS filled liposomes served as a control besides untreated islets. PBS filled liposomes alone seem to have an effect already on macrophages, most of the macrophage genes show a tendency to decrease upon liposome treatment and this trend was not detectable for β-cell genes. This could be explained by the composition of the liposomes. The phospholipid bilayers are prepared of phosphatidylcholine and cholesterol[150], which are naturally occurring molecules and not toxic for cells. But macrophages swallow the liposomes and an overload of intracellular cholesterol induces the unfolded protein response in macrophages and leads to apoptosis[151]. mRNA analysis of the clodronate treated islets showed significantly decreased macrophage markers CD68, CD11b and F4/80 compared to the PBS control, whereas the β-cell markers Ins1, Ins2 and Pdx1 stayed the same, indicating the specific macrophage depletion. Along with macrophage markers, Siglec-E decreased significantly and Siglec–F was not even detectable upon clodronate treatment, marking macrophages as the most likely Siglec source in islets.

Diabetes mellitus is a complex disease that involves a lot of tissues and cells, and the absence of Siglecs in the islet cells themselves does not exclude a possible role of mouse Siglecs in the development of diabetes. We found that Siglec expression in human monocytes is changed due to diabetogenic stimuli, and Siglec-F is known to

have a modulatory role in eosinophils during airway inflammation. Siglec-F is upregulated on eosinophils during ovalbumin induced lung inflammation together with the upregulation of Siglec-F ligands in lung tissue[117]. Activating of Siglec-F via antibodies leads to increased eosinophil apoptosis, showing a feedback loop modulating eosinophilic inflammation[118,119]. If the same would be true for the inflammation during diabetes progression, Siglec-F knockout mice should develop a more severe diabetes mellitus, because of the missing feedback loop and increased macrophage promoted inflammation.

To see, if Siglec-F takes part in inflammatory processes during diabetes development, we investigated its participation in an *in vivo* model for diabetes. Siglec-F whole body knockout mice and their littermate wildtype and heterozygous controls were injected with STZ to induce diabetes[152]. Rising random blood sugar levels in STZ injected mice showed diabetes progression due to β-cell destruction while the control injected mice had constant blood sugar levels. Increase was the same for all genotypes, there was no visible effect of Siglec-F knockout. Same was found for glucose tolerance that was strongly impaired in STZ injected mice compared to the control group, but revealed no differences in between genotypes. β-cell loss was additionally proven by measuring the insulin secretion. All control mice showed nice stimulation of 3-fold, whereas all STZ injected mice were not stimulated at all. Also here knockout of Siglec-F did not influence the results.

Additionally we isolated islets from the different genotypes and treated them with diabetogenic stimuli, to see if the knockout of Siglec-F in the resident macrophages within the islet influences their behavior. As expected islets were less stimulated when treated with diabetogenic conditions, but Siglec-F absence did not have any effect here, too. All this together hint to an unlikely participation of Siglecs in the development of diabetes in mice.

This is not in agreement with Siglecs behavior in diabetes development in humans, but does not speak against it. It could be explained by interspecies differences. Animal models have been generated to study the underlying pathology and to develop potential treatments for diabetes, but these models do not exactly replicate human diabetes. For example, while humans have only one β-cell-specific and glucose-regulated insulin gene, mice carry two functional forms[153,154]. Insulin promoter reveals only ~45-48% sequence homology between rodents and humans[155], revealing possible different mechanisms for transcriptional control. Also

glucose uptake differs in between species. While uptake in human skeletal muscle involves clathrin heavy chain 22, it exists only as a pseudogene in mice[156]. All this important functions of glucose homeostasis are altered between human and mouse and shows that different protein expression is not unusual in between species. CD33 related Siglecs show already species differential expression in their main research field, the immune system, so absence of Siglecs in mouse islets while it is expressed in humans is possible, giving an additional example for interspecies differences.

Taking this together, Siglecs display a protective role in human islets, but no CD33 related Siglec is expressed in mouse endocrine islet cells and make mice an inappropriate model for studying Siglec function in diabetes.

References

1. Gray, H. Anatomy of the Human Body. Vol. 20 (LEA & FEBIGER, PHILADELPHIA, 1918).
2. Permutt, A., Chirgwin, J., Giddings, S., Kakita, K. & Rotwein, P. Insulin biosynthesis and diabetes mellitus. *Clin Biochem* **14**, 230-6 (1981).
3. Youos, J.G. The role of alpha-, delta- and F cells in insulin secretion and action. *Diabetes Res Clin Pract* **93 Suppl 1**, S25-6 (2011).
4. Bardeesy, N., Sharpless, N.E., DePinho, R.A. & Merlino, G. The genetics of pancreatic adenocarcinoma: a roadmap for a mouse model. *Semin Cancer Biol* **11**, 201-18 (2001).
5. Wierup, N., Sundler, F. & Heller, R.S. The islet ghrelin cell. *J Mol Endocrinol* **52**, R35-49 (2014).
6. http://classroom.sdmesa.net/eschmid/Chapter13-Zoo145.htm.
7. Suckale, J. & Solimena, M. Pancreas islets in metabolic signaling--focus on the beta-cell. *Front Biosci* **13**, 7156-71 (2008).
8. Quesada, I., Tuduri, E., Ripoll, C. & Nadal, A. Physiology of the pancreatic alpha-cell and glucagon secretion: role in glucose homeostasis and diabetes. *J Endocrinol* **199**, 5-19 (2008).
9. Hauge-Evans, A.C. et al. Somatostatin secreted by islet delta-cells fulfills multiple roles as a paracrine regulator of islet function. *Diabetes* **58**, 403-11 (2009).
10. Asakawa, A. et al. Characterization of the effects of pancreatic polypeptide in the regulation of energy balance. *Gastroenterology* **124**, 1325-36 (2003).
11. Joshi, S.R., Parikh, R.M. & Das, A.K. Insulin--history, biochemistry, physiology and pharmacology. *J Assoc Physicians India* **55 Suppl**, 19-25 (2007).
12. Fauci, B., Kasper, Hauser, Longo, Jameson, Loscalzo. *Harrison`s principles of internal medicine*, (2008).
13. Henquin, J.C. Triggering and amplifying pathways of regulation of insulin secretion by glucose. *Diabetes* **49**, 1751-60 (2000).
14. Rouille, Y., Martin, S. & Steiner, D.F. Differential processing of proglucagon by the subtilisin-like prohormone convertases PC2 and PC3 to generate either glucagon or glucagon-like peptide. *J Biol Chem* **270**, 26488-96 (1995).
15. Rouille, Y., Westermark, G., Martin, S.K. & Steiner, D.F. Proglucagon is processed to glucagon by prohormone convertase PC2 in alpha TC1-6 cells. *Proc Natl Acad Sci U S A* **91**, 3242-6 (1994).
16. Wendt, A. et al. Glucose inhibition of glucagon secretion from rat alpha-cells is mediated by GABA released from neighboring beta-cells. *Diabetes* **53**, 1038-45 (2004).
17. Cejvan, K., Coy, D.H. & Efendic, S. Intra-islet somatostatin regulates glucagon release via type 2 somatostatin receptors in rats. *Diabetes* **52**, 1176-81 (2003).
18. Gonzalez, M. et al. Loss of insulin-induced inhibition of glucagon gene transcription in hamster pancreatic islet alpha cells by long-term insulin exposure. *Diabetologia* **51**, 2012-21 (2008).
19. Rorsman, P., Braun, M. & Zhang, Q. Regulation of calcium in pancreatic alpha- and beta-cells in health and disease. *Cell Calcium* **51**, 300-8 (2012).
20. Walker, J.N. et al. Regulation of glucagon secretion by glucose: paracrine, intrinsic or both? *Diabetes Obes Metab* **13 Suppl 1**, 95-105 (2011).
21. Federation, I.D. IDF Diabetes Atlas. **6th edition**(2013).
22. Organization, W.H. Global status report on noncommunicable diseases 2010. *Geneva* (2011).
23. Pirot, P., Cardozo, A.K. & Eizirik, D.L. Mediators and mechanisms of pancreatic beta-cell death in type 1 diabetes. *Arq Bras Endocrinol Metabol* **52**, 156-65 (2008).
24. van Belle, T.L., Coppieters, K.T. & von Herrath, M.G. Type 1 diabetes: etiology, immunology, and therapeutic strategies. *Physiol Rev* **91**, 79-118 (2011).
25. Tisch, R. & McDevitt, H. Insulin-dependent diabetes mellitus. *Cell* **85**, 291-7 (1996).
26. Kim, M.S. & Polychronakos, C. Immunogenetics of type 1 diabetes. *Horm Res* **64**, 180-8 (2005).

27. Wagner, D. *Type 1 Diabetes - Pathogenesis, Genetics and Immunotherapy*, (2011).
28. Mathis, D., Vence, L. & Benoist, C. beta-Cell death during progression to diabetes. *Nature* **414**, 792-8 (2001).
29. Cogger, K. & Cristina Nostro, M. Recent advances in cell replacement therapies for the treatment of type 1 diabetes. *Endocrinology*, en20141691 (2014).
30. Daifotis, A.G., Koenig, S., Chatenoud, L. & Herold, K.C. Anti-CD3 clinical trials in type 1 diabetes mellitus. *Clin Immunol* **149**, 268-78 (2013).
31. Donath, M.Y. & Halban, P.A. Decreased beta-cell mass in diabetes: significance, mechanisms and therapeutic implications. *Diabetologia* **47**, 581-9 (2004).
32. Tooley, J.E., Waldron-Lynch, F. & Herold, K.C. New and future immunomodulatory therapy in type 1 diabetes. *Trends Mol Med* **18**, 173-81 (2012).
33. Every, A.L., Kramer, D.R., Mannering, S.I., Lew, A.M. & Harrison, L.C. Intranasal vaccination with proinsulin DNA induces regulatory CD4+ T cells that prevent experimental autoimmune diabetes. *J Immunol* **176**, 4608-15 (2006).
34. Romao, I. & Roth, J. Genetic and environmental interactions in obesity and type 2 diabetes. *J Am Diet Assoc* **108**, S24-8 (2008).
35. Chen, C., Hosokawa, H., Bumbalo, L.M. & Leahy, J.L. Mechanism of compensatory hyperinsulinemia in normoglycemic insulin-resistant spontaneously hypertensive rats. Augmented enzymatic activity of glucokinase in beta-cells. *J Clin Invest* **94**, 399-404 (1994).
36. Steil, G.M. et al. Adaptation of beta-cell mass to substrate oversupply: enhanced function with normal gene expression. *Am J Physiol Endocrinol Metab* **280**, E788-96 (2001).
37. Bonner-Weir, S. Islet growth and development in the adult. *J Mol Endocrinol* **24**, 297-302 (2000).
38. Weir, G.C. & Bonner-Weir, S. Five stages of evolving beta-cell dysfunction during progression to diabetes. *Diabetes* **53 Suppl 3**, S16-21 (2004).
39. Butler, A.E. et al. Beta-cell deficit and increased beta-cell apoptosis in humans with type 2 diabetes. *Diabetes* **52**, 102-10 (2003).
40. Wajchenberg, B.L. beta-cell failure in diabetes and preservation by clinical treatment. *Endocr Rev* **28**, 187-218 (2007).
41. Lim, E.L. et al. Reversal of type 2 diabetes: normalisation of beta cell function in association with decreased pancreas and liver triacylglycerol. *Diabetologia* **54**, 2506-14 (2011).
42. Thomas, H.E., McKenzie, M.D., Angstetra, E., Campbell, P.D. & Kay, T.W. Beta cell apoptosis in diabetes. *Apoptosis* **14**, 1389-404 (2009).
43. Maedler, K. Beta cells in type 2 diabetes - a crucial contribution to pathogenesis. *Diabetes Obes Metab* **10**, 408-20 (2008).
44. Bensellam, M., Laybutt, D.R. & Jonas, J.C. The molecular mechanisms of pancreatic beta-cell glucotoxicity: recent findings and future research directions. *Mol Cell Endocrinol* **364**, 1-27 (2012).
45. Robertson, R.P., Harmon, J., Tran, P.O. & Poitout, V. Beta-cell glucose toxicity, lipotoxicity, and chronic oxidative stress in type 2 diabetes. *Diabetes* **53 Suppl 1**, S119-24 (2004).
46. de Luca, C. & Olefsky, J.M. Inflammation and insulin resistance. *FEBS Lett* **582**, 97-105 (2008).
47. Schmidt, A.M. Insulin resistance and metabolic syndrome: mechanisms and consequences. *Arterioscler Thromb Vasc Biol* **32**, 1753 (2012).
48. Baker, R.G., Hayden, M.S. & Ghosh, S. NF-kappaB, inflammation, and metabolic disease. *Cell Metab* **13**, 11-22 (2011).
49. Bluher, M. Adipokines - removing road blocks to obesity and diabetes therapy. *Mol Metab* **3**, 230-40 (2014).
50. Dunmore, S.J. & Brown, J.E. The role of adipokines in beta-cell failure of type 2 diabetes. *J Endocrinol* **216**, T37-45 (2013).
51. Maury, E. & Brichard, S.M. Adipokine dysregulation, adipose tissue inflammation and metabolic syndrome. *Mol Cell Endocrinol* **314**, 1-16 (2010).

52. Kennedy, A.J., Ellacott, K.L., King, V.L. & Hasty, A.H. Mouse models of the metabolic syndrome. *Dis Model Mech* **3**, 156-66 (2010).
53. Sainz, N., Barrenetxe, J., Moreno-Aliaga, M.J. & Martinez, J.A. Leptin resistance and diet-induced obesity: central and peripheral actions of leptin. *Metabolism* **64**, 35-46 (2015).
54. Marroqui, L. et al. Role of leptin in the pancreatic beta-cell: effects and signaling pathways. *J Mol Endocrinol* **49**, R9-17 (2012).
55. Revollo, J.R. et al. Nampt/PBEF/Visfatin regulates insulin secretion in beta cells as a systemic NAD biosynthetic enzyme. *Cell Metab* **6**, 363-75 (2007).
56. Revollo, J.R., Grimm, A.A. & Imai, S. The NAD biosynthesis pathway mediated by nicotinamide phosphoribosyltransferase regulates Sir2 activity in mammalian cells. *J Biol Chem* **279**, 50754-63 (2004).
57. Yoshino, J., Mills, K.F., Yoon, M.J. & Imai, S. Nicotinamide mononucleotide, a key NAD(+) intermediate, treats the pathophysiology of diet- and age-induced diabetes in mice. *Cell Metab* **14**, 528-36 (2011).
58. Romacho, T. et al. Extracellular PBEF/NAMPT/visfatin activates pro-inflammatory signalling in human vascular smooth muscle cells through nicotinamide phosphoribosyltransferase activity. *Diabetologia* **52**, 2455-63 (2009).
59. Cheng, Q., Dong, W., Qian, L., Wu, J. & Peng, Y. Visfatin inhibits apoptosis of pancreatic beta-cell line, MIN6, via the mitogen-activated protein kinase/phosphoinositide 3-kinase pathway. *J Mol Endocrinol* **47**, 13-21 (2011).
60. El-Mesallamy, H.O., Kassem, D.H., El-Demerdash, E. & Amin, A.I. Vaspin and visfatin/Nampt are interesting interrelated adipokines playing a role in the pathogenesis of type 2 diabetes mellitus. *Metabolism* **60**, 63-70 (2011).
61. Andralojc, K. et al. Obstacles on the way to the clinical visualisation of beta cells: looking for the Aeneas of molecular imaging to navigate between Scylla and Charybdis. *Diabetologia* **55**, 1247-57 (2012).
62. Yang, L., Ji, W., Xue, Y. & Chen, L. Imaging beta-cell mass and function in situ and in vivo. *J Mol Med (Berl)* **91**, 929-38 (2013).
63. Ichise, M. & Harris, P.E. Imaging of beta-cell mass and function. *J Nucl Med* **51**, 1001-4 (2010).
64. Blomberg, B.A., Codreanu, I., Cheng, G., Werner, T.J. & Alavi, A. Beta-cell imaging: call for evidence-based and scientific approach. *Mol Imaging Biol* **15**, 123-30 (2013).
65. Souza, F. et al. Longitudinal noninvasive PET-based beta cell mass estimates in a spontaneous diabetes rat model. *J Clin Invest* **116**, 1506-13 (2006).
66. Simpson, N.R. et al. Visualizing pancreatic beta-cell mass with [11C]DTBZ. *Nucl Med Biol* **33**, 855-64 (2006).
67. Veluthakal, R. & Harris, P. In vivo beta-cell imaging with VMAT 2 ligands--current state-of-the-art and future perspective. *Curr Pharm Des* **16**, 1568-81 (2010).
68. Saisho, Y. et al. Relationship between pancreatic vesicular monoamine transporter 2 (VMAT2) and insulin expression in human pancreas. *J Mol Histol* **39**, 543-51 (2008).
69. Malaisse, W.J. & Maedler, K. Imaging of the beta-cells of the islets of Langerhans. *Diabetes Res Clin Pract* **98**, 11-8 (2012).
70. Moore, A., Bonner-Weir, S. & Weissleder, R. Noninvasive in vivo measurement of beta-cell mass in mouse model of diabetes. *Diabetes* **50**, 2231-6 (2001).
71. Ueberberg, S. et al. Generation of novel single-chain antibodies by phage-display technology to direct imaging agents highly selective to pancreatic beta- or alpha-cells in vivo. *Diabetes* **58**, 2324-34 (2009).
72. Malaisse, W.J. & Ladriere, L. Assessment of B-cell mass in isolated islets exposed to D-[3H]mannoheptulose. *Int J Mol Med* **7**, 405-6 (2001).
73. Simon, E. & Kraicer, P.F. The blockade of insulin secretion by mannoheptulose. *Isr J Med Sci* **2**, 785-99 (1966).
74. Mukai, E. et al. GLP-1 receptor antagonist as a potential probe for pancreatic beta-cell imaging. *Biochem Biophys Res Commun* **389**, 523-6 (2009).

75. Brom, M., Andralojc, K., Oyen, W.J., Boerman, O.C. & Gotthardt, M. Development of radiotracers for the determination of the beta-cell mass in vivo. *Curr Pharm Des* **16**, 1561-7 (2010).
76. Xu, G. et al. Downregulation of GLP-1 and GIP receptor expression by hyperglycemia: possible contribution to impaired incretin effects in diabetes. *Diabetes* **56**, 1551-8 (2007).
77. Biancone, L. et al. Magnetic resonance imaging of gadolinium-labeled pancreatic islets for experimental transplantation. *NMR Biomed* **20**, 40-8 (2007).
78. Gauden, A.J., Phal, P.M. & Drummond, K.J. MRI safety: nephrogenic systemic fibrosis and other risks. *J Clin Neurosci* **17**, 1097-104 (2010).
79. Evgenov, N.V., Medarova, Z., Dai, G., Bonner-Weir, S. & Moore, A. In vivo imaging of islet transplantation. *Nat Med* **12**, 144-8 (2006).
80. Evgenov, N.V. et al. In vivo imaging of immune rejection in transplanted pancreatic islets. *Diabetes* **55**, 2419-28 (2006).
81. Toso, C. et al. Clinical magnetic resonance imaging of pancreatic islet grafts after iron nanoparticle labeling. *Am J Transplant* **8**, 701-6 (2008).
82. Antkowiak, P.F., Vandsburger, M.H. & Epstein, F.H. Quantitative pancreatic beta cell MRI using manganese-enhanced Look-Locker imaging and two-site water exchange analysis. *Magn Reson Med* **67**, 1730-9 (2012).
83. Antkowiak, P.F. et al. Noninvasive assessment of pancreatic beta-cell function in vivo with manganese-enhanced magnetic resonance imaging. *Am J Physiol Endocrinol Metab* **296**, E573-8 (2009).
84. Angata, T. Molecular diversity and evolution of the Siglec family of cell-surface lectins. *Mol Divers* **10**, 555-66 (2006).
85. Crocker, P.R., Paulson, J.C. & Varki, A. Siglecs and their roles in the immune system. *Nat Rev Immunol* **7**, 255-66 (2007).
86. von Gunten, S. & Bochner, B.S. Basic and clinical immunology of Siglecs. *Ann N Y Acad Sci* **1143**, 61-82 (2008).
87. *Essentials of Glycobiology*, (Cold Spring Harbor (NY): Cold Spring Harbor Laboratory Press, 2009).
88. Pillai, S., Netravali, I.A., Cariappa, A. & Mattoo, H. Siglecs and immune regulation. *Annu Rev Immunol* **30**, 357-92 (2012).
89. Yu, Z., Maoui, M., Wu, L., Banville, D. & Shen, S. mSiglec-E, a novel mouse CD33-related siglec (sialic acid-binding immunoglobulin-like lectin) that recruits Src homology 2 (SH2)-domain-containing protein tyrosine phosphatases SHP-1 and SHP-2. *Biochem J* **353**, 483-92 (2001).
90. Zhang, J.Q., Biedermann, B., Nitschke, L. & Crocker, P.R. The murine inhibitory receptor mSiglec-E is expressed broadly on cells of the innate immune system whereas mSiglec-F is restricted to eosinophils. *Eur J Immunol* **34**, 1175-84 (2004).
91. Liu, Y. et al. Neoglycolipid probes prepared via oxime ligation for microarray analysis of oligosaccharide-protein interactions. *Chem Biol* **14**, 847-59 (2007).
92. Linnartz-Gerlach, B., Kopatz, J. & Neumann, H. Siglec functions of microglia. *Glycobiology* **24**, 794-9 (2014).
93. Nitschke, L. CD22 and Siglec-G: B-cell inhibitory receptors with distinct functions. *Immunol Rev* **230**, 128-43 (2009).
94. Munday, J. et al. Identification, characterization and leucocyte expression of Siglec-10, a novel human sialic acid-binding receptor. *Biochem J* **355**, 489-97 (2001).
95. Hoffmann, A. et al. Siglec-G is a B1 cell-inhibitory receptor that controls expansion and calcium signaling of the B1 cell population. *Nat Immunol* **8**, 695-704 (2007).
96. Zhang, J. et al. Characterization of Siglec-H as a novel endocytic receptor expressed on murine plasmacytoid dendritic cell precursors. *Blood* **107**, 3600-8 (2006).
97. Crocker, P.R., McMillan, S.J. & Richards, H.E. CD33-related siglecs as potential modulators of inflammatory responses. *Ann N Y Acad Sci* **1253**, 102-11 (2012).

98. Jones, C., Virji, M. & Crocker, P.R. Recognition of sialylated meningococcal lipopolysaccharide by siglecs expressed on myeloid cells leads to enhanced bacterial uptake. *Mol Microbiol* **49**, 1213-25 (2003).
99. Monteiro, V.G. et al. Increased association of Trypanosoma cruzi with sialoadhesin positive mice macrophages. *Parasitol Res* **97**, 380-5 (2005).
100. Vanderheijden, N. et al. Involvement of sialoadhesin in entry of porcine reproductive and respiratory syndrome virus into porcine alveolar macrophages. *J Virol* **77**, 8207-15 (2003).
101. Tateno, H. et al. Distinct endocytic mechanisms of CD22 (Siglec-2) and Siglec-F reflect roles in cell signaling and innate immunity. *Mol Cell Biol* **27**, 5699-710 (2007).
102. Chen, G.Y., Tang, J., Zheng, P. & Liu, Y. CD24 and Siglec-10 selectively repress tissue damage-induced immune responses. *Science* **323**, 1722-5 (2009).
103. Bjorck, P., Leong, H.X. & Engleman, E.G. Plasmacytoid dendritic cell dichotomy: identification of IFN-alpha producing cells as a phenotypically and functionally distinct subset. *J Immunol* **186**, 1477-85 (2011).
104. Blasius, A.L., Cella, M., Maldonado, J., Takai, T. & Colonna, M. Siglec-H is an IPC-specific receptor that modulates type I IFN secretion through DAP12. *Blood* **107**, 2474-6 (2006).
105. Yamanaka, M., Kato, Y., Angata, T. & Narimatsu, H. Deletion polymorphism of SIGLEC14 and its functional implications. *Glycobiology* **19**, 841-6 (2009).
106. Kirchberger, S. et al. Human rhinoviruses inhibit the accessory function of dendritic cells by inducing sialoadhesin and B7-H1 expression. *J Immunol* **175**, 1145-52 (2005).
107. Lock, K., Zhang, J., Lu, J., Lee, S.H. & Crocker, P.R. Expression of CD33-related siglecs on human mononuclear phagocytes, monocyte-derived dendritic cells and plasmacytoid dendritic cells. *Immunobiology* **209**, 199-207 (2004).
108. Boyd, C.R. et al. Siglec-E is up-regulated and phosphorylated following lipopolysaccharide stimulation in order to limit TLR-driven cytokine production. *J Immunol* **183**, 7703-9 (2009).
109. Ando, M., Tu, W., Nishijima, K. & Iijima, S. Siglec-9 enhances IL-10 production in macrophages via tyrosine-based motifs. *Biochem Biophys Res Commun* **369**, 878-83 (2008).
110. Dharmadhikari, G. (2013).
111. Tateno, H., Crocker, P.R. & Paulson, J.C. Mouse Siglec-F and human Siglec-8 are functionally convergent paralogs that are selectively expressed on eosinophils and recognize 6'-sulfo-sialyl Lewis X as a preferred glycan ligand. *Glycobiology* **15**, 1125-35 (2005).
112. Angata, T., Hingorani, R., Varki, N.M. & Varki, A. Cloning and characterization of a novel mouse Siglec, mSiglec-F: differential evolution of the mouse and human (CD33) Siglec-3-related gene clusters. *J Biol Chem* **276**, 45128-36 (2001).
113. Aizawa, H. et al. Molecular analysis of human Siglec-8 orthologs relevant to mouse eosinophils: identification of mouse orthologs of Siglec-5 (mSiglec-F) and Siglec-10 (mSiglec-G). *Genomics* **82**, 521-30 (2003).
114. Kiwamoto, T., Kawasaki, N., Paulson, J.C. & Bochner, B.S. Siglec-8 as a drugable target to treat eosinophil and mast cell-associated conditions. *Pharmacol Ther* **135**, 327-36 (2012).
115. Feng, Y.H. & Mao, H. Expression and preliminary functional analysis of Siglec-F on mouse macrophages. *J Zhejiang Univ Sci B* **13**, 386-94 (2012).
116. Bochner, B.S. Siglec-8 on human eosinophils and mast cells, and Siglec-F on murine eosinophils, are functionally related inhibitory receptors. *Clin Exp Allergy* **39**, 317-24 (2009).
117. Zhang, M. et al. Defining the in vivo function of Siglec-F, a CD33-related Siglec expressed on mouse eosinophils. *Blood* **109**, 4280-7 (2007).
118. Zimmermann, N. et al. Siglec-F antibody administration to mice selectively reduces blood and tissue eosinophils. *Allergy* **63**, 1156-63 (2008).
119. Song, D.J. et al. Anti-Siglec-F antibody reduces allergen-induced eosinophilic inflammation and airway remodeling. *J Immunol* **183**, 5333-41 (2009).
120. Song, D.J. et al. Anti-Siglec-F antibody inhibits oral egg allergen induced intestinal eosinophilic inflammation in a mouse model. *Clin Immunol* **131**, 157-69 (2009).

121. Rubinstein, E. et al. Siglec-F inhibition reduces esophageal eosinophilia and angiogenesis in a mouse model of eosinophilic esophagitis. *J Pediatr Gastroenterol Nutr* **53**, 409-16 (2011).
122. Staiger, K. et al. Adiponectin is functionally active in human islets but does not affect insulin secretory function or beta-cell lipoapoptosis. *J Clin Endocrinol Metab* **90**, 6707-13 (2005).
123. Rakatzi, I., Mueller, H., Ritzeler, O., Tennagels, N. & Eckel, J. Adiponectin counteracts cytokine- and fatty acid-induced apoptosis in the pancreatic beta-cell line INS-1. *Diabetologia* **47**, 249-58 (2004).
124. Maedler, K. et al. Glucose and leptin induce apoptosis in human beta-cells and impair glucose-stimulated insulin secretion through activation of c-Jun N-terminal kinases. *FASEB J* **22**, 1905-13 (2008).
125. Dahl, T.B. et al. Intracellular nicotinamide phosphoribosyltransferase protects against hepatocyte apoptosis and is down-regulated in nonalcoholic fatty liver disease. *J Clin Endocrinol Metab* **95**, 3039-47 (2010).
126. Li, Y. et al. Extracellular Nampt promotes macrophage survival via a nonenzymatic interleukin-6/STAT3 signaling mechanism. *J Biol Chem* **283**, 34833-43 (2008).
127. Caton, P.W., Kieswich, J., Yaqoob, M.M., Holness, M.J. & Sugden, M.C. Nicotinamide mononucleotide protects against pro-inflammatory cytokine-mediated impairment of mouse islet function. *Diabetologia* **54**, 3083-92 (2011).
128. Belenky, P., Bogan, K.L. & Brenner, C. NAD+ metabolism in health and disease. *Trends Biochem Sci* **32**, 12-9 (2007).
129. Rongvaux, A., Andris, F., Van Gool, F. & Leo, O. Reconstructing eukaryotic NAD metabolism. *Bioessays* **25**, 683-90 (2003).
130. Lin, S.J. & Guarente, L. Nicotinamide adenine dinucleotide, a metabolic regulator of transcription, longevity and disease. *Curr Opin Cell Biol* **15**, 241-6 (2003).
131. Imai, S. Dissecting systemic control of metabolism and aging in the NAD World: the importance of SIRT1 and NAMPT-mediated NAD biosynthesis. *FEBS Lett* **585**, 1657-62 (2011).
132. Van Gool, F. et al. Intracellular NAD levels regulate tumor necrosis factor protein synthesis in a sirtuin-dependent manner. *Nat Med* **15**, 206-10 (2009).
133. Busso, N. et al. Pharmacological inhibition of nicotinamide phosphoribosyltransferase/visfatin enzymatic activity identifies a new inflammatory pathway linked to NAD. *PLoS One* **3**, e2267 (2008).
134. Watson, M. et al. The small molecule GMX1778 is a potent inhibitor of NAD+ biosynthesis: strategy for enhanced therapy in nicotinic acid phosphoribosyltransferase 1-deficient tumors. *Mol Cell Biol* **29**, 5872-88 (2009).
135. Hasmann, M. & Schemainda, I. FK866, a highly specific noncompetitive inhibitor of nicotinamide phosphoribosyltransferase, represents a novel mechanism for induction of tumor cell apoptosis. *Cancer Res* **63**, 7436-42 (2003).
136. Audrito, V. et al. Extracellular nicotinamide phosphoribosyltransferase (NAMPT) promotes M2 macrophage polarization in chronic lymphocytic leukemia. *Blood* (2014).
137. Robertson, R.P. Estimation of beta-cell mass by metabolic tests: necessary, but how sufficient? *Diabetes* **56**, 2420-4 (2007).
138. Polonsky, K.S. & Rubenstein, A.H. C-peptide as a measure of the secretion and hepatic extraction of insulin. Pitfalls and limitations. *Diabetes* **33**, 486-94 (1984).
139. Dryselius, S., Grapengiesser, E., Hellman, B. & Gylfe, E. Voltage-dependent entry and generation of slow Ca2+ oscillations in glucose-stimulated pancreatic beta-cells. *Am J Physiol* **276**, E512-8 (1999).
140. Winzell, M.S. & Ahren, B. The high-fat diet-fed mouse: a model for studying mechanisms and treatment of impaired glucose tolerance and type 2 diabetes. *Diabetes* **53 Suppl 3**, S215-9 (2004).
141. Roat, R. et al. Alterations of pancreatic islet structure, metabolism and gene expression in diet-induced obese C57BL/6J mice. *PLoS One* **9**, e86815 (2014).

142. Hull, R.L. et al. Dietary-fat-induced obesity in mice results in beta cell hyperplasia but not increased insulin release: evidence for specificity of impaired beta cell adaptation. *Diabetologia* **48**, 1350-8 (2005).
143. Meier, J.J. & Bonadonna, R.C. Role of reduced beta-cell mass versus impaired beta-cell function in the pathogenesis of type 2 diabetes. *Diabetes Care* **36 Suppl 2**, S113-9 (2013).
144. Deeds, M.C. et al. Single dose streptozotocin-induced diabetes: considerations for study design in islet transplantation models. *Lab Anim* **45**, 131-40 (2011).
145. Ogawa, A. et al. Functional localization of glucose transporter 2 in rat liver. *J Histochem Cytochem* **44**, 1231-6 (1996).
146. Simoes, C. et al. Remodeling of liver phospholipidomic profile in streptozotocin-induced diabetic rats. *Arch Biochem Biophys* **538**, 95-102 (2013).
147. Michalke, B. & Fernsebner, K. New insights into manganese toxicity and speciation. *J Trace Elem Med Biol* **28**, 106-16 (2014).
148. Gimi, B. et al. Functional MR microimaging of pancreatic beta-cell activation. *Cell Transplant* **15**, 195-203 (2006).
149. Ehses, J.A., et al., Increased number of islet-associated macrophages in type 2 diabetes. Diabetes, **56**(9): p. 2356-70 (2007)
150. van Rooijen, N. et al., Apoptosis of macrophages induced by liposome-mediated intracellular delivery of clodronate and propamidine. J Immunol Methods. 193(1):93-9 (1996)
151. Feng, B., et al., The endoplasmic reticulum is the site of cholesterol-induced cytotoxicity in macrophages. Nat Cell Biol. 5(9):781-92 (2003)
152. Sakata, N., Yoshimatsu, G., Tsuchiya, H., Egawa, S. & Unno, M. Animal models of diabetes mellitus for islet transplantation. *Exp Diabetes Res* **2012**, 256707 (2012).
153. Owerbach, D., Bell, G.I., Rutter, W.J. & Shows, T.B. The insulin gene is located on chromosome 11 in humans. *Nature* **286**, 82-4 (1980).
154. Wentworth, B.M., Schaefer, I.M., Villa-Komaroff, L. & Chirgwin, J.M. Characterization of the two nonallelic genes encoding mouse preproinsulin. *J Mol Evol* **23**, 305-12 (1986).
155. Chandrasekera, P.C. & Pippin, J.J. Of rodents and men: species-specific glucose regulation and type 2 diabetes research. *ALTEX* **31**, 157-76 (2014).
156. Wakeham, D.E. et al. Clathrin heavy and light chain isoforms originated by independent mechanisms of gene duplication during chordate evolution. *Proc Natl Acad Sci U S A* **102**, 7209-14 (2005).

Acknowledgements

This dissertation would not have been possible without the guidance, help and support of several people…

First, I would like to thank Prof. Dr. Kathrin Mädler for giving me the opportunity to perform my PhD thesis in her lab and for her support and guidance throughout my work.

I thank Prof. Dr. Annette Schürmann for reviewing my thesis.

My special thanks goes to Gitanjali Dharmadhikari, who introduced me to the lab and worked side by side with me on this project for several years. She was always there and encouraged and supported me in the first three years of my thesis.

I also want to thank Jenny, without whose help and knowledge in laboratory organisation and experimental design my work would have been so much more complicated.

Many thanks to Payal, Anke, Fede, Katrin, Niels, Katrischa, Amin, Zahra, Erna, Wei, Ting, Durga and all the others for their support and help.

At last I want to thank my biggest supporters, my family, who were always there for me, although they do not know what I did in the last few years!

Appendix

Siglec Expression in C57Bl/6J mice

C57Bl/6J mice were fed a HFD for 16 weeks and tissue was collected directly afterwards and put directly into Trizol for RNA isolation. Reverse transcription and subsequent qRT-PCR revealed increased signals for Siglec-E and –G in HFD islets that go along with the increase of the macrophage markers CD11c and F4/80, showing an increased infiltration during diabetes progression. Siglec-F was not detectable in most of this tissue samples.

Siglec expression in bone marrow showed only increasing Siglec-G expression, whereas the other Siglecs did not change upon HFD. But macrophage markers were upregulated, indicating the activation of the immune system during HFD.

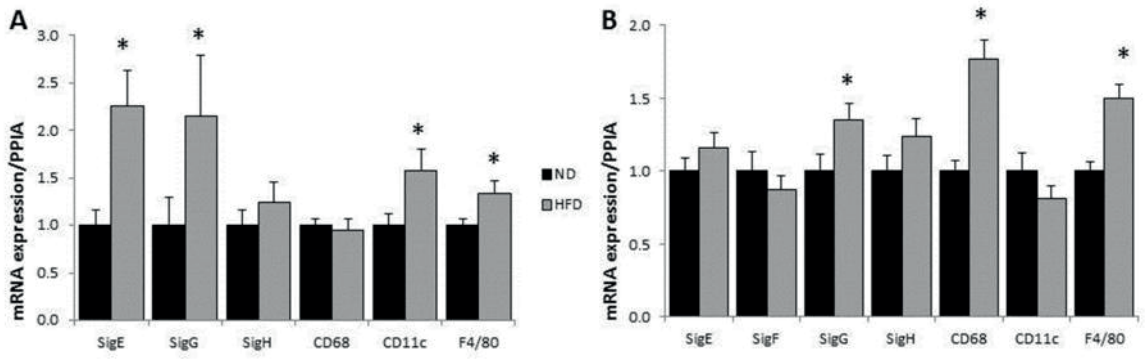

C57Bl/6J mice were fed a HFD for 16 weeks. Islets **(A)** and bone marrow **(B)** were isolated and RNA was directly isolated, transcribed and analyzed by qRT- PCR for the indicated genes. **(A)** n=11-15, **(B)** n=7-10. Data are shown as mean +/-SE, *p<0.05 ND to HFD

Coculture of WT islets with peritoneal macrophages

Macrophages from WT, SigF$^{+/-}$ and SigF$^{-/-}$ mice were isolated and cultured in a suspension dish for 1 day, to get rid of non-adherent cells. Islets from C57Bl/6J mice were isolated the next day and seeded into ECM dishes with or without different numbers of peritoneal macrophages. Medium was changed after two days; GSIS was performed three days later. None of the two experiments revealed significant differences in islet function, presence and number of macrophages did not influence stimulatory index.

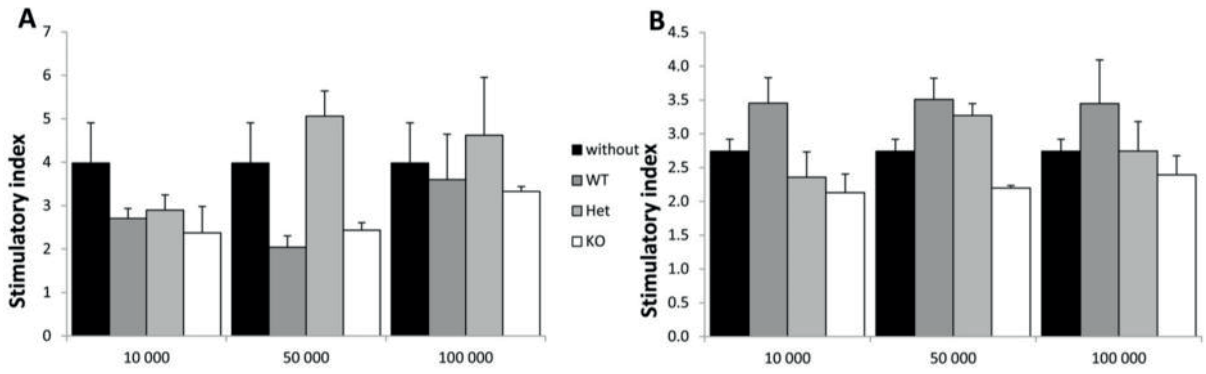

C57Bl/6J mouse islets were isolated and cocultured with or without peritoneal macrophages for five days. Experiment was done two times (**A,B**). Data are shown as mean +/-SE of three internal repeats